Maternal Health & Diet Programs Offspring Metabolism

by

Keenan Thomas Greyslak, M.S.

A dissertation accepted & approved in partial fulfillment
of the requirements for the degree of
Doctor of Philosophy in
Human Physiology

Dissertation Committee:

Carrie E. McCurdy, PhD, Chairperson & Advisor
Adrianne G. Huxtable, PhD, Core Member
Hans C. Dreyer, PhD, Core Member
Kryn Stankunas, PhD, Institutional Representative

University of Oregon

Spring 2024

DISSERTATION ABSTRACT

Keenan Thomas Greyslak
Doctor of Philosophy in Human Physiology
Title: Maternal Health & Diet Programs Offspring Metabolism

Although adult sedentary behavior and poor dietary patterns can impact metabolic health and disease outcomes, studies in animal models and human populations have generated a convincing body of evidence to suggest that nutritional and hormonal insults during critical windows of development in early life can redirect future metabolic health outcomes in offspring independent of future lifestyle choices. Specifically, maternal phenotypes derived from chronic consumption of high-fat, high-sugar, low fiber "Western-Style" diets (WD), the presence of obesity, and/or the presence of maternal hyperandrogenemia (HA) during pregnancy place them and their unborn child at higher risk for developing chronic metabolic diseases like Cardiovascular Disease, Type 2 Diabetes, and Nonalcoholic Fatty Liver Disease.

To better understand the mechanisms that lay the groundwork for metabolic dysfunction in offspring tissues beginning *in utero*, this dissertation has utilized a nonhuman primate model of chronic maternal WD consumption with and without the development of obesity on the metabolic health outcomes in juvenile and adolescent offspring. The added contributions introduced by postweaning diet style was also examined in these offspring. Finally, this thesis builds upon previous work tracking the reproductive and metabolic profiles associated with WD-induced obesity with and without HA in young female primates beginning in prepubescent juveniles and extending into adulthood. Finally, the independent and combined influence of HA with/without obesity during pregnancy on key aspects of fetal metabolism was also assessed.

This dissertation includes previously published co-authored material.

CURRICULUM VITAE

NAME OF AUTHOR: Keenan Thomas Greyslak

GRADUATE AND UNDERGRADUATE SCHOOLS ATTENDED:

University of Oregon, Eugene, OR

University of Arizona, Tucson, AZ

DEGREES AWARDED:

Doctor of Philosophy, Human Physiology, 2024, University of Oregon

Master of Science, Human Physiology, 2018, University of Oregon

Bachelor of Science, Physiology, 2014, University of Arizona

W.A. Franke Honors College

AREAS OF SPECIAL INTEREST:

Developmental Origins of Health & Disease

Mitochondrial Physiology

Metabolism

Skeletal Muscle Metabolism

Endocrinology

Insulin Signaling/Diabetes

Sex Hormones

Polycystic Ovary Syndrome/Hyperandrogenemia

PROFESSIONAL EXPERIENCE:

Graduate Employee, Department of Human Physiology, University of Oregon

Graduate Research Assistant, 2016-Present

Graduate Teaching Fellow, 2016-Present

Instructor, 2020 & 2021

Instructor, Pro-tempore, Department of Human Physiology, University of Oregon

GRANTS, AWARDS, AND HONORS:

Broekhoff Fellowship, Dept. of Human Physiology, University of Oregon, 2023.

Shapiro Family Scholarship, Dept. of Human Physiology, University of Oregon, 2023.

Fieldman Scholarship, Dept. of Human Physiology, University of Oregon, 2022.

Starr Scholarship Fund, University Scholarship, University of Oregon, 2022.

Evonuk Fellowship, Dept. of Human Physiology, University of Oregon, 2021.

Teaching Excellence Award, Dept. of Human Physiology, University of Oregon, 2021.

Gary E. Smith Professional Development Award, University of Oregon, 2020.

Shapiro Family Scholarship, Dept. of Human Physiology, University of Oregon, 2020.

Elma Hendricks Scholarship, University Scholarship, University of Oregon, 2020.

Baird Scholarship, University of Arizona, 2010-2014.

Wildcat Excellence Tuition Award, University of Arizona, 2010-2014.

PUBLICATIONS:

KT Greyslak, B Hetrick, BC Bergman, TA Dean, SR Wesolowski, M Gannon, S Schenk, EL Sullivan, KM Aagaard, P Kievit, AJ Chicco, JE Friedman, CE McCurdy. A maternal Western-style diet impairs skeletal muscle lipid metabolism in adolescent Japanese macaques. Diabetes. 2023 Sep 19. doi: 10.2337/db23-0289. PMID: 37725952.

KT Greyslak. Taken to Heart: Lessons from the Japanese Macaque Model of Obesogenic Pregnancy. Academy of Nutrition and Dietetics Dietetic Practice Group of Sports, Cardiovascular, and Wellness Nutrition's (SCAN's): Pulse. 2020;40(4).

JR Dent, B Hetrick, S Tahvilian, A Sathe, **K Greyslak**, SA LaBarge, K Svensson, CE McCurdy, S Schenk. Skeletal muscle mitochondrial function and exercise capacity are not impaired in mice with knockout of STAT3. J Appl Physiol. 127: 1117-1127. J Appl Physiol (1985). 2019 Oct 1. doi: 10.1152/japplphysiol.00003.2019. PMID: 31513449.

K Svensson, S Tahvilian, V Martins, JR Dent, A Lemanek, N Barooni, **K Greyslak**, CE McCurdy, and S Schenk. Combined overexpression of SIRT1 and knockout of GCN5 in adult skeletal muscle does not affect glucose homeostasis or exercise performance in mice. Am J Physiol Endocrinol Metab. 2020 Feb. doi: 10.1152/ajpendo.00370.2019. PMID: 31794263.

KT Greyslak, A Sharma, B Hetrick, C Meza, K Carey, TA Dean, KM Aagaard, M Gannon, SR Wesolowski, JE Friedman, P Kievit, K Funai, CE McCurdy. Exposure to Western-

style diet disrupts mitochondrial architecture in muscle of juvenile Japanese macaques. *Manuscript in preparation.*

KT Greyslak, W Campodonico-Burnett, B Hetrick, K Carey, C True, DL Takahashi, I Gertsman, EE Spangenburg, RL Stouffer, CT Roberts, CE McCurdy. Chronic hyperandrogenemia impairs skeletal muscle insulin sensitivity and mitochondrial metabolism in the absence of obesity in female Rhesus macaques. *Manuscript in preparation.*

MB Gillingham, A Gregor, O Varlamov, CE McCurdy, **KT Greyslak**, D Choi, E Baetscher, W Rooney, CO Harding, JQ Purnell. Reduced fatty acid oxidation prevents intralipid-induced hepatic insulin resistance but does not alter the development of peripheral insulin resistance independent of tissue lipid accumulation in humans. *Manuscript in preparation.*

ACKNOWLEDGMENTS

Thank you to all the mothers – past, present, and future – for not only giving me purpose in life through my research but for so gracefully shouldering the burden of our entire species. Every cell in my body thanks you for your sacrifice and for so selflessly sharing your mitochondria with the rest of us.

Y'all are the true Powerhouse of this story.

Thank you to the veterinarians and staff at ONPRC who have made this work possible – especially Tyler Dean and Diana Takahashi. Thank you to the many brilliant scientists and collaborators responsible for creating and establishing the models that this thesis is founded upon. It is a privilege to stand on the shoulders of such giants and I hope this dissertation does you, and the monkeys invested in these studies, the justice that y'all deserve. Thank you, thank you, thank you.

Thank you to my committee – Dr. Stankunas, Dr. Dreyer, Dr. Huxtable, and Dr. McCurdy – for your oversight and guidance throughout my dissertation process. **Dr. Stankunas**: thank you for not giving up on me. Your patience is very appreciated. I promise I know things and I look forward to proving it to you with this dissertation. Thank you for participating! **Dr. Dreyer**: thank you for the impromptu 30-minute hallway conversations over the years – a practice I believe embodies the true spirit of science. These chats are some of my favorite memories during my time in Oregon. I fondly refer to you as my "favorite soccer dad" among fellow lab mates because of your endless support and constant encouragement as a member of our committees – the only thing missing are the orange slices and shin guards. Thank you for taking care of me and, more importantly, for taking such good care of my lab mates. **Dr. Huxtable**: thank you for being so unapologetically you. Specifically, thank you for advocating on behalf of individuals like me who struggle to advocate for themselves. You have taught me how to own my opinion and how to disagree with others, respectfully, in a professional arena. Thank you for teaching me how to separate the work from the individual; that disagreement and critical feedback isn't personal but is critical for good science. Your "strong personality" is not only appreciated but celebrated. **Dr.**

McCurdy: thank you for always putting me and my wellbeing before the science at hand, regardless of the cost. It has been an absolute honor to grow with you over these last eight years and, while it certainly hasn't always been easy, I wouldn't want to experience this journey with anyone other than you. For better or worse, I am yours for life and I look forward to our future work and collaborations together. Never forget, "The squeaky wheel gets the oil." -my mother (:

Finally, thank you to the 2021 Evonuk Fellowship Award Committee. The kindness extended to me by this committee is truly a testament to the memory, impact, and legacy of the Evonuks. I promise to pay this kindness, and their generosity, forward for the duration of my career.

DEDICATION

This body of work is dedicated to **my mother**, Nancy Marie Greyslak, the woman responsible for my own fetal programming and whose mitochondria continue to allow me to pursue the things that I love with the people that I love.

Mama bear: you're my whole world now just as much as you were my first 1,000 days of life.

I love you, you love me. Always and forever <3

TABLE OF CONTENTS

Chapter Page

Chapter Page

LIST OF FIGURES

Figure Page

LIST OF TABLES

Table Page

LIST OF SUPPLEMENTAL MATERIALS

LIST OF ABBREVIATIONS

3Y/1Y	3-year-old/1-year-old
AUC	Area under the curve
BCA	Bicinchoninic acid
BIOPS	Biopsy preservation media
C(I-V)	Mitochondrial complexes I-V
CD	Control diet
CHO	Carbohydrate; non-lipid
CL	Cardiolipin
CoQ	Coenzyme Q
CS	Citrate synthase
CVD	Cardiovascular Disease
DEXA	Dual-energy x-ray absorptiometry
DG/DAGs	Diacylglycerol
DNPH	2,4-dinitrophenylhydrazine
DOHaD	Developmental Origins of Health and Disease
ER	Endoplasmic reticulum
ETS	Electron transport system
F	Female
FAO	Fatty acid oxidation; lipid
FCCP	Carbonyl cyanide-p-trifluoromethoxyphenylhydrazone
FFA	Free fatty acid
FGR	Fetal growth restriction
G	Glutamate
GD	Gestational day
GAS/Gastroc	Gastrocnemius (muscle)
GDM	Gestational diabetes mellitus
GLUT4	Glucose transporter type 4
GnRH	Gonadotropin hormone-releasing hormone

HA	Hyperandrogenemia
HDL	High-density lipoprotein cholesterol
HOMA-IR	Homeostatic model assessment for insulin resistance
i.v. GTT	Intravenous glucose tolerance test
IMM	Inner mitochondrial membrane
IUGR	Intrauterine growth restriction
LDL	Low-density lipoprotein cholesterol
LEAK	Proton leak (from mitochondrial intermembrane space)
LGA	Large for gestational age
LH	Luteinizing hormone
LIP	Lipid
Ln	Lean
m(mWD)	Maternal (i.e., maternal western diet)
M	Male
MAM	Mitochondrial associated membrane
MDA	Malondialdehyde
MetS	Metabolic Syndrome
mtDNA	Mitochondrial DNA
MSCs	Mesenchymal stem cells
NAFLD	Nonalcoholic Fatty Liver Disease
NHP	Nonhuman primate
Ob	Obese
OMM	Outer mitochondrial membrane
OXPHOS	Oxidative phosphorylation
PCA	Principal component analysis
PCOS	Polycystic Ovary Syndrome
PG	Phosphatidylglycerol
PMFB	Permeabilized muscle fiber bundle
PS	Phosphatidylserine
pw	Postweaning diet (a.k.a. offspring diet)
PYR	Pyruvate; non-lipid

ROS	Reactive oxygen species
S	Succinate
Sat	Saturated
SOL	Soleus (muscle)
SPMs	Sphingomyelin
T	Testosterone
T2D	Type 2 Diabetes
TBARS	Thiobarbituric acid reactive substances
TG/TAGs	Triacylglycerol
U	Uncoupled respiration
W/WD	Western diet
Y	Year

I. INTRODUCTION

SIGNIFICANCE

1 in 3 children in the U.S. have overweight or obesity (1; 2). Current growth trajectories predict that **almost 60% of children in the U.S. today will develop obesity by age 35** (3). While excess adiposity alone is not inherently lethal, the presence of obesity has been implicated with a constellation of degenerative metabolic disturbances – including dyslipidemia, hyperglycemia, hypertension, and insulin resistance – that are involved in the etiology of the Metabolic Syndrome (MetS) (4; 5). Individuals diagnosed with MetS are at an elevated risk of developing cardiovascular disease (CVD), Type 2 Diabetes (T2D), and Nonalcoholic Fatty Liver Disease (NAFLD) (6). Indeed, these chronic diseases previously thought to be "adult-onset" have become increasingly prevalent among American youth (7; 8). Furthermore, the social, clinical, and economic burden of these comorbidities cannot be overstated. CVD is the leading cause of mortality globally and in the United States (9; 10) with a projected annual cost of $1.1 trillion within the next decade in the U.S. alone (11). Therefore, in addition to therapies and interventions designed to slow the progression and mitigate the severity of CVD-related illnesses, the prevention of these diseases requires an improved understanding of how phenotypic shifts initiated *in utero* can result in such dangerous pathological outcomes. To this end, an abundance of work in both animal models and clinical cohorts of humans have identified an increased risk for MetS in individuals with early life exposure to maternal obesity, maternal high-fat/high-sugar diet (i.e., "Western-style" diet, WD), and hyperandrogenemia (12-16). Further investigation into causal mechanisms is needed to adequately understand, effectively address, and ultimately prevent the propagation of cardiometabolic maladies into future generations.

REVIEW of the LITERATURE

Critical Windows of Development

There are periods of time in the earliest stages of growth and development – e.g., embryogenesis, gestation, lactation – when tissues, organs, and physiological systems become increasingly plastic or malleable, placing them at a heightened sensitivity to adapt their physiology in response to acute and chronic environmental signals (17). These impressionable intervals during development are known as "critical windows" (18). While necessary or even advantageous for embryonic and fetal tissues to adapt structurally and functionally to ensure their survival *in utero*, retaining the subsequent phenotypes associated with such adaptations can result in irreversible, maladaptive outcomes once the window of plasticity for the newly "reprogrammed" tissue, organ, or system has closed (12; 19). This increased susceptibility to environmental insults for structures like the spine, head, appendages (arms and legs), and select internal organs like the heart is present throughout the first trimester (i.e., the first 13 weeks of human pregnancy) (20). During this time, harmful exposures are *most likely* to result in major **structural** abnormalities, birth defects, or embryonic/fetal demise (21). The growth of these structures occurs throughout the second and third trimesters, when harmful exposures or restriction of nutrients result *primarily* in **functional** abnormalities in the developing offspring (20). These potentially harmful exposures are strongly influenced by maternal health and behavior patterns. Therefore, in addition to potential health complications during and after pregnancy, the presence of adverse metabolic health in pregnant individuals comes with the risk of unintentional, pathophysiological outcomes in their unborn child (22).

Developmental Origins of Health and Disease

The Developmental Origins of Health and Disease (DOHaD) hypothesis, also known as "Barker's Hypothesis" or "Fetal Programming", is a paradigm established by Dr. David Barker and associates that laid the groundwork for our contemporary understanding of early life factors that contribute to the development of noncommunicable diseases like CVD (23-25). DOHaD was forged in epidemiological studies conducted across England and Wales, where a strong geographic

association was observed between newborn death rates and adult coronary heart disease decades later (23). At that time, low birthweight was the primary cause of neonatal mortality, suggesting that prenatal/intrauterine stress caused by maternal undernutrition was not only responsible for increased infant mortality but was also predictive of heart disease in similarly exposed middle-aged adults who survived infancy (25; 26). Since its inception, DOHaD has grown to include a battery of clinical, nutritional, pathological, and physiologically stressful conditions shown to impact maternal and offspring health outcomes. These include, but are not limited to, maternal: protein restricted diets (27; 28), Western-style diet (29-31), under/overnutrition (32-34), tobacco and alcohol consumption (35; 36), exercise (37-39), acute and chronic inflammation (40; 41), trauma and stress (42; 43), hyperandrogenemia (44; 45), insulin resistance (46; 47), and obesity (48). While each of these conditions are associated with their own unique medley of metabolic and hormonal elements, the mechanisms through which they reprogram offspring anatomy and physiology are consistently observed and conserved across model species.

Mechanisms of DOHaD

Placental Insufficiency & Fetal Growth Restriction

The placenta is the lifeline distinguishing what is "fetal" from what is "maternal", operating to provide protection, nutrients, and waste management on behalf of the newly developing fetus (49). Placental insufficiency is synonymous with poor placental function that may result from instances of vascular abnormalities or other adverse circumstances that restrict the placenta's capacity to exchange oxygen, nutrients, and metabolic waste between maternal and fetal circulations (50; 51). This loss of placental function induces Fetal Growth Restriction (FGR, a.k.a. Intrauterine Growth Restriction or IUGR), which is characterized by fetal hypoxia, acidosis, and a dearth of anabolic substrates necessary for healthy growth and development (49). FGR is most common in underweight pregnancies or pregnancies experiencing chronic nutrient deprivation/micronutrient deficiency (52). Delayed growth during gestation results in low birthweight/smaller babies, a neonatal phenotype strongly associated with development of CVD and T2D in adulthood (53). Mice from pregnancies of chronic undernutrition experience dysregulated insulin secretion from β-cells at 2 months old followed by severe glucose intolerance in young adulthood (6 months old) (54). Similarly, a study in humans by Phipps and colleagues

found that men and women at ~50 years old with impaired glucose tolerance or T2D had the lowest birthweights of the 140 men and 126 women included in their sample (55). One hypothesis connecting low birthweight to glucose intolerance and altered insulin dynamics in adulthood is the "Thrifty" hypothesis (56). This hypothesis describes a resource management strategy executed by the undernourished fetus that prioritizes critical tissues by redirecting nutrients to organs most likely to ensure survival (57; 58). In this context, developing insulin resistance *in utero* would ensure nutrients like glucose and lipid remain in circulation to spare brain growth from fuel deprivation, albeit at the cost of growth in tissues like muscle (59-61). The long-term metabolic repercussions of remaining insulin resistant postnatally would likely devolve into MetS and, ultimately, CVD and T2D. This phenotype would be especially maladaptive if intrauterine undernutrition is followed by lifestyle overnutrition in childhood and/or adulthood as this mismatch in pre- and postnatal environments would exacerbate offspring risk of developing MetS (12).

Epigenetic Modifications

In a monastery garden, Gregor Mendel and his pedigree of peas introduced humanity to the tenets of familial inheritance and the laws of modern genetics (62). Mendelian Dogma dictates a unidirectional transition of traits from parent to child through genes, thereby explaining the transmission of similar traits observed among members of the same family. While genes have been identified among cohorts of youth with diabetes (8) and obesity (63) that support the notion of MetS inheritability, genetic inheritance alone cannot explain the 35% increase in T2D among children and adolescents within a decade (64; 65). Therefore, potential influences formulated by one's surroundings presents a putative explanation for these alarming trends in T2D diagnoses in the U.S. and around the world (66; 67).

This reprogramming in offspring phenotypes in response to internal and external stressors is achieved through changes in the expression of genes. This code switching is managed by modifications at the level of chromatin accessibility – i.e., via DNA methylation, histone modification, and the activities of non-coding RNAs – which exerts control over the transcriptome without revisions to the genetic code itself (68-70). Silencing genes can be executed through cytosine methylation of CpG islands located within promotor regions of DNA (71; 72). DNA accessibility by transcription factors is modulated through chemical modifications to histone

proteins to alter how they bind and organize chromatin, thereby enhancing or repressing transcription of certain genes/gene programs (72). Finally, non-coding RNAs, which are RNA molecules that include long non-coding RNAs and micro RNAs, function in a wide variety of cellular processes that extend beyond the traditional role of mRNA to transport information outside the nucleus (73; 74). These epigenetic mechanisms operate at the intersection of routine environmental stimuli, originating from sources like diet, and individual genetic configurations to manufacture a kaleidoscope of possible phenotypic outcomes.

Dominguez-Salas et al., designed a creative study to assess the critical window when offspring were most susceptible to epigenetic modifications resulting from maternal diet. To do so, they leveraged ethnographically isolated, seasonally unique (maternal) diets that varied significantly in their methyl-donor composition throughout the year (75). In infants born to these rural Gambian mothers who participated, researchers noninvasively collected and compared DNA methylation across multiple offspring tissues to the methyl content present in the maternal diet and relating the associated season/time of year with the date the child was born. They discovered that maternal nutrition in proximity to conception and early pregnancy associated strongest with offspring DNA methylation patterns (75). While a creative approach to examining the gestational timing and interaction of maternal diet and fetal epigenome, chronic exposure to WD and the hormonal and chemical fluctuations associated with it across a genetically diverse population establishes a quagmire of complications that challenge the conclusions drawn by human studies of maternal diet.

Inheritance of Dysfunctional Mitochondria

It is widely accepted that mitochondria and mitochondrial DNA (mtDNA) are homogeneous and maternally inherited (76). As every cell in a human results from a single cell manifested upon conception, all mitochondria are therefore descended from a single population of founder mitochondria occupying one primordial germ cell created during *maternal* embryogenesis (77). Essentially, the entirety of an individual's mitochondria (F2) can be traced back to a single haploid cell generated in their grandmother's (F0) womb. This small but mighty population of mitochondria divide and amplify during maternal oogenesis (78) and folliculogenesis (79). Upon fertilization, this vanguard of mitochondria is gifted to the newly established diploid cell that serves as the precursor for every cell of the future offspring created by this union (80). Therefore,

formation of the primordial (maternal) oogonium and early embryogenesis of the offspring represent critical inflection points when mtDNA content is minimal and mitochondrial capacity to buffer damage or correct mtDNA mutations is suppressed (81), thereby making them particularly vulnerable to adverse environmental inputs (78; 81-83). Such insults during this time can have multigenerational ramifications (13). Subsequent divisions, parceling, and amplification of damage accrued by these predecessor pools of mitochondria transcend the female germline (84), potentially complicating aspects of embryo implantation (83) and fetal growth (85). The variety and magnitude of offspring metabolic outcomes caused by these dysfunctional mitochondria can be augmented or exacerbated by features previously discussed, including hostile intrauterine environments created by nutrient or hormonal stress (86-88).

Potential for Paternal Programming

The prospect of "paternal programming" is most convincingly portrayed by studies that investigate the impact of paternal age (89) and paternal psychosocial and traumatic stress (42; 90; 91) on aberrant offspring neurodevelopment and acquisition of anxiety-like behaviors. The proposed mechanisms through which this occurs involve epigenetic modifications to sperm (91-94) and alterations to components of the seminal fluid that protects and nourishes them (90; 95; 96). While mitochondria in sperm are unable to be transmitted directly to the embryo (97), the energetic investment provided by paternal mitochondria for spermatogenesis, sperm motility and viability, and formulation of seminal fluid are influential factors that impact fetal outcomes (98), albeit in a more indirect fashion (99).

In contrast to the influence of paternal stress on offspring mental health outcomes, strong evidence supporting paternal programming of offspring cardiometabolic dysfunction in the absence of maternal influence is more limited (100-102) and highly contested (103; 104). An interesting study of chronic alcohol exposure in male mice found increased mtDNA copy number and altered transcriptional regulation of mitochondrial oxidative phosphorylation (OXPHOS) pathways in the epididymis of alcohol-exposed males (99). After four weeks of alcohol cessation, mtDNA content remained elevated with ~100-fold increase in the abundance of an antioxidant-specific microRNA (99). While concerning that alcohol-derived biological elements remain in the male reproductive tract of mice one month after alcohol exposure, and while these mitochondrial-related adaptations may diminish sperm quality and viability, the retention of these phenotypes

and subsequent long-term metabolic repercussions following fertilization is unsubstantiated. In contrast to these findings, there is much evidence to suggest that (i) sperm mitochondria are culled by egg-derived mitophagy to prevent the transmission of paternal mitochondria to subsequent generations (105-107) and (ii) the epigenome (nuclear DNA) is reset following fertilization (71). Therefore, more evidence is needed to support the premise that these mitochondrial alterations in sperm persist, in a more meaningful capacity, beyond fertilization to program future offspring health and disease outcomes.

Another rodent study demonstrated that male mice (F1) exposed to maternal (F0) gestational undernutrition can serve as conduits impacting male (F2) offspring body fat, glucose tolerance, and insulin sensitivity (108). Important to note, these phenotypes required male sires (F1) to be crossed with female dams (F1) that were also exposed to early life undernutrition (108). Alternatively, exposure to maternal high-fat diet had a modest increase on female offspring (F3) body weight and length strictly through the paternal F1/F2 lineage (all generations but F0 fed chow diets) (109). In an experiment by Ferey et al., F2 offspring born to male F1 mice from obesogenic pregnancies (i.e., F1 males exposed to intrauterine obesogenic stress) displayed structural abnormalities and mitochondrial defects in cardiac tissue without additional nutrient stress in either F1 or F2 animals (110). In lieu of a direct or casual role in response to paternal programming, these data suggest that paternal contributions to adverse metabolic outcomes in offspring originate from the male's exposure to early life stress, thereby making sires more akin to vectors than "fetal programmers" *per se*. Regardless, more work is required before such findings can be applied within a clinically relevant context.

Early Life Stress & Risk of Cardiometabolic Disease

Maternal Obesogenic Stress

Two-thirds of reproductive-aged U.S. females have overweight or obesity (111). The risk of developing Gestational Diabetes Mellitus (GDM) is two, four, and eight times more likely with overweight, obesity, and severe obesity, respectively (112; 113). Of concern, GDM and obese pregnancies are at higher risk of cesarean delivery, preterm birth, and still birth (112; 114). In contrast to FGR, pregnancies complicated by obesity, GDM, and WD are significantly more likely to result in overgrowth of the fetus, i.e., macrosomia (birthweight greater than 4 kg) or Large for

Gestational Age (LGA, birthweight above the 90th percentile) (115; 116). The presence of excess glucose and lipids in maternal circulation – typical of gestational obesity, GDM, and WD – is hypothesized to mediate this escalation in fetal growth (116). In fact, maternal triacylglyceride (TG) content in early pregnancy has been shown to predict neonatal adiposity (117) which is a strong predictor of childhood obesity and MetS in offspring (118; 119). Maternal TGs, which are 40-50% higher in obese and GDM pregnancies (120), are cleaved by placental lipases (116; 121) prior to their entry into fetal circulation as free fatty acids (FFA). Once FFAs have crossed the placenta, they are stored in the fetus due to insufficient fatty acid oxidation (FAO) capacity (122). This storage of lipid is further exacerbated by the presence of fetal hyperinsulinemia from chronic exposure to maternal hyperglycemia (123). This elevated lipid storage in adipose tissue depots is believed to be responsible for the observed elevations in offspring adiposity (120). Furthermore, this abnormal lipid accumulation also occurs in metabolic organs like fetal liver due to lack of subcutaneous adipose tissue development, thereby promoting development of NAFLD in neonates, infants, and children from obese and GDM pregnancies (124; 125).

Intrauterine metabolic and hormonal stress found in diabetic and obese pregnancies confer an epigenetic fingerprint on fetal and placental tissues (126; 127). Methylation of genes regulating fatty acid oxidation (FAO) and the nutrient stress sensor AMPK was observed in mesenchymal stem cells isolated from umbilical cords (uMSCs) of obese pregnancies (128). These methylation patterns corresponded with functional deficits in FAO and AMPK activity (128). Similar findings in cord blood show DNA methylation of genes involved in lipid metabolism and immune function that correlated with maternal circulating triacylglycerides (TG) and offspring childhood adiposity (129). In rodent models, poor nutrition during gestation also changes gene expression in adipose tissue and skeletal muscle of exposed offspring by modifying chromatin architecture to reprogram pathways involved in glucose uptake and lipid accumulation (130; 131). In baboon placenta and fetal liver, exposure to maternal WD disrupted non-coding micro-RNAs with roles in lipid handling, inflammation, and offspring growth and obesity (132). Notably, these epigenetic changes that influence offspring phenotypic outcomes occurred in the absence of obesity in WD-consuming dams (132).

While it is evident that maternal nutrition programs metabolic phenotypes of different cell types during early life development, there is evidence that it can permanently reprogram cellular identity. Of interest are multipotent stem cells like MSCs with the capacity to differentiate into

different cell types including myocytes (skeletal muscle), adipocytes (fat), and connective tissues (fibroblasts) (133). The fate of MSC commitment is orchestrated by hormonal, nutritional, and inflammatory signals during embryonic and fetal development (133). An appropriate allocation of MSCs toward myogenesis during prenatal development is critical for long-term offspring health. This is because fibrosis and intramuscular lipid accumulation is common with aging (134; 135) and adult obesity/T2D (136; 137). Therefore, redirecting MSCs away from myogenesis in early life – a potential outcome observed in human MSCs from obese pregnancies with heightened adipogenic potential (138) – would restrict the pool of myogenic progenitor cells available to commit to myogenesis to improve future myogenic plasticity. This would restrict skeletal muscle's ability to adapt or mitigate future metabolic stressors, placing offspring at an increased risk of earlier development of MetS.

Maternal Hyperandrogenemia

Polycystic Ovary Syndrome (PCOS) impacts 6-20% of reproductive-aged females, making it the most common endocrinopathy among this demographic (139-141). A hallmark symptom of PCOS is hyperandrogenemia (HA) (142). Importantly, HA is strongly associated with the presence of obesity in pre/peripubertal girls (143; 144) and reproductive-aged women (145; 146). Even in BMI-matched controls, women with HA are more insulin resistant (147; 148) and at a higher risk for developing T2D (149) and CVD (150; 151). It is unknown whether obesity and/or MetS is a cause or effect of HA and HA-associated dysfunction. Like maternal obesogenic exposure in early life, maternal HA during fetal development has been shown to transmit adverse metabolic and reproductive outcomes to offspring (152-157). Symptoms like hyperandrogenism and metabolic dysfunction that are associated with PCOS tend to aggregate within families (158; 159), suggesting a genetic element involved in the heritability of PCOS (160-162). While candidate genes have been identified via family-based and genome-wide sequencing, these "risk" genes increase susceptibility for PCOS but are not causal as they are estimated to account for less than 10% of PCOS heritability observed (141; 163; 164). Therefore, the additional influence of epigenetic modifiers and features of early life environment in combination with these genetic or polygenic susceptibility genes are likely responsible for the reproductive and metabolic phenotypes associated with PCOS (141; 165-167). However, a better understanding of the progression of metabolic dysfunction in insulin sensitive tissues in populations with androgen excess is needed

to understand the etiology of this complicated, heterogeneous endocrine, metabolic, and reproductive disorder.

Skeletal Muscle Insulin Resistance

Insulin signaling determines systemic glucose and lipid homeostasis primarily through the regulation of intermediate metabolism in liver, adipose, and skeletal muscle tissues (168). Loss of insulin action/sensitivity to insulin in these target tissues, i.e., insulin resistance, is a defining feature of obesity and MetS, making it a strong predictor of adult CVD (169-173). The presence of insulin resistance is a predictor of all-cause and cardiovascular mortality in nondiabetic (174-176) and non-overweight (177) populations prior to the development of overt metabolic illness.

In addition to systemic insulin resistance, there is evidence of "selective" or "partial" insulin resistance (178; 179) pertaining to the inhibition of specific arms of the intracellular insulin signaling cascade rather than a global loss of signal transduction. This partial insulin resistance can vary by tissue and is documented in canonical insulin-targeted cells like hepatocytes (180; 181) and also noncanonical insulin-sensitive tissues like the microvasculature (182). This partial insulin resistance has also been observed in human skeletal muscle (183). In a study by Cusi et al., signal transduction through PI3-kinase in response to insulin stimulation was significantly decreased in nondiabetic, obese muscle and essentially absent in T2D muscle (183). Surprisingly, insulin's action through the MAP-kinase pathway in skeletal muscle was consistent across these same groups. The significance of this finding is highlighted by the fact that skeletal muscle accounts for ~80% of insulin-stimulated glucose uptake, a feat that is reduced by 50% with T2D (184). Therefore, the specific loss of metabolic action, i.e., glucose uptake, due to insulin resistance in skeletal muscle is a key contributor to the degeneration of systemic metabolic homeostasis and subsequent development of cardiometabolic illnesses.

Putative mechanisms underlying this loss in muscle insulin signaling involve dysregulated substrate utilization. Specifically, chronic exposure to excess intramuscular lipid content from systemic dyslipidemia, obesity, or consumption of high-fat diets results in the accumulation of toxic lipid intermediates and increased oxidative stress (185; 186). These lipotoxic, bioactive molecules – namely diacylglycerols and ceramides – interfere with insulin signaling to inhibit GLUT4 translocation and subsequent glucose uptake (187-190). This metabolic signature of

elevated cellular stress/damage, loss of insulin signaling, and dramatic reduction in insulin-stimulated glucose uptake seen in muscle from adults with obesity or T2D (184; 191-193) has been replicated in fetal skeletal muscle of nonhuman primates exposed to obesogenic stress *in utero* (194; 195). The mechanisms underlying this phenotype, and whether this programmed muscle insulin resistance persists postnatally, requires further investigation.

Role of Mitochondrial Dysfunction in Metabolic Disease

In both the literal and colloquial sense of the term "powerhouse", mitochondria occupy the central bioenergetic hub of cellular metabolism (196; 197). The mitochondrion fulfills energetic demands while integrating intracellular signals with environmental insults in almost every cell from gametogenesis through the rigors of fertilization and mitosis until their eventual dismemberment, retirement, or imprisonment via mitophagy, apoptosis, or cellular senescence, respectively (77; 198; 199).

In skeletal muscle tissue, mitochondria determine glucose and lipid metabolism (200). The ability of skeletal muscle mitochondria to respond to environmental cues and adapt to adverse cellular conditions is critical for maintaining whole-body energetic flux (201). Diminished mitochondrial abundance or function is intimately tied to the development of insulin resistance and MetS (186; 202). Further elaboration of what "mitochondrial function/dysfunction" means is necessary in describing its role in skeletal muscle insulin resistance. While mitochondrial "oxidative capacity" (i.e., OXPHOS) and mitochondrial "function" are frequently used interchangeably, this modest oversight neglects to acknowledge the battery of other critical metabolic niches and responsibilities fulfilled by the mitochondrial compartment. These roles include mitochondrial network: dynamics (203-205), morphology (206-208), and quality control (209; 210); ROS generation (211; 212) and signaling (213); antioxidant buffering capacity (213; 214); redox balance (215; 216); and ATP production (217) – all features extending beyond the boundaries of maximal OXPHOS capacity that are equally relevant to mitochondrial fitness, vitality, and survival (198; 200).

Discussion surrounding whether mitochondrial insufficiencies, in either function or content, precedes insulin resistance in skeletal muscle or vice versa is highly contested (202; 218-221). The presence of both can be seen in skeletal muscle from adults with obesity or T2D (222-

224). These findings are replicated within the context of DOHaD, as dysfunctional mitochondria are present in skeletal muscle of young, lean human offspring born to parents with T2D (225-229). While the argument could be made that such findings are indicative of genetic inheritance of metabolic dysfunction at the level of insulin signaling and/or skeletal muscle mitochondria, the abundance of confounding factors featured in human studies, e.g., nutrient, hormonal, genetic, and epigenetic variabilities, complicate the interpretation of these findings. Therefore, further investigation providing a more rigorously controlled, chronological timeline reflective of the human lifespan using a model that prioritizes nutritional environment and consistency in nutrient handling, gestational timing of development, and intrauterine environment relative to humans is necessary.

CURRENT GAPS in KNOWLEDGE

Chronic nutrient and hormonal stress during pregnancy generates an adverse intrauterine environment that increases risk of prenatal complications for both the mother and their unborn child. Metabolic dysfunction in offspring observed *in utero* can persist postnatally, increasing their risk for cardiometabolic diseases previously thought to be adult-onset. Unfortunately, critical insight into mechanisms that drive metabolic dysfunction during fetal, juvenile, and adolescent timepoints in human development require invasive procedures, making these research pursuits untenable. Even with the use of indirect, noninvasive approaches, this gap in knowledge is deepened by the inability to regulate important aspects of human lifestyle choices and behaviors in a controlled experimental setting over the exceedingly long period of time required for human growth and development. Therefore, this dissertation aims to assist in bridging this gap in knowledge using a clinically relevant, translational nonhuman primate (NHP) model with *two primary objectives:* **(1)** to assess the persistence of metabolic dysfunction in juvenile and adolescent offspring in response to maternal high-fat, high-sugar diet (Western Diet, WD) consumption prior to and throughout pregnancy/lactation. The influence of a postweaning WD in addition to, or in the absence of, maternal WD will also be evaluated. **(2)** To evaluate skeletal muscle metabolism and insulin sensitivity in young females with chronic hyperandrogenemia with and without diet-induced obesity. Preliminary assessment of how this physiological status translates to fetal skeletal muscle metabolism will also be explored.

OVERARCHING HYPOTHESIS

The overarching hypothesis of this dissertation is that maternal WD will permanently alter skeletal muscle metabolism and muscle mitochondrial function in juvenile and adolescent offspring. These phenotypes will be exacerbated upon weaning to WD. Hyperandrogenemia will diminish skeletal muscle function and drive insulin resistance in young female monkeys. This deficit will be amplified with the addition of WD-induced obesity. Fetal offspring exposed to excess androgens will have reduced muscle function that will be worsened with maternal diet-induced obesity.

SPECIFIC AIMS & HYPOTHESES

AIM #1. To investigate key points of regulation that govern mitochondrial efficiency in offspring skeletal muscle exposed to maternal WD (Chapter III)

Rationale. Oxidative Phosphorylation (OXPHOS) complexes determine mitochondrial efficiency and oxidative capacity. Reduced complex abundance, particularly in complex I (CI), and loss of transporters that traffic metabolites and substrates into the mitochondrion decreases oxidative capacity as seen in tissues from obese humans and rodents. **Hypothesis.** Maternal WD will reduce oxidative capacity in offspring skeletal muscle and will correlate with decreased CI-CV gene expression and complex abundance. Skeletal muscle from offspring exposed to maternal WD will be compared to offspring of lean dams on a healthy control diet with offspring from both groups weaned to either CD or WD. **(a)** Skeletal muscle mitochondrial function will be assessed as rate of oxygen consumption in the presence of lipid or non-lipid substrates. **(b)** Abundance of (i) individual respiratory complex (CI-CV) enzymes, (ii) rate-limiting substrate transporters, and (iii) lipid subspecies and intermediates will be measured in whole muscle tissue. **(c)** Nuclear- and mitochondrial-encoded gene expression of CI-CV subunits will be measured in exposed offspring skeletal muscle.

AIM #2. To investigate whether maternal obesity *in utero* further influences mitochondrial network dynamics in skeletal muscle of offspring weaned to WD (Chapter IV)

Rationale. Mitochondrial network quality is maintained through tightly regulated fusion (merging) and fission (dividing) events in response to environmental signals. Mitochondrial networks also maintain interactions with the Endoplasmic Reticulum (ER) at Mito-ER associated membrane (MAM) junctions where phospholipid precursors are integrated into the mitochondrial membrane. Instances of mitochondrial damage from chronic oxidative stress and lipotoxicity compromise MAM-contacts and fragment mitochondrial networks as seen in obese and diabetic muscle. Skeletal muscle from offspring weaned to WD with and without exposure to maternal WD-induced obesity will be compared to offspring of lean dams weaned to control diet. **Hypothesis.** Maternal obesity will exaggerate mitochondrial network fission and reduce markers of MAM junctions in muscle of offspring weaned to WD. **(a)** Protein abundance of mitochondrial fission/fusion machinery and network quality control markers will be measured in offspring

muscle. **(b)** MAM contacts will be determined by measuring: (i) markers localized at MAM junctions, (ii) mito DNA copy number and (iii) mitochondrial membrane lipids originating from the ER.

AIM #3. To investigate how chronic hyperandrogenism with and without obesity impacts skeletal muscle metabolism in young females and exposed fetal offspring (Chapter VI)

Rationale. Polycystic Ovary Syndrome (PCOS) is the most common endocrine disorder in premenopausal females and is associated with increased rates of MetS and risk for CVD. Previous work has shown that hyperandrogenemia (HA) and obesity, both phenotypes associated with PCOS, impact metabolism in a tissue-specific manner. Fetal offspring exposed to maternal PCOS display signs of altered metabolism. The additional impact of HA with and without WD-induced obesity on skeletal muscle physiology in young females will be measured after 2-years of treatment. The metabolic impact of these maternal phenotypes on fetal skeletal muscle will also be investigated. **Hypothesis.** HA combined with obesity will decrease oxidative capacity and insulin sensitivity in female skeletal muscle more than either treatment alone. Fetal muscle oxidative capacity will be lowest in offspring of gestational HA+WD. **(a)** Skeletal muscle metabolism in young females will be characterized by: (i) oxidative capacity and (ii) insulin signaling in response to glucose *in vivo*. **(b)** Oxidative capacity will be measured in fetal offspring skeletal muscle.

II. EXPERIMENTAL PARADIGM: MATERNAL WESTERN DIET

MODELS of MATERNAL NUTRIENT STRESS

Research on human pregnancy and embryonic, fetal, and neonatal development can be sensitive. Necessary moral and ethical considerations prevent the use of invasive techniques on pregnant individuals and their young, newborn, or unborn child. Relatedly, the inclusion of necessary experimental controls over human lifestyle and behaviors is improbable for long-term, scientifically rigorous studies – especially regarding nutrition and diet patterns. Participant withdrawal from longitudinal studies further complicates these endeavors. For these reasons, animal models have proven to be an indispensable tool to better understand human health and disease.

Every animal model system is characterized by a unique combination of strengths and limitations that determine whether it is the appropriate means to answer the question at hand. In perinatal studies, rodents are relatively quick breeders, inexpensive, and manageable (230). Transgenic manipulation of mouse models provides a powerful approach to determine the importance of specific genes at the cellular, tissue, and physiological/systemic levels. Genetic manipulation can be executed at specified periods during development (i.e., inducible) and in a tissue(s)-specific manner. While transgenic rat models are less common, more ubiquitous rat strains like Sprague-Dawley and Wistar are outbred, more docile, larger, and more resistant to environmental insults than mice (231). Like rodents, rabbits are affordable, easy to breed, but have lipid metabolisms (232; 233) and placentation that more closely resemble that of humans (234). Unlike humans, rabbits and rodents are polytocous with multiple embryos/fetuses per pregnancy (230). Sheep are closer in size to humans, have a longer gestational period (five months), and can undergo invasive surgical catheterization during pregnancy that allow for repetitive sampling from fetal and maternal circulation, making them the primary source of translatable knowledge in placental development and function in its role on fetal physiology (e.g., IUGR/FGR) (235). Discrepancies in the anatomy of the digestive system and glucose metabolism in ruminant animals like sheep limit their capacity to recapitulate maternal hyperglycemia and/or intrauterine

obesity/WD consumption on fetal developmental outcomes (230). Unlike sheep, pigs are omnivorous with digestive tracts more akin to humans, making nutrition studies in pigs more readily translatable to human health (236; 237). However, human placental development is more accurately modeled by rabbits than pigs or sheep (230). In summary, while no animal perfectly models all aspects of human development, health, or disease, the utilization of different models to probe various aspects of human anatomy and physiology has promoted the advancement of human biomedical sciences in a manner that would be unattainable via human research alone.

DEPICTION of the JAPANESE MACAQUE

To date, animal models have provided consistent and reliable insight into the epidemiology of metabolic diseases resulting from early-life exposures to maternal WD, obesity, and GDM (238). To build upon this knowledge, our group at the Oregon National Primate Research Center (ONPRC) established a nonhuman primate (NHP), Japanese macaque model of fetal development in response to maternal obesogenic diet consumption starting 2-8 years before mating, during conception, and throughout pregnancy and lactation (239). Japanese macaques have similar placental (240), pancreatic islet (241), and neural (242; 243) developmental trajectories relative to humans, making them a readily translatable model of DOHaD (16). To this end, the Japanese macaque mimics key aspects of human nutrient handling, gestational timing of development, and intrauterine environment while allowing the necessary degree of nutritional control over an extended period in both dams and their offspring. By characterizing maternal metabolic phenotypes, as well as offspring physiology and anatomy in key tissues during fetal and juvenile timepoints of development (~14-months and ~40-months, respectively), the Japanese macaque allows critical, chronological insight into potential mechanisms that drive adverse cardiometabolic outcomes in offspring exposed to early life obesogenic stress.

Important to note: approximately one-third of dams chronically consuming WD remained lean and insulin sensitive (244-246). This resistance to diet-induced obesity and insulin resistance is reflective of variations in human sensitivity/resistance to the development of obesity (247; 248), making this NHP system a clinically relevant and translatable model of maternal WD stress, independent of maternal obesity or insulin resistance, on offspring metabolic outcomes.

Previous Findings in Japanese macaque

Prior work in this model support the observation that exposure to an obesogenic gestational environment alters offspring metabolism (249-251), neural development (252) and behavior (242; 253; 254). Tissues displaying altered structure or function in response to maternal obesity and WD include the liver (239; 245; 255; 256), pancreas (241; 257-259), vasculature (260), and microbiome (261). Previously, our lab has found decreased mitochondrial efficiency (194) and insulin stimulated glucose uptake (195) in fetal muscle exposed to maternal WD and obesity. The loss in mitochondrial function could not be reversed at the fetal stage of development by switching obese mothers to a healthy control diet prior to pregnancy with exposure to WD in the absence of obesity *in utero* displaying an intermediate phenotype in fetal muscle of these offspring (194). The retention of these phenotypes seen in skeletal muscle mitochondrial function after gestation, i.e., during childhood, is unknown. Furthermore, the potential to reverse mitochondrial dysfunction in fetal muscle by weaning offspring to a healthy postweaning CD has not been investigated in this model.

PROJECT DESIGN

Adult Japanese macaques housed in indoor/outdoor pens were maintained on CD (Monkey Diet no. 5000; Purina Mills) or WD (TAD Primate Diet no. 5LOP, Test Diet, Purina Mills) fed *ad libitum* for up to 7 years prior to pregnancy as previously described (29; 194; 195). WD represents a typical Western diet with respect to percent of caloric contribution from fat and saturated fat content (Table 2.1). Carbohydrate content differed between the two diets, with sugars (mainly sucrose and fructose) constituting 19% of WD but only 3% CD (Table 2.1). Monkeys on the WD were also given calorically dense treats (35.7% of calories from fat, 56.2% of calories from carbohydrates, and 8.1% of calories from protein) once daily.

A subset of adult females consuming WD remained lean based on percentage body fat obtained by dual-energy X-ray absorptiometry (DEXA). Lean (Ln) was defined as body fat less than 25% (~2 SD above baseline mean) and obese (Ob) as body fat greater than 30%. Offspring were born naturally to Ln/CD, Ln/WD, or Ob/WD mothers and remained in their home colony until weaning. Infants begin independent ingestion of the maternal diet at ~4 months old and were

consuming this diet as their primary food source by 6 months of age. At 7-8 months of age, juvenile offspring were weaned to new group housing with 6–10 similarly aged juveniles from both maternal diet groups and 1–2 unrelated adult females. Offspring either continued consuming the same maternal diet after weaning or were switched to the other diet style. Offspring were maintained on this postweaning (pw) diet for ~30-months (Aim #1) or ~7 months (Aim #2), at which time skeletal muscle tissues were collected.

Aim #1

Aim #1 will investigate how maternal WD, independent of obesity or insulin resistance, during pregnancy and lactation impacts adolescent 3-year-old offspring skeletal muscle metabolism. Additionally, this study will assess whether a postweaning (pw)CD is a viable intervention to improve disparate metabolic outcomes in the skeletal muscle of offspring exposed to early life WD stress. Offspring measures of interest will include anthropometric and glucose homeostatic outcomes, mitochondrial oxidative capacity (OXPHOS), OXPHOS gene expression/protein abundance, skeletal muscle lipidome profile, and markers of oxidative stress.

Aim #2

Aim #2 will pursue the impact of pwWD with and without early-life obesogenic exposure on underlying mitochondrial network dynamics in 1-year-old juvenile offspring skeletal muscle. Anthropometric measures, glucose/insulin homeostasis, and mitochondrial lipidome and networking dynamics will be interrogated in the pursuit of better understanding of how offspring pwWD impacts metabolic predisposition for skeletal muscle mitochondrial dysfunction, both independently and in conjunction with early life exposure to obesogenic stress.

III. AIM #1

A MATERNAL WESTERN-STYLE DIET IMPAIRS SKELETAL MUSCLE LIPID METABOLISM in ADOLESCENT JAPANESE MACAQUES

Previously published material:

Greyslak KT, Hetrick B, Bergman BC, Dean TA, Wesolowski SR, Gannon M, Schenk S, Sullivan EL, Aagaard KM, Kievit P, Chicco AJ, Friedman JE, McCurdy CE: A Maternal Western-Style Diet Impairs Skeletal Muscle Lipid Metabolism in Adolescent Japanese Macaques. Diabetes 2023;72:1766-1780.

INTRODUCTION

Intrauterine exposure to maternal obesity, diabetes, or a poor-quality diet (i.e., Westernized high-fat, high-sugar diet [WD]) during development is associated with increased risk for cardiometabolic diseases in youth including insulin resistance, nonalcoholic fatty liver disease, cardiovascular disease, and type 2 diabetes (16; 262). Skeletal muscle is a principal regulator of insulin sensitivity and metabolic homeostasis, accounting for the majority of systemic fatty acid oxidation and insulin-mediated glucose disposal (184; 263). As such, metabolic dysregulation in muscle, in part due to reductions in mitochondrial mass and function, is a primary contributor to the development and progression of metabolic diseases in adults (186; 202; 224; 264). Specifically, skeletal muscle insulin resistance has been associated with reduced mitochondrial abundance, less oxidative phosphorylation (OXPHOS) capacity, blunted lipid oxidation, increased de novo synthesis of bioactive fatty acid species (e.g., diacylglycerides [DGs], ceramides) and/or greater reactive oxygen species (ROS) production in adults (184; 212; 225) with reduced mitochondrial function observed in overweight children (265). Similar markers of metabolic dysregulation including reduced oxidative capacity, altered gene expression, and development of insulin resistance have also been observed in skeletal muscle of adult offspring exposed to maternal obesity in rodents (13; 266-268). Of concern, metabolic dysregulation is already found in mesenchymal stem cells isolated from umbilical cords of infants born to women with obesity

(128). However, few studies have evaluated whether maternal (m)WD in the absence of obesity or insulin resistance induces changes in offspring skeletal muscle.

Previous studies in our established Japanese macaque model of WD-induced maternal obesity identified metabolic dysregulation in multiple tissues of fetal and juvenile offspring (194; 239; 245; 255; 258; 261; 269) including reduced insulin sensitivity in skeletal muscle (195) and decreased oxidative metabolism in fetal muscle (194). In this model, we have consistently observed that chronic WD consumption induces obesity and insulin resistance in the majority of, but not all, adult females (270). Leveraging this unique subset of lean and insulin- sensitive dams, we tested whether a WD chronically fed to lean, insulin-sensitive dams during pregnancy and lactation would result in a persistent impairment in offspring skeletal muscle OXPHOS capacity and lipid metabolism. We also evaluated whether weaning offspring exposed to mWD onto a healthy chow diet (postweaning [pw]CD) would attenuate programmed effects at 3 years of age (i.e., early adolescence).

METHODS

Animals

All animal procedures were conducted under regulatory compliance at the Oregon National Primate Research Center (ONPRC) and Oregon Health & Science University, which is accredited by the Association for Assessment and Accreditation of Laboratory Animal Care (AAALAC) International. Experiments were designed and reported with reference to the Animals in Research: Reporting In Vivo Experiments (ARRIVE) guidelines (271).

Experimental Design

Adult Japanese macaques were housed in indoor/outdoor pens and fed a CD (15% of calories from fat primarily from soybeans and corn, monkey diet no. 5000; Purina Mills) or WD (37% of calories from fat primarily from corn oil, egg, and animal fat, no. 5LOP, TAD Primate Diet; Test-Diet and Purina Mills) ad libitum. Carbohydrate content differed between diets, with sucrose and fructose constituting 19% of WD but only 3% of CD. Females consumed WD for 1–3 years prior to and during the pregnancy from which offspring were studied. Maternal prepregnancy demographics are presented by offspring cohort in Supplementary Table 1. More extensive phenotyping of the

adult female macaques has previously been described (272). All births were singleton and delivered vaginally after spontaneous labor. Offspring remained in their home colony until weaning at 7–8 months of age, when they were grouped with 6–10 similarly aged juveniles from both maternal diet groups and 1–2 adult females. These new social housing groups were fed either CD orWD.

Offspring from 17 mCD dams and 17 mWD dams were included in this study. The offspring groups include 13 mCD/pwCD (8 female [F], 5 male [M]), 6 mCD/pwWD (2 F, 4 M), 13 mWD/pwCD (5 F, 8 M), and 9 mWD/pwWD (5 F, 4 M). No more than two offspring from the same dam were included in any offspring group per analysis. If two offspring from the same dam were included in the same group, offspring were of the opposite sex. Offspring sex is indicated in figures with use of different symbols.

Offspring Anthropometric Measures

Nonfat mass, fat mass, lean mass, and bone mineral content were measured with DEXA in offspring <1 month prior to necropsy as previously described (258). Offspring body mass, retroperitoneal fat pad mass, crown rump length, and subscapular skin fold thickness were measured at necropsy.

Offspring Intravenous Glucose Tolerance Testing

Intravenous glucose tolerance tests (i.v. GTT) were conducted within 2 months prior to offspring necropsy (at 36 months of age) as previously described (195; 258). Baseline blood samples were obtained prior to the infusion and at 1, 3, 5, 10, 20, 40, and 60 min after infusion. Glucose was measured immediately with OneTouch Ultra blood glucose monitor (LifeScan), and the remainder of the blood was kept in heparinized tubes on ice for insulin measurement. After centrifugation, samples were stored at -80°C until assayed. Insulin measurements were performed by the Endocrine Technologies Core at ONPRC using a chemiluminescence-based automatic clinical platform (cobase 411; Roche Diagnostics, Indianapolis, IN). HOMA of insulin resistance (HOMA-IR) was calculated from fasting insulin and glucose values with the following formula: (insulin (mU/L) * glucose (mg/dL))/405.

Offspring Activity Monitoring

Physical activity was continuously monitored in group housed offspring with Actical accelerometers (Mini Mitter, Bend, OR) affixed to loose-fitting plastic collars (Primate Products, Miami, FL) as previously described (252). These monitors record the total number of activity counts, detected as changes in acceleration in all directions per minute. Activity count data over a 1-month period preceding necropsy are reported as average counts per hour for 24-h and 12-h day and night activities. All data were collected in late spring or early summer to control potential seasonal variability.

Offspring Necropsy Collection

Animals were sacrificed as previously described (252; 254; 256) between 37 and 40 months of age. Blood was collected in appropriate tubes for later analysis of insulin, triglycerides, and cholesterol and stored at -80°C for batch analysis by Endocrine Technologies Core at ONPRC. Skeletal muscles including gastrocnemius (gastroc), soleus, vastus lateralis, and rectus femoris were rapidly dissected of fascia and portions were either flash frozen in liquid nitrogen or transferred to a biopsy preservation solution (BIOPS) and shipped overnight for respirometry experiments. Frozen muscle was stored at -80°C until analysis.

Protein Analysis

Frozen gastroc and soleus muscles (50–100 mg) were homogenized mechanically in 0.6 mL buffer (195) with six 2.8-mm ceramic beads (VWR International) in a Bead Ruptor (OMNI International, Kennesaw, GA) at a rate of 6 m/s for 2 × 30 s intervals kept at 4°C with a cryo-cool instrument adaptor. Homogenate was then rotated for 1 h at 4°C on an orbital platform and then centrifuged at 13,000g for 15 min at 4°C. Protein concentration was determined with a BCA kit (Pierce and Thermo Fisher Scientific). Protein abundance was analyzed by capillary immunoassay on a Wes instrument per manufacturer instructions (ProteinSimple, Bio-Techne; San Jose, CA) with 3 mL of 0.25 or 1.25 mg/mL of sample. Antibody concentrations were optimized and multiplexed with target protein abundance quantified with Compass software (ProteinSimple, Bio-Techne) and normalized to a loading control protein. For OXPHOS analysis, abundance of individual complexes was normalized to an internal fluorescent loading control. Equal loading of total protein in soleus and gastroc homogenate was also measured with Stain-Free technology (Bio-Rad Laboratories, Hercules, CA) (Supplementary Figs. 1 and 2). Traditional Western blot was used to

measure HADHA and was normalized to GAPDH, as previously described (194). Data were analyzed with Image Lab 5.2 software (Bio-Rad Laboratories). Primary and secondary antibody information can be found in Supplementary Table 2.

Citrate Synthase Activity Assay

Frozen gastroc and soleus muscles (20 mg) were homogenized in 0.7 mL buffer and enzyme activity was measured by spectrophotometry as previously described (194).

Muscle Lipid Analysis

Frozen offspring gastroc (50 mg) was dissected of extramuscular adipose tissue and fascia, lyophilized, weighed, and homogenized in 0.9 mL high-performance liquid chromatography–grade water. Homogenate (0.75 mL) plus methyl tert-butyl, as an internal lipid standard, was added to 0.9 mL methanol, and lipid species were serially extracted (194; 273; 274). Skeletal muscle lipid abundance and composition were analyzed with liquid chromatography–tandem mass spectrometry as previously described (273; 274).

Permeabilized Muscle Fiber Bundle Preparation & Respirometry

Mitochondrial respiratory function was measured in permeabilized muscle fiber bundles (PMFBs) with high-resolution respirometry with an Oxygraph-2k system (Oroboros Instruments, Innsbruck, Austria). Muscles fiber bundles (3–5 mg) were dissected from gastroc and soleus and then permeabilized with 30 mg/mL saponin in BIOPS for 30 min, washed, blotted dry, and weighed. All respirometry data were collected at 37°C in a super-oxygenated environment (200–400 mmol/L O2), and two titration protocols were run in parallel to measure respiration with lipid and nonlipid substrates as previously described (194). Mitochondrial integrity was confirmed by measurement of respiratory responses to cytochrome c.

Gene Expression

RNA was isolated from frozen gastroc and soleus (25 mg) with Direct-zol RNA MiniPrep kits (Zymo Research, Irvine, CA). cDNA was synthesized from extracted RNA with qScript cDNA Synthesis Kit from Quantabio (Beverly, MA) in a thermal cycler (Eppendorf, Enfield, CT). Expression of target genes were measured with PerfeCTa SYBR Green FastMix (Quantabio) using

a CFX384 PCR Detection System (Bio-Rad Laboratories). Gene expression was normalized to the geometric mean of three housekeeping genes, and fold change was calculated with DDCt analysis (275). Primer sequence, efficiencies, genome of origin, and experimental conditions per target/control genes can be found in Supplementary Table 3.

Lipid Peroxidation

Malondialdehyde (MDA) was measured in gastroc (50 mg) with a commercially available kit (no. 700870; Cayman Chemical) according to the manufacturer's protocol and as previously described (194). Briefly, sample reaction mixture was loaded in duplicate onto a 96-well plate with standards and measured fluorometrically. MDA concentration is expressed relative to protein content.

Protein Carbonylation

Protein carbonyl content in gastroc (40 mg) was measured with a commercially available kit (ab126287; Abcam) per the manufacturer's instructions. Sample homogenate was loaded in duplicate onto a 96-well plate, and data were normalized to total protein content of reaction mixture with the BCA method.

Statistical Analysis

Individual-sample data points with group minimum, maximum, median, and interquartile range are graphed. We calculated sample size using variance from previously published fetal muscle respirometry data, a primary outcome for the current study. For detection of a medium effect size with a = 0.05 and 80% power, this study requires 11 offspring (n) for main effects (i.e., m diet or pw diet). Using a factorial design, we tested for interactions of sex by treatment [i.e., m or pw diet] in main outcome measures as previously described (276)) (Supplementary Tables 4 and 5). Sexes were combined when no interactive effect of sex was identified. In subsequent analysis, data were analyzed with a two-way ANOVA for fixed effects of m diet and pw diet, and the interaction (m diet × pw diet). When significant main effects or interactions were identified, a Sidak post hoc analysis was used to test for significance within subgroups. Significant main effects ($p < 0.05$) are listed above each graph. For post hoc analysis, carets (^) indicate significant differences between m diets within the same pw diet group, while asterisks (*) indicate significant differences between pw diets within the same m diet group. An unpaired t test was used to compare data sets with only

two groups. OXPHOS and VDAC protein abundance were correlated to oxidative stress markers (protein carbonylation and/or lipid peroxidation content) in the following groupings: all offspring, all mCD offspring, and all mWD offspring. All *P* values for OXPHOS (CI–CV and CI+III) protein abundance and lipid peroxidation were adjusted for multiple comparisons with Bonferroni correction (Supplementary Table 6). All analyses were completed with Prism 9.2 software (GraphPad).

RESULTS

Adolescent Offspring Physiology is Altered by mWD and pwWD

At 3 years of age, offspring body weight, nonfat mass, and crown-rump length were not different by group (Table 3.1). Surprisingly, total fat mass was reduced in offspring consuming pwWD (Table 3.1). Despite less total fat mass, retroperitoneal fat mass and subscapular skinfold thickness were significantly higher with pwWD, mirroring shifts in body fat distribution typically associated with poorer insulin sensitivity (277). Average daily activity in mWD offspring was significantly greater than mCD, with mWD/pwWD having the highest activity counts (Table 3.1). There was also an observed increase in activity with pwWD in both groups that did not reach statistical significance ($p = 0.08$). These data suggest that greater physical activity levels may contribute to reduced total fat mass but do not protect against metabolically unfavorable visceral fat accumulation, especially in mWD offspring.

Insulin sensitivity and glucose metabolism were impacted by both m and pw diet. Fasting glucose was not different, but fasting insulin was significantly increased by pwWD and to a greater extent in mCD/pwWD offspring (Table 3.1). During an i.v. GTT, total insulin area under the curve (AUC) was significantly higher in offspring consuming pwWD (main effect, pw diet, $p = 0.008$). However, when accounting for higher fasting insulin concentrations, we observed a main effect of m diet ($p = 0.03$) with higher insulin AUCs calculated from baseline in mWD offspring (Table 3.1), suggesting that mWD may increase peripheral insulin resistance as seen at younger ages (195) requiring greater insulin response. The higher insulin AUC measured may also account for the lower glucose AUC observed in offspring consuming the pwWD. Calculation of HOMA-IR indicates increased insulin resistance with pwWD that is higher in offspring from mCD compared with mWD. Lastly, fasting total cholesterol was significantly increased with pwWD, driven by

increases in both HDL and LDL cholesterol (Table 3.1). There was no difference in offspring fasting triglycerides by m or pw diet.

Persistent Reduction in Muscle Oxidative Capacity in Offspring Exposed to mWD

Skeletal muscle mitochondrial function and/or abundance is strongly associated with systemic insulin sensitivity (202). We previously reported reduced OXPHOS in PMFBs and differentiated myocytes isolated from fetal skeletal muscle exposed to maternal obesity and mWD (194). Here, we examined whether these adaptations persist into adolescence. To address potential muscle-specific differences, we interrogated substrate-specific respiration (i.e., with and without lipids) in the presence of saturating ADP in both the soleus, a highly aerobic muscle with majority type I fibers, and the gastroc, a mixed fiber–type muscle. In the soleus, rates of fatty acid oxidation with palmitoylcarnitine were impacted by m and pw diet (interaction, $p = 0.04$) such that in the case of mWD fatty acid oxidation was lower for pwCD versus pwWD—with the opposite pattern of response in mCD offspring (Fig. 3.1A and Supplementary Fig. 3.3A). However, after the addition of pyruvate (Fig. 3.1B), respiration was lower with mWD to a similar extent in both pw diet groups (main effect, m diet, $p = 0.002$). Similarly, maximal CI- and CI+CII-linked respirations were also lower in mWD offspring in the presence of palmitoylcarnitine, with greater reduction in mWD/pwCD offspring (Fig. 3.1C and D). However, in the absence of palmitoylcarnitine, maximal CI-linked respiration was not different between mWD and mCD (Fig. 3.1E and Supplementary Fig. 3.3B), indicating that the presence of long-chain acylcarnitine limited flux of convergent substrate oxidation pathways at CI in mWD groups (Fig. 3.1C and D). Indeed, when succinate was added (contributing electrons downstream of CI) the maximal CI+II-supported respiration rate in the absence of fatty acids was similar between mCD and mWD offspring and higher in mWD/pwWD than in mWD/pwCD (Fig. 3.1F). Finally, soleus citrate synthase activity, a marker of mitochondrial content, was not different by group (Fig. 3.1G), further suggesting that mWD impacts the capacity of skeletal muscle to integrate oxidation of fatty acids with other substrates rather than suppressing total oxidative capacity.

In the gastroc, fatty acid oxidation capacity was again lower in mWD offspring on the pwCD (Fig. 3.1H and Supplementary Fig. 3C). Like in the soleus, CI-linked respiration rates in the gastroc supported by subsequent titrations of pyruvate and glutamate were lower in mWD compared with mCD offspring in the presence of palmitoylcarnitine (main effect, m diet [Fig. 3.1I

and J]) but similar across groups after addition of succinate (Fig. 3.1K), and with all substrates in the absence of palmitoylcarnitine (Fig. 3.1L and M and Supplementary Fig. 3D). Again, citrate synthase activity was also similar across groups (Fig. 3.1N). These data indicate that early-life programming by mWD decreases the capacity of muscle to oxidize a combination of metabolic substrates, particularly through CI, when high concentrations of fatty acid are present.

mWD Reduces OXPHOS Enzymes in Exposed Offspring

As a potential mechanism for reduced respiratory capacity in mWD-exposed offspring, we measured the enzymes responsible for mitochondrial OXPHOS. In the soleus, mWD had a main effect to reduce the abundance of subunits in all five OXPHOS complexes while pwWD had a main effect to increase complex abundance. The increase in OXPHOS complexes in the soleus parallels the observed increase in activity levels with pwWD. In pairwise comparisons, CI, CIV, and CV abundance were significantly reduced with mWD compared with mCD in offspring on the pwWD, while CII and CV were significantly reduced with mWD in both offspring pw diet groups (Fig. 3.2A–G). In contrast, there was no main effect of mWD on expression of electron-transferring flavoprotein (ETF) or ETF dehydrogenase (ETFDH), which coordinate electron transfer from fatty acid b-oxidation to the respiratory chain downstream of CI (Fig. 3.2F and G). In pairwise comparisons, pwWD increased CIV in mCD offspring and increased CV in both mCD and mWD offspring (Fig. 3.2D and E). Additionally, there was a main effect of pw diet to increase ETF and ETFDH, with a significant increase in ETF in the mWD group by pairwise comparison (Fig. 3.2F and G).

Similar to the soleus, there was a main effect of mWD to decrease the expression of all five OXPHOS complex proteins in the gastroc (Fig. 3.2I–M) but not ETF or ETFDH (Fig. 3.2N and O). Pairwise comparisons revealed lower expression of CII through CIV in mWD/pwCD groups (Fig. 3.2I–L) and reduced CV in both pw diet groups (Fig. 3.2M). In contrast to the soleus, there was no significant main effect of the pw diet on OXPHOS complexes or ETF/ETFDH proteins in the gastroc. Taken together, these data indicate that mWD reduces offspring skeletal muscle expression of respiratory chain complexes but not ETF/ETFDH. This shift may favor a greater flow of electrons from fatty acid b-oxidation to ubiquinone relative to CI and CII in mWD versus mCD offspring, perhaps explaining the partial inhibition of CI- and CI+II-dependent oxidative capacity during convergent palmitoylcarnitine oxidation.

Transcriptional Regulation of OXPHOS in Response to WD

To test whether reductions in OXPHOS proteins in mWD offspring were due to difference in gene transcription, we evaluated the expression of genes that code for subunits of CI–CV from both the mitochondrial and nuclear genomes in soleus and gastroc. In the soleus, COXII (CIV, mitochondrial genome) and UQCRC2 (CIII, nuclear genome) expression was greater with pwWD with post hoc analysis showing a significant increase in UQCRC2 between pw diet in mWD offspring (Fig. 3.3C and G). Only the nuclear encoded gene for CI, NDUFB8, had a main effect of m diet with a significant decrease in expression in mWD compared with mCD offspring on pwCD (Fig. 3.3E). In the gastroc, neither mitochondrial nor nuclear encoded OXPHOS genes are significantly impacted by m or pw diets (Supplementary Fig. 4). Although modest, the alterations in gene expression recapitulate patterns observed in the protein abundance of the mitochondrial complexes but do not fully explain either the downregulation of OXPHOS abundance, particularly in the gastroc, nor the subsequent reduction in oxidative capacities in offspring exposed to mWD and pwWD.

m and pw Diets Alter Muscle Acylcarnitine Accumulation but Not Lipid Transport or Oxidation Enzyme Abundance

Given the impact of m diet on lipid-associated oxidative capacity in offspring gastroc without reduced ETF or ETFDH abundance (Fig. 3.2N and O), we next measured upstream regulators of lipid trafficking and b-oxidation. There was no difference in the abundance of two key b-oxidation enzymes, very-long-chain acyl-CoA dehydrogenase (VLCAD) or hydroxyacyl-CoA dehydrogenase a (HADHA) (Fig. 3.4A and B), by m or pw diet. There was also no difference in the abundance of the inner or outer mitochondrial membrane (OMM) long-chain fatty acid transporters, CPT1b or CPT2, respectively (Fig. 3.4C and D). Although b-oxidation and lipid transport enzymes were not different, the abundance of intramuscular acylcarnitines was significantly different by pw and m diet, suggesting potential differences in activity and/or lipid transport. Specifically, medium- and long-chain acylcarnitines, C10, C12, C14, C16:1, C18, and C18:1, were much lower with a pwCD in mWD offspring (Supplementary Table 6). Short-chain acylcarnitines, C4 and C6, (main effect, m diet) as well as the unsaturated long-chain

acylcarnitines, C18:2 and C18:3 (interactive effect), were also less concentrated with pwCD in mWD compared tomCD offspring.

AMP-activated protein kinase (AMPK) and acetyl-CoA carboxylase (ACC), key enzymes involved in nutrient sensing and metabolic fuel use, showed a significant decrease in abundance in mWD compared with mCD offspring when consuming pwWD (Fig. 3.4E and F). Phosphorylation of AMPK and ACC were not different (Fig. 3.4G and H). Lastly, PGC1a abundance, a master regulator of mitochondrial metabolism and biogenesis, was not different across groups (Fig. 3.4I).

Prior Exposure to mWD Exacerbates Accumulation of Lipid Metabolites Associated with Muscle Insulin Resistance

Since the shift in the abundance and composition of intramyocellular lipids is associated with muscle insulin resistance (188; 273; 278), we examined the lipid composition and abundance in offspring gastroc. As expected, the abundance of individual triacylglyceride (TG) species and total TGs (Fig. 3.5A and B and Supplementary Table 7) increased with pwWD. The composition of the TG pool also changed with pwWD with an increased accumulation of more saturated and shorter-length TGs (Fig. 3.5A). This shift in TG saturation was exacerbated in mWD offspring with a fivefold greater accumulation with pwWD relative to pwCD animals (Fig. 3.5C). The abundance of total DGs, including both 1,3-DGs (derived from intramuscular TG lipolysis) and 1,2-DGs (a product of de novo synthesis and phospholipid degradation) (Fig. 3.5K), was dependent on both the m and pw diet (interaction, $p = 0.04$). Within mCD offspring, total DGs were lower with pwWD, while the pattern was reversed for mWD offspring (Fig. 3.5D). However, the percent of 1,2-DGs (Fig. 3.5E) and the percent of saturated 1,2-DGs (Fig. 3.5F) was significantly elevated by pwWD in both m groups. Interestingly, the greater difference in the pool of 1,2-AGs and saturated 1,2-DAGS in mWD offspring was not driven by greater accumulation with pwWD but, rather, was due to reduced content in mWD/pwCD offspring, which have the lowest amount of these intramuscular lipid species (Fig. 3.5C, E, and F). Total ceramide, saturated ceramide, and total sphingomyelin (SPM) content were not different by m or pw diet (Supplementary Fig. 3.5A–C). However, saturated SPM, specifically SPM C18:0, and the upstream metabolite ceramide C18:0, a lipid species associated with insulin resistance (188), were most abundant in mWD offspring on pwWD (Fig. 3.5G–I). The abundance of ceramide C16:0 was not increased with either diet,

indicating specificity rather than global enrichment of saturated fatty acids (Fig. 3.5J). Together, these data suggest that mWD leads to persistent change in lipid handling and metabolism in offspring muscle that is dependent on pw diet; mWD/pwCD offspring have decreased content and mWD/pwWD offspring have equal or higher amounts of saturated TGs and DGs relative to pw-matched controls. The increased accumulation of specific bioactive lipid species—namely, saturated SPM, SPM C18:0, and ceramide C18:0—in response to pwWD may contribute to an earlier decline in skeletal muscle insulin sensitivity (Fig. 3.5K).

Oxidative Stress Linked to CI and VDAC1 Abundance in Muscle from Offspring with Prior Exposure to mWD

Reduced mitochondrial function is often associated with greater oxidative damage and impaired insulin sensitivity (212; 279). We previously observed elevated markers of oxidative stress in fetal muscle from offspring of obese dams on mWD (194). Therefore, we assessed markers of oxidative stress in adolescent offspring skeletal muscle. Surprisingly, MDA, a marker of lipid peroxidation, was reduced with mWD (main effect, m diet) in gastroc (Fig. 3.6A). Similarly, protein carbonylation, a marker of oxidative stress that is not influenced by membrane lipid saturation, was also reduced with pwWD in mWD offspring (Fig. 3.6B). We next measured the voltage-dependent anion channel (VDAC1/2) abundance, an outer mitochondrial membrane transporter associated with ROS release (280). VDAC1/2 abundance was significantly lower in mWD offspring compared with pw diet–matched mCD offspring (Fig. 3.6C and D). Indeed, VDAC abundance was approximately fourfold lower in mWD/pwWD offspring relative to mCD/pwCD offspring muscle despite no differences observed in citrate synthase activity (Fig. 3.1N). VDAC2 was not different, indicating a VDAC1-specific downregulation in mWD offspring (Fig. 3.6D).

Correlation analysis was performed for assessment of relationships between markers of oxidative stress and VDAC and OXPHOS abundance in offspring muscle. We found a significant positive linear relationship between VDAC1/2 and MDA ($R2 = 0.3$, $p < 0.002$) or protein carbonylation concentration ($R2 = 0.3$, $p < 0.009$) across all offspring (Fig. 3.6E and G) with significant relationships maintained in mWD offspring (Fig. 3.6F and H). We also found a positive linear relationship between MDA and CI, CIII, and CI+CIII abundance, primary sites for ROS generation, and CV in all offspring (Fig. 3.6G and Supplementary Table 8). Only CI remained significant in analysis within the mWD offspring (Fig. 3.6J). These data suggest that reduced

OXPHOS content and/or limiting ROS release via VDAC1 may reflect fetal adaptations to elevated ROS in skeletal muscle during development.

DISCUSSION

Future risk for the development of obesity and cardiometabolic disease in youth, including type 2 diabetes, is increased by exposure to maternal obesity and diabetes in utero (46; 281; 282). These early exposures may "program" the offspring for metabolic dysfunction; however, the mechanisms and cellular targets mediating these outcomes are not known. Here, we examined the long-term metabolic impact of exposure to mWD during pregnancy and lactation, in the absence of either maternal obesity or insulin resistance, on 3-year-old offspring body composition, glucose homeostasis, and skeletal muscle metabolism. We also evaluated the efficacy of a healthy pw diet intervention at ameliorating the effects of early-life exposure to mWD. In summary, offspring exposed to mWD during gestation and lactation weaned to a healthy pw diet had elevated insulin release during i.v. GTT despite a similar body composition compared to mCD offspring and higher physical activity. In skeletal muscle, offspring had significant reductions in oxidative metabolism in the presence of fatty acids concomitant with reduced OXPHOS complex abundance and VDAC1. Further exposure to the pwWD in mWD offspring revealed a greater change in the accumulation of saturated lipids and some bioactive lipid species associated with insulin resistance despite increases in visceral fat accruement similar to those of mCD offspring. The increased accumulation of saturated ceramides in skeletal muscle coupled with reduced oxidative capacity may contribute to worsening systemic insulin sensitivity and partitioning of lipids to adipose stores.

The coordination of mitochondrial oxidation in response to nutrient availability and energy demand (i.e., metabolic flexibility) decreases in parallel with the development of systemic insulin resistance (283; 284) and metabolic dysfunction (264). We observed lower oxidative capacity in isolated soleus and gastroc muscle fibers from mWD offspring, regardless of pw diet, when provided a combination of fatty acid and pyruvate. Our data could not be explained by reduced mitochondrial content or decreased abundance of critical lipid trafficking or b-oxidation enzymes or ETF/ETFDH but may be linked to reduced OXPHOS complex abundance. Importantly, skeletal muscle from mWD offspring, including mWD offspring switched to a healthy diet, contained

approximately one-half the volume of OXPHOS complexes like CI relative to controls. We propose that the observed loss in maximal CI- and CI+II-linked respiration in the presence of lipids may be due, in part, to greater flow of electrons from fatty acid b-oxidation to ubiquinone via ETF/ETFDH relative to electrons coming from CI and CII in mWD versus mCD offspring. Additionally, patients with CI deficiency have reduced [NAD^+]-to-[NADH] ratios that also coincide with impaired β-oxidation (285). As both pathways for lipid and pyruvate oxidation are dependent on an adequate [NAD^+]-to-[NADH] ratio to proceed, insufficient CI abundance would shift redox circuitry toward NADH excess and may also explain why flux is most limited when both pathways converge at CI.

Interestingly, with the exception of the CI nuclear gene NDUFB8 in soleus, reduced OXPHOS protein abundance was not related to decreased nuclear or mitochondrial gene expression. Furthermore, in soleus, a more oxidative muscle, pwWD increased the protein abundance of OXPHOS complex, even in the mWD offspring, suggesting an ability to respond to nutrient stresses, albeit starting at a lower baseline level. These baseline differences may be due to posttranscriptional mechanisms related to higher mitochondrial protein turnover and/or less synthesis.

Exposure to the pwWD revealed altered lipid handling in mWD offspring compared with control offspring also on the pwWD. Increased saturated intramyocellular lipid content is a strong predictor of muscle insulin resistance in sedentary adults and children with obesity (136; 188; 286) and is often associated with impaired lipid oxidation or lipid trafficking in muscle (287). A predominate and unexpected finding across our muscle lipid analysis was a reduction in lipid species accumulation in mWD offspring weaned to pwCD, suggesting reduced uptake or altered fatty acid metabolism. In both soleus and gastroc, reductions in fatty acid oxidation were greatest in this group (i.e., mWD/pwCD) despite no difference in the abundance of key fatty acid oxidation enzymes. However, the activity of CPT1b and/or the abundance of other fatty acid transporters may be responsible for the lower accumulation of fatty acids and fatty acid metabolites in mWD/pwCD muscle. At the molecular level, bioactive lipid metabolites, like 1,2-DG and ceramide, activate signaling cascades that impede insulin signaling transduction (288). The activation of canonical and/or atypical PKCs by elevated 1,2-DG to promote inhibitory phosphorylation of IRS proteins or by ceramide to inhibit Akt activation (289; 290) and suppression of insulin signaling is well described in human and animal models of insulin resistance

(193). Specifically, in total and saturated 1,2-DGs, there was a greater difference between pw diet treatments in mWD offspring driven by the lower baseline in pwCD muscle. However, whether the magnitude of change in 1,2-DGs (or other lipid species) with pwWD is as important as the total accumulation has not been investigated but may reflect a unique response associated with developmental programming. In contrast to the 1,2-DGs, exposure to mWD led to a greater accumulation of another saturated lipid species, ceramide C18:0, and its downstream metabolite SPM C18:0, in muscle in response to pwWD. Indeed, increased mitochondrial ceramide accumulation has been linked to reduced coenzyme Q levels and reduced electron transport system components and, subsequently, impaired mitochondrial function similar to that seen in skeletal muscle of mWD offspring (291). Importantly, our findings are consistent with an intracellular environment characterized in obesity and type 2 diabetes (188; 273; 278; 292; 293).

Increased ROS production and elevated oxidative damage to intracellular molecules are features of mitochondrial dysfunction (294; 295). We previously reported increased ROS damage in fetal skeletal muscle, pancreas, and livers from obese mWD dams (194; 239; 257). Therefore, the absence of elevated markers of lipid peroxidation or protein carbonylation in skeletal muscle of mWD was unanticipated. Indeed, we observed lower levels of oxidative damage in mWD offspring on the pwWD. Lower levels of oxidative damage may result from decreased VDAC1 abundance, which functions in the formation of the mitochondrial permeability transition pore to allow ROS efflux and/or stimulate apoptosis (296). Thus, reduced VDAC may lower oxidative damage by trapping ROS within the mitochondria. Reduced CI and overall lower OXPHOS flux may also act as a countermeasure to ameliorate ROS production (297). Along these lines, we show strong correlations between ROS damage and VDAC1 abundance driven by mWD offspring. We also see a relationship between CI, CI+CIII, and CV and lipid peroxidation. Reduced VDAC1 and OXPHOS abundance may be an adaptation that reprograms ROS handling as a strategy to mediate the excessive oxidative stress previously observed in fetal skeletal muscle, albeit at the cost of mitochondrial health and oxidative efficiency. A higher antioxidant system may also be induced to sequester excess ROS, although this has not been explored here. Further work is required to determine the mechanisms that underlie changes in ROS handling and mitochondrial integrity.

Overall, we show that exposure to an mWD during pregnancy and lactation, even in the absence of maternal obesity and insulin resistance, is sufficient to reprogram offspring lipid handling and impair oxidative metabolism in skeletal muscle, a phenotype typically associated

with metabolic disease states or the functional decline in muscle health with aging (16; 298). Sex-specific difference in metabolic outcomes including insulin resistance and obesity have been identified in adult offspring exposed to maternal obesity (299). We postulate that these changes observed in cellular metabolism in our peripubertal animals will be exacerbated by future physiological stresses including weight gain, puberty, lack of physical activity, or a chronic pwWD, revealing the elevated and sex specific risk of cardiometabolic diseases observed in adults from pregnancies complicated by poor maternal nutrition and obesity. Future studies will be aimed at interrogating regulators of cellular quality control processes contributing to downregulated OXPHOS abundance and function with exposure to mWD or obesity.

NOTES

Funding. This research was supported by National Institutes of Health (NIH) grants R24 DK090964 (to J.E.F., K.M.A., and P.K.), R01 DK128187 (K.M.A., P.K., and J.E.F.), R01 MH107508 (E.L.S.), and R01 DK089201 (K.M.A.) and by an NIH Center Grant (P51 OD011092) to ONPRC. This work was also supported by the Eugene and Clarissa Evonuk Memorial Graduate Fellowship (K.T.G.). The Endocrine Technologies Core at ONPRC is supported (in part) by NIH grant P51 OD011092 for operation of the ONPRC.

Duality of Interest. No potential conflicts of interest relevant to this article were reported.

Author Contributions. S.R.W., M.G., E.L.S., K.M.A., P.K., J.E.F., and C.E.M. established and supported the experimental animal model. K.T.G., B.H., B.C.B., T.A.D., S.S., P.K., A.J.C., and C.E.M. collected and analyzed data. K.T.G. and C.E.M. drafted the manuscript. All authors provided critical feedback and reviewed the final manuscript. C.E.M. is the guarantor of this work and, as such, had full access to all the data in the study and takes responsibility for the integrity of the data and the accuracy of the data analysis.

Prior Presentation. Parts of this study were presented in abstract form at the 83rd Scientific Sessions of the American Diabetes Association, San Diego, CA, 23–26 June 2023.

Anthropometrics	**CD/CD** (*n*=10-11)	**CD/WD** (*n*=4-5)	**WD/CD** (*n*=11-12)	**WD/WD** (*n*=8-9)	**m diet**	**pw diet**	**m x pw**
Body mass (kg)	6.1±0.3	6.1±0.5	6.3±0.3	6.3±0.3	*ns*	*ns*	*ns*
Non-fat mass (kg)	5.1±0.2	5.0±0.3	5.2±0.3	5.3±0.3	*ns*	*ns*	*ns*
Fat mass (kg)	0.9±0.06	0.8±0.10	0.9±0.04	0.8±0.07	*ns*	**0.04**	*ns*
Crown rump (cm)	49±0.8	47±1.3	48±1.0	48±0.8	*ns*	*ns*	*ns*
Subscapular skinfold thickness (mm)	3.5±0.3	3.9±0.4	3.1±0.2	4.0±0.3	*ns*	**0.04**	*ns*
Retroperitoneal fat mass (g)	0.8±0.1	2.5±1.0**	0.9±0.1	2.5±0.4**	*ns*	**0.0001**	*ns*
Activity	**CD/CD** (*n*=8)	**CD/WD** (*n*=5)	**WD/CD** (*n*=9)	**WD/WD** (*n*=9)	**m diet**	**pw diet**	**m x pw**
Daily (24h) (counts/hr)	356±31	385±11	413±12	453±21	**0.009**	*ns*	*ns*
Daytime (12h) (counts/hr)	299±26	315±7	331±17	385±22	**0.03**	*ns*	*ns*
Nighttime (12h) (counts/hr)	57±6	60±5	66±6	66±10	*ns*	*ns*	*ns*
Glucose metabolism	**CD/CD** (*n*=9-10)	**CD/WD** (*n*=5)	**WD/CD** (*n*=11-12)	**WD/WD** (*n*=9)	**m diet**	**pw diet**	**m x pw**
Fasting glucose (mg/dL)	54±4	63±6	49±2	55±2	*ns*	**0.04**	*ns*
Fasting insulin (μU/mL)	4±1	25±8****	4±1	10±2^^	**0.01**	**0.0001**	**0.01**
Glucose AUC, zero (x10^3; a.u.)	10.1±0.5	8.5±0.4	8.2±0.4^^	8.2±0.4	**0.02**	*ns*	*ns*
Insulin AUC, zero (x10^3; a.u.)	1.6±0.2	2.4±0.3	1.7±0.2	2.3±0.2	*ns*	**0.01**	*ns*
Insulin AUC, baseline (x10^3; a.u.)	1.0±0.3	1.0±0.2	1.4±0.2	1.7±0.2	**0.03**	*ns*	*ns*
HOMA-IR	0.7±0.1	4.2±1.8***	0.5±0.1	1.4±0.3^^	**0.009**	**0.0002**	**0.02**
Plasma lipids	**CD/CD** (*n*=10)	**CD/WD** (*n*=5)	**WD/CD** (*n*=10-11)	**WD/WD** (*n*=9)	**m diet**	**pw diet**	**m x pw**
Triglycerides (mg/dL)	46±6	52±12	40±5	33±5	*ns*	*ns*	*ns*
Cholesterol (mg/dL)	129±5	**160±6***	134±8	**170±9****	*ns*	**0.0003**	*ns*
HDL (mg/dL)	58±2	**87±6*****	61±4	**90±4******	*ns*	**0.0001**	*ns*
LDL (mg/dL)	67±5	73±4	72±7	83±10	*ns*	*ns*	*ns*

Table 3.1 – Adolescent offspring physiological measures and activity at 34 months.

Body composition, fasting serum values and activity data are shown as mean ± SEM. Glucose area under the curve was calculated either from zero or from fasting baseline during an i.v. GTT. Statistical significance was determined by 2-way ANOVA. *P*-values are listed for main effects of maternal (m) diet, postweaning (pw) diet and interactions (m x pw). Multiple comparisons following Sidak's post hoc analysis are represented by asterisks (*p<0.05, **p<0.01, ***p<0.001, ****p<0.0001) for significant differences between postweaning diet within the same maternal diet group and carets (^^p<0.01) for differences between maternal diet within same postweaning diet. *ns*, no significant difference; a.u., arbitrary units.

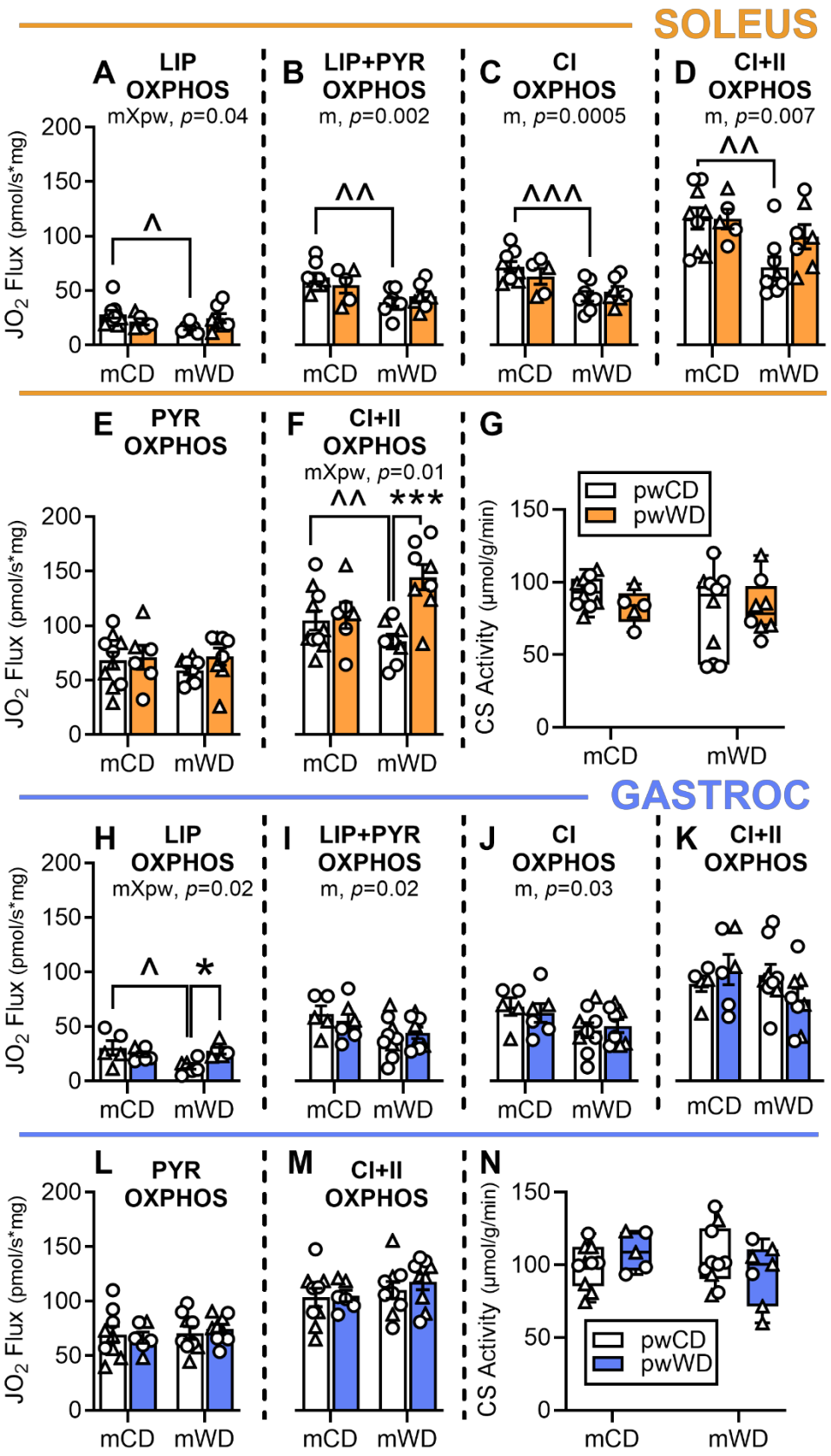
SOLEUS
A
LIP
OXPHOS
mXpw, p=0.04
B
LIP+PYR
OXPHOS
m, p=0.002
C
CI
OXPHOS
m, p=0.0005
D
CI+II
OXPHOS
m, p=0.007
E
PYR
OXPHOS
F
CI+II
OXPHOS
mXpw, p=0.01
G
pwCD
pwWD
JO2 Flux (pmol/s*mg)
CS Activity (µmol/g/min)
mCD
mWD
GASTROC
H
LIP
OXPHOS
mXpw, p=0.02
I
LIP+PYR
OXPHOS
m, p=0.02
J
CI
OXPHOS
m, p=0.03
K
CI+II
OXPHOS
L
PYR
OXPHOS
M
CI+II
OXPHOS
N

Figure 3.1 – Substrate oxidation in skeletal muscle of adolescent offspring.

Average group oxygen flux (JO_2; pmols/s*mg) was measured in permeabilized muscle fiber bundles (PMFB) with or without lipid (palmitoyl-carnitine; LIP) and normalized to tissue wet weight in soleus (orange figures, A-F) or gastrocnemius (blue figures, H-M). In soleus, rate was measured in the presence of saturating ADP with serial additions of (A) LIP and malate, (B) Pyruvate (PYR), (C) glutamate for CI OXPHOS capacity and (D) succinate for maximal CI+CII OXPHOS capacity. Respiration rate without lipid was measured in the presence of saturating ADP after titrations of (E) pyruvate and malate and (F) glutamate and succinate CI+CII OXPHOS capacity. These measures were repeated, in the same order listed above, in the gastrocnemius (blue figures, H-M). Citrate synthase activity (μmols/min*g) is shown in soleus (G) and gastroc (N). Respiratory flux and CS activity were analyzed by 2-way ANOVA with Sidak's multiple comparisons. *P*-values for significant main effects of maternal (m) or postweaning (pw) diet are listed above each graph. For post-hoc analysis, carets (^^p<.01, ^^^p<.001) indicate significant differences by maternal diet within the same postweaning diet group; asterisks (**p<.01) indicate significant differences by postweaning diet within the same maternal diet group. Individual data points with group mean and SEM (A-F, H-M) or with the minimum, maximum, median and interquartile range (G and N) are shown. Male (M) offspring are indicated by circles and female (F) offspring by triangles. Sample size for each group by sex: mCD/pwCD, 5-6F/4M; mCD/pwWD, 2F/4M; mWD/pwCD, 3F/5-6M; mWD/pwWD, 4-5F/4M.

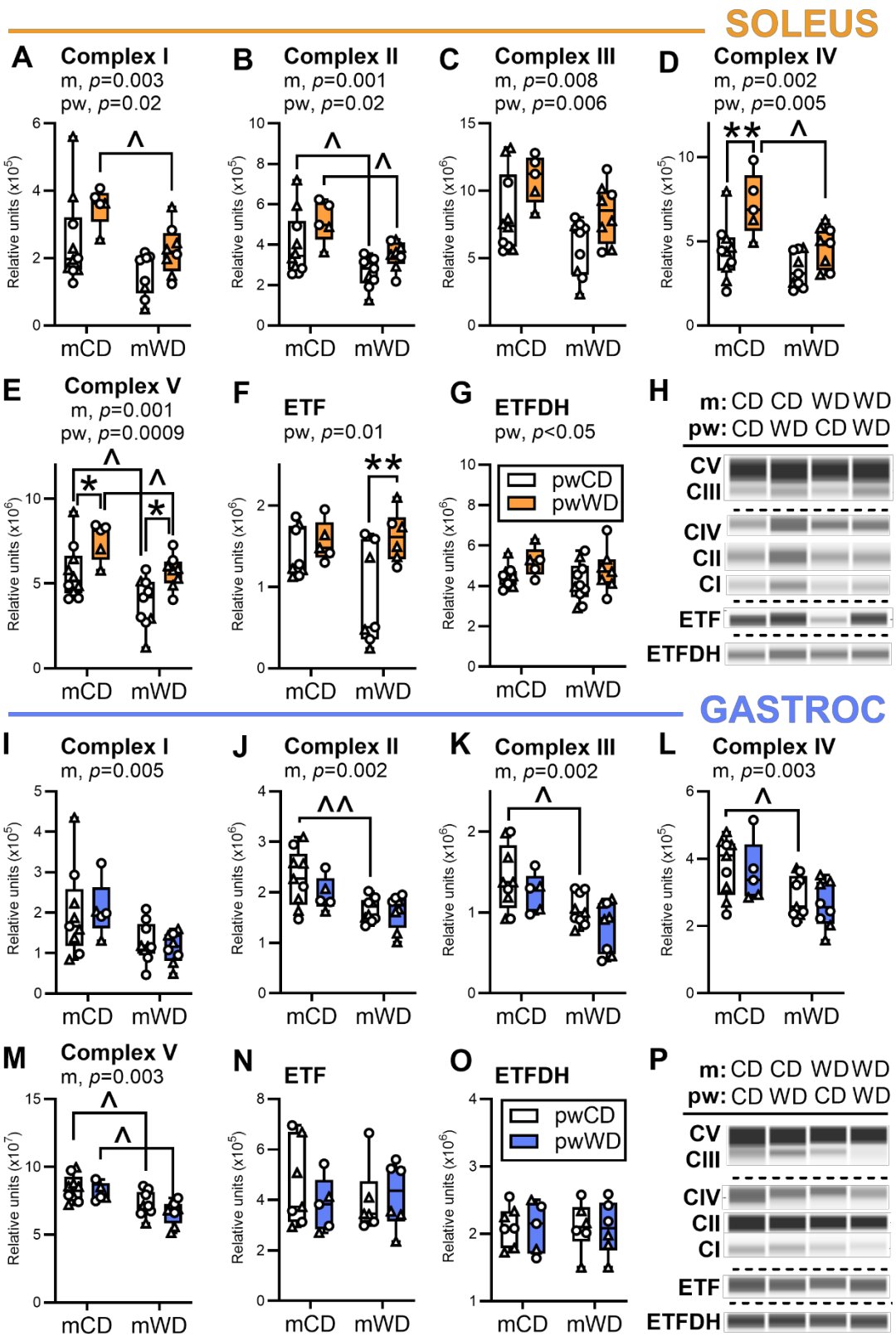
SOLEUS
A
Complex I
m, p=0.003
pw, p=0.02
B
Complex II
m, p=0.001
pw, p=0.02
C
Complex III
m, p=0.008
pw, p=0.006
D
Complex IV
m, p=0.002
pw, p=0.005
E
Complex V
m, p=0.001
pw, p=0.0009
F
ETF
pw, p=0.01
G
ETFDH
pw, p<0.05
pwCD
pwWD
H
m: CD CD WD WD
pw: CD WD CD WD
CV
CIII
CIV
CII
CI
ETF
ETFDH
GASTROC
I
Complex I
m, p=0.005
J
Complex II
m, p=0.002
K
Complex III
m, p=0.002
L
Complex IV
m, p=0.003
M
Complex V
m, p=0.003
N
ETF
O
ETFDH
pwCD
pwWD
P
m: CD CD WD WD
pw: CD WD CD WD
CV
CIII
CIV
CII
CI
ETF
ETFDH
Relative units (x10^5)
Relative units (x10^6)
Relative units (x10^7)
mCD
mWD

Figure 3.2 – Mitochondrial oxidative phosphorylation (OXPHOS) enzyme abundance in offspring skeletal muscle.

Protein abundance of electron transport system (ETS) and OXPHOS complexes were measured by Simple Western for CI (A), CII (B), CIII (C), and CIV (D), CV (E), ETF (F) and ETFDH (G) in offspring soleus (orange bars). Individual protein abundance was normalized to an internal fluorescent loading control and CI-CV abundance was normalized to total protein. These measures were repeated in the gastrocnemius (blue figures, I-P). Representative immunoassay images for soleus (H) and gastroc (P) are shown. Dashed horizontal lines indicate different contrast levels. Data were analyzed by 2-way ANOVA for significant main effects of maternal or postweaning diet or interactions with Sidak's multiple comparisons test. *P*-values for significant main effects are listed above each graph. For post-hoc analysis, carets (^p<.05, ^^p<.01) indicate significant differences by maternal diet within the same postweaning diet group and asterisks (*p<.05, **p<.01) indicate significant differences by postweaning diet within the same maternal diet group. Individual data points for offspring on pwCD (open bars) or pwWD (closed bars) are shown along with group minimum, maximum, median and interquartile range. Male (M) offspring are indicated by circles and female (F) offspring by triangles. Sample size for each group by sex: mCD/pwCD, 6F/3M; mCD/pwWD, 2F/3M; mWD/pwCD, 3F/6M; mWD/pwWD, 5F/3M. For ETF and ETFDH n= mCD/pwCD, 4F/3-4M; mCD/pwWD, 2F/3M; mWD/pwCD, 3F/3-4M; mWD/pwWD, 3-5F/2-3M.

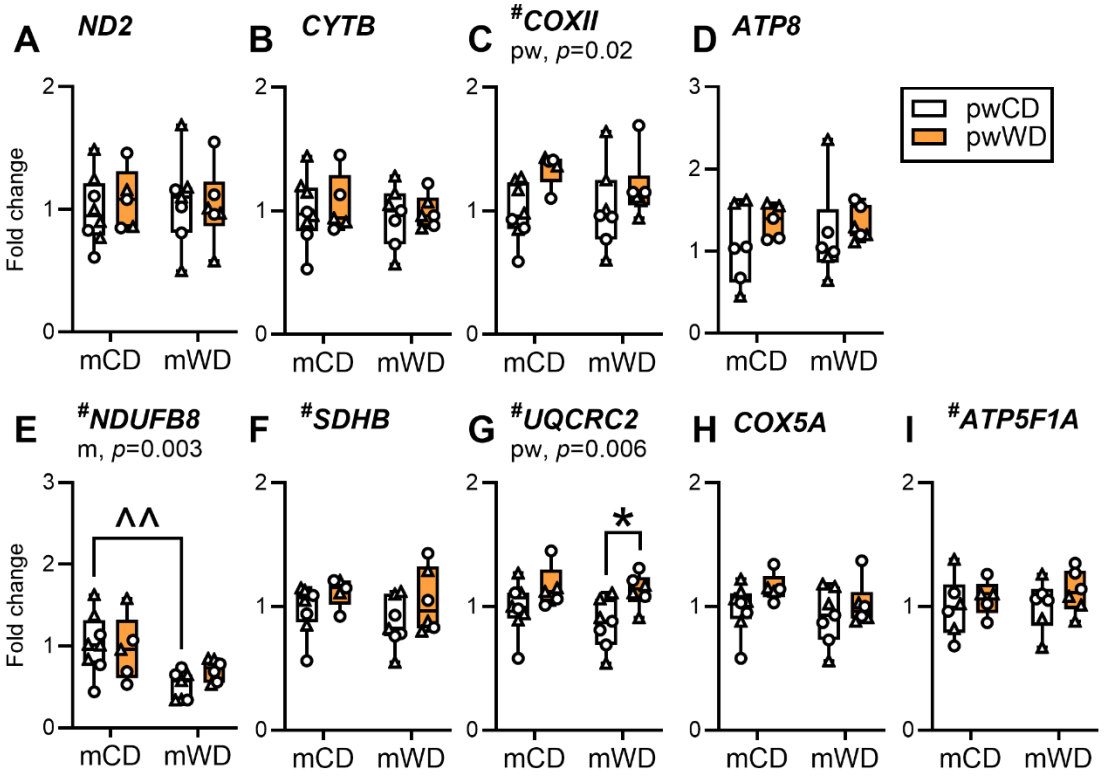

Figure 3.3 – OXPHOS gene expression in offspring soleus.

Gene expression of key mitochondrial and nuclear encoded OXPHOS proteins were measured by qPCR in offspring soleus (orange bars). Mitochondrial encoded genes measured were (A) *ND2* for CI, (B) *CYTB* for CIII, (C) *COXII* for CIV and (D) *ATP8* for CV. Nuclear encoded genes measured were (E) *NDUFB8* for CI, (F) *SDHB* for CII, (G) *UQCRC2* for CIII, (H) *COX5A* for CIV and (I) *ATP5F1A* for CV. Individual gene expression was adjusted to the geometric mean for the expression of housekeeper genes, *RPS15*, *28S* and *RPL13A*, and are presented as fold-change. Data were analyzed by 2-way ANOVA for significant main effects of maternal or postweaning diet or interactions using Sidak's multiple comparisons test. The p-values for significant main effects are listed in each graph. For post-hoc analysis, carets (^^p<.01) indicate significant differences by maternal diet within the same postweaning diet group and asterisks (*p<.05) indicate significant differences by postweaning diet within the same maternal diet group. Individual data points for offspring on pwCD (open bars) or pwWD (closed bars) are shown along with group minimum, maximum, median, and interquartile range. Male (M) offspring are indicated by circles and female (F) offspring by triangles. Sample size for each group by sex: mCD/pwCD, 5F/3M; mCD/pwWD, 2F/3M; mWD/pwCD, 4F/3M; mWD/pwWD, 3F/3M.

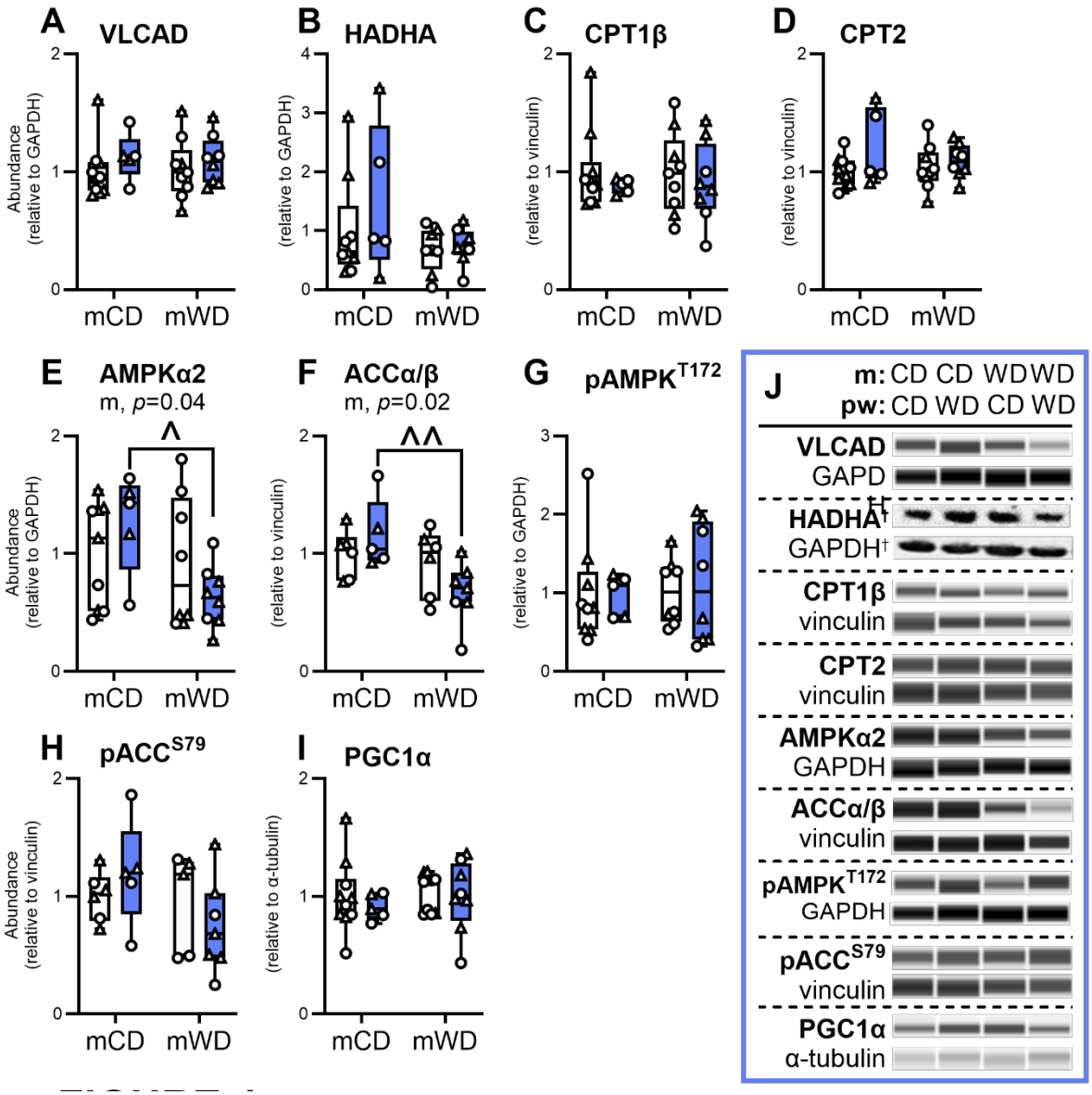
A
VLCAD
Abundance (relative to GAPDH)
mCD
mWD
B
HADHA
(relative to GAPDH)
C
CPT1β
(relative to vinculin)
D
CPT2
(relative to vinculin)
E
AMPKα2
m, p=0.04
^
F
ACCα/β
m, p=0.02
^^
G
pAMPK T172
H
pACC S79
(relative to vinculin)
I
PGC1α
(relative to α-tubulin)
J
m: CD CD WD WD
pw: CD WD CD WD
VLCAD
GAPD
HADHA†
GAPDH†
CPT1β
vinculin
CPT2
vinculin
AMPKα2
GAPDH
ACCα/β
vinculin
pAMPK T172
GAPDH
pACC S79
vinculin
PGC1α
α-tubulin

Figure 3.4 – Lipid oxidation and signaling enzymes in offspring gastroc.

Protein abundance of key regulators of lipid metabolism, including (A) VLCAD, (B) HADHA, (C) CPT1β and (D) CPT2, upstream signaling kinases, (E) AMPKα2, (F) ACCα/β, (G) phosphorylated (p)AMPK (T172) and (H) pACC (S79), and (I) PGC1α were measured by immunoassay in offspring gastrocnemius. Individual protein abundance was adjusted to GAPDH, vinculin, or α-tubulin and ratios expressed relative to the mCD/pwCD group. (J) Representative immunoassay images with loading controls. Dashed horizontal lines indicate different contrast levels. Data were analyzed by 2-way ANOVA for significant main effects of maternal or postweaning diet or interactions with Sidak's multiple comparisons test. *P*-values for significant main effects are listed in each graph. For post-hoc analysis, carets (^p<.05, ^^p<.01) indicate significant differences by maternal diet within the same postweaning diet group. Individual data points for offspring on pwCD (open bars) or pwWD (blue bars) are shown along with group minimum, maximum, median, and interquartile range. Male (M) offspring are indicated by circles and female (F) offspring by triangles. Sample size for each group by sex: mCD/pwCD, 5-6F/4M; mCD/pwWD, 2F/3M; mWD/pwCD, 3F/5-6M; mWD/pwWD, 5F/3M.

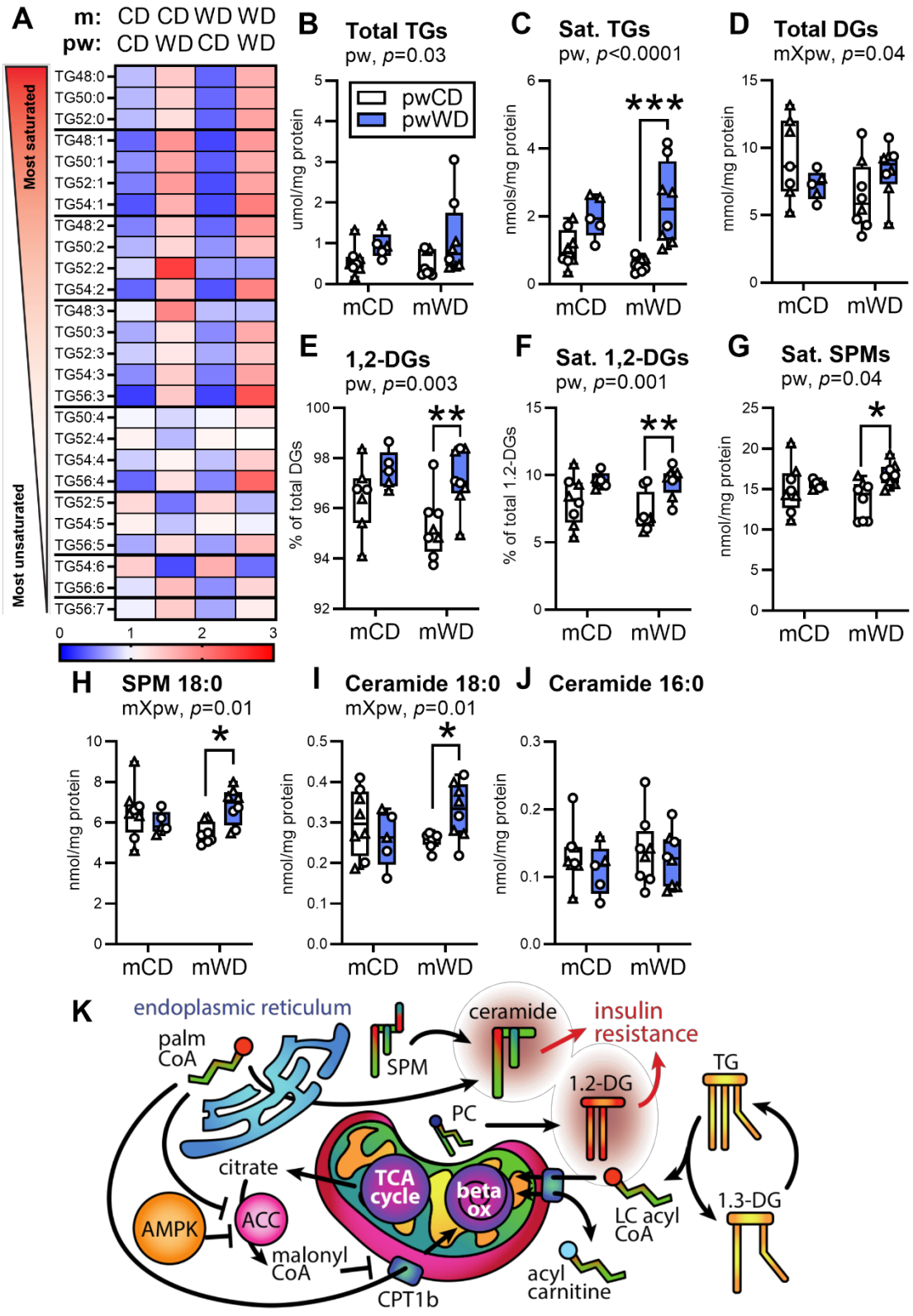
A
m: CD CD WD WD
pw: CD WD CD WD
Most saturated
Most unsaturated
TG48:0
TG50:0
TG52:0
TG48:1
TG50:1
TG52:1
TG54:1
TG48:2
TG50:2
TG52:2
TG54:2
TG48:3
TG50:3
TG52:3
TG54:3
TG56:3
TG50:4
TG52:4
TG54:4
TG56:4
TG52:5
TG54:5
TG56:5
TG54:6
TG56:6
TG56:7
0 1 2 3
B Total TGs
pw, p=0.03
pwCD
pwWD
umol/mg protein
mCD mWD
C Sat. TGs
pw, p<0.0001
***
nmols/mg protein
D Total DGs
mXpw, p=0.04
mmol/mg protein
E 1,2-DGs
pw, p=0.003
**
% of total DGs
F Sat. 1,2-DGs
pw, p=0.001
% of total 1.2-DGs
G Sat. SPMs
pw, p=0.04
*
nmol/mg protein
H SPM 18:0
mXpw, p=0.01
I Ceramide 18:0
mXpw, p=0.01
J Ceramide 16:0
K
endoplasmic reticulum
palm CoA
SPM
ceramide
insulin resistance
TG
1.2-DG
PC
citrate
TCA cycle
beta ox
AMPK
ACC
malonyl CoA
CPT1b
LC acyl CoA
1.3-DG
acyl carnitine

Figure 3.5 – Measurement of intramuscular lipids in offspring skeletal muscle.

Saturated triacylglycerol (TG) species (A), total TG content (B) and saturated TG abundance (C) were measured in gastroc of 3Y offspring. Diacylglycerol (DG) abundance (D), percent of 1,2-DGs of total DGs (E), percent of saturated 1,2-DGs out of total 1,2-DGs (F), saturated sphingomyelin (SPM) abundance (G) 18:0 SPM (H), 18:0 ceramide (I) and 16:0 ceramide (J) content were also measured in the same samples. Data were analyzed by 2-way ANOVA with Sidak's multiple comparisons test. *P*-values for significant effects are listed in each graph. For post-hoc analysis, asterisks (*p<.05, **p<.01, ***p<.001) indicate significant differences between postweaning diets within the same maternal diet group. Individual data points for offspring with minimum, maximum, median and interquartile range per group are shown. Male (M)offspring are indicated by circles and female (F) offspring by triangles. Sample size for each group by sex: mCD/pwCD, 5F/3M; mCD/pwWD, 2F/3M; mWD/pwCD, 2F/6M; mWD/pwWD, 5F/3M. An illustration summarizing offspring intramuscular lipid metabolism (K).

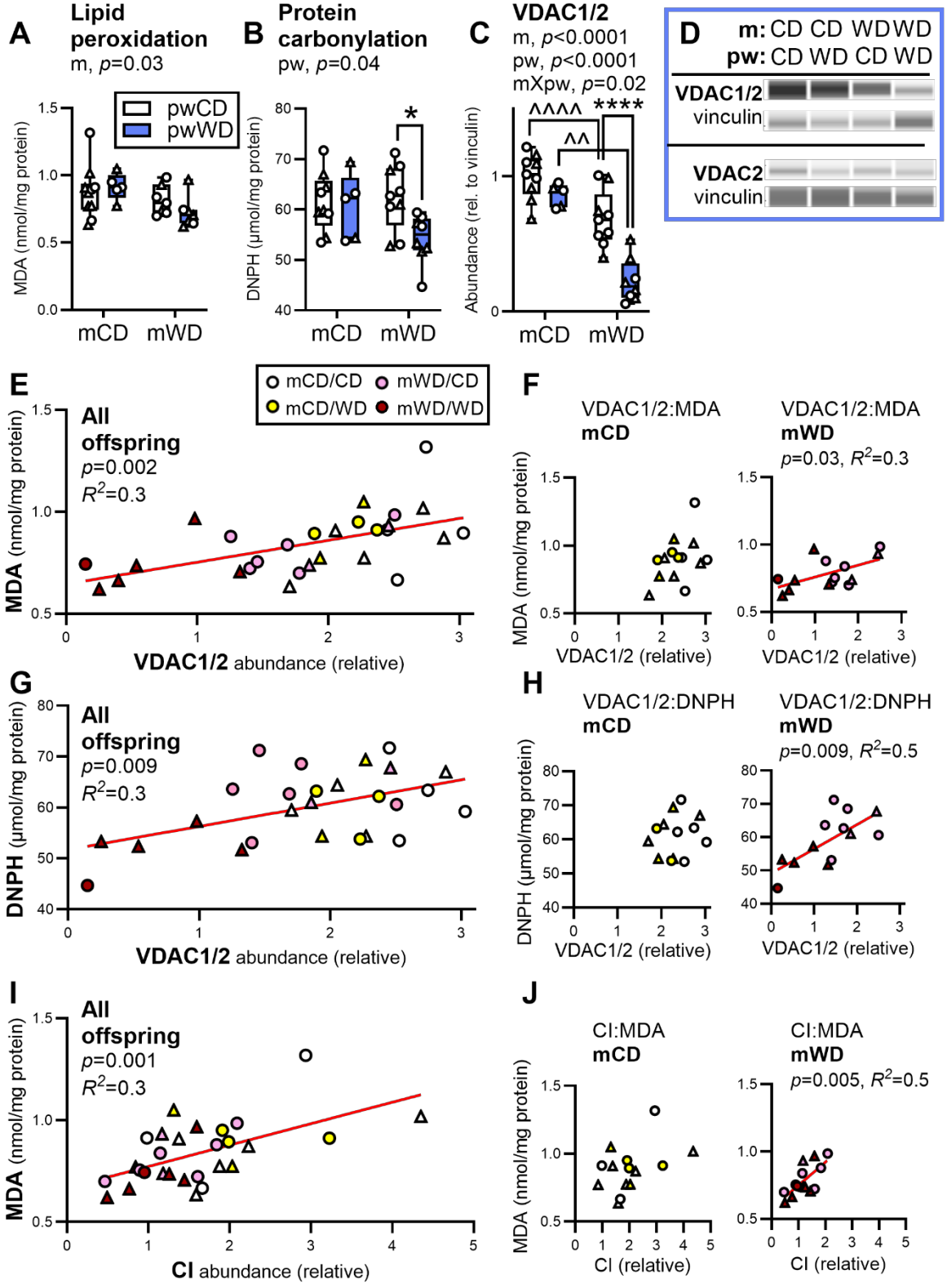
A
Lipid peroxidation
m, p=0.03
pwCD
pwWD
MDA (nmol/mg protein)
mCD
mWD
B
Protein carbonylation
pw, p=0.04
DNPH (µmol/mg protein)
*
C
VDAC1/2
m, p<0.0001
pw, p<0.0001
mXpw, p=0.02
Abundance (rel. to vinculin)
^^^^
****
^^
D
m: CD CD WD WD
pw: CD WD CD WD
VDAC1/2
vinculin
VDAC2
vinculin
E
mCD/CD
mWD/CD
mCD/WD
mWD/WD
All offspring
p=0.002
R2=0.3
MDA (nmol/mg protein)
VDAC1/2 abundance (relative)
F
VDAC1/2:MDA
mCD
VDAC1/2:MDA
mWD
p=0.03, R2=0.3
MDA (nmol/mg protein)
VDAC1/2 (relative)
G
All offspring
p=0.009
R2=0.3
DNPH (µmol/mg protein)
VDAC1/2 abundance (relative)
H
VDAC1/2:DNPH
mCD
VDAC1/2:DNPH
mWD
p=0.009, R2=0.5
DNPH (µmol/mg protein)
VDAC1/2 (relative)
I
All offspring
p=0.001
R2=0.3
MDA (nmol/mg protein)
CI abundance (relative)
J
CI:MDA
mCD
CI:MDA
mWD
p=0.005, R2=0.5
MDA (nmol/mg protein)
CI (relative)

Figure 3.6 – Intramuscular oxidative stress is lower in mWD offspring.

Lipid peroxidation (MDA, A), protein carbonylation (DNPH, B) and the protein abundance of VDAC1/2 (C) and VDAC2 (D) were measured in 3Y offspring gastroc. Protein abundance data was collected using Simple Western and adjusted to vinculin. Representative immunoassay images are shown (D). Data were analyzed by 2-way ANOVA with Sidak's multiple comparisons test. *P*-values for significant effects are listed in each graph. For post-hoc analysis, carets (^^p<.01, ^^^^p<.0001) indicate significant differences between maternal diets within the same postweaning diet group while asterisks (*p<.05, ****p<.0001) indicate significant differences between postweaning diets within the same maternal diet group. Male (M)offspring are indicated by circles and female (F) offspring by triangles. Sample size for A-C: mCD/pwCD, 5-6F/4M; mCD/pwWD, 2-3F/3M; mWD/pwCD, 2-3F/5-6M; mWD/pwWD, 4-5F/2-4M.Simple regression analysis was run for VDAC1/2 abundance and MDA across all offspring, n=28 (E) and within maternal groups (F) or DNPH across all offspring, n=26 (G) or within maternal groups (H). Correlations were also run between MDA and Complex I abundance in all offspring, n=28 (I) or within maternal groups (J). Individual data points for offspring are shown with minimum, maximum, median and interquartile range per group (A-C). Statistically significant correlations are indicated by red lines (E-J) with *p*-value and correlation coefficient *(R^2)* listed.

IV. AIM #2

EXPOSURE to WESTERN-STYLE DIET DISRUPTS MITOCHONDRIAL ARCHITECTURE & FUNCTION in MUSCLE of JUVENILE JAPANESE MACAQUES

Greyslak KT, Sharma A, Hetrick B, Meza C, Carey K, Dean TA, Aagaard KM, Gannon M, Wesolowski SR, Friedman JE, Kievit P, Funai K, McCurdy CE. *Manuscript in preparation.*

INTRODUCTION

The first 1,000 days of life represent a critical window of development when nutrient and hormonal stress can redirect future health and disease in the exposed offspring. This is seen in children of obese or diabetic pregnancies who are more likely to develop obesity and diabetes themselves (112; 300). Importantly, these chronic metabolic illnesses develop in the presence of systemic insulin resistance (301). Skeletal muscle is a primary target tissue for insulin and is responsible for up to 80% of insulin-stimulated glucose uptake, thereby making it a driver of systemic insulin resistance (184; 301). Furthermore, the loss of skeletal muscle insulin sensitivity has been implicated in the pathogenesis of metabolic diseases in offspring exposed to early life obesogenic stress (302). In skeletal muscle, insulin resistance is strongly associated with reduced mitochondrial abundance and function (221; 279). Mitochondria are highly dynamic organelles with critical roles extending beyond their bioenergetic niche. As a network, mitochondria buffer intracellular stress through coordinated functional and structural adaptations that ensure homeostasis and, ultimately, cellular survival (303). There are several mechanisms that contribute to these necessary adaptations, including: fission and fusion events (199), mitochondrial biogenesis (304), endoplasmic reticulum (ER) tethering (305; 306), mitochondrial-specific autophagy (i.e., mitophagy) (307), and global redox balance (215). Studies in humans and animals have demonstrated that reduced mitochondrial abundance, increased network fission, and loss of

MAM contacts are metabolically unfavorable and develop in tandem with insulin resistance (203; 302; 308) and obesity (224).

To this end, our group has previously reported that insulin resistance and mitochondrial dysfunction are present in skeletal muscle of offspring chronically exposed to maternal high-fat, high-sugar diet (i.e., Western Diet, WD) during early life (29; 194; 195). However, other features associated with mitochondrial physiology, including mitochondrial network dynamics and quality control, remain incompletely understood in offspring skeletal muscle in our model of maternal nutrient and obesogenic stress. Therefore, the purpose of the present study is to better understand how offspring diet with and without maternal WD-induced obesity corresponds with altered parameters of mitochondrial network dynamics in skeletal muscle of juvenile offspring.

METHODS

Experimental Design

Adult Japanese macaques were fed a high-fiber chow diet (CD, 15% calories from fats; Monkey Diet #5000, Purina Mills) or Western-style diet (WD, 37% calories from fat; TAD Primate Diet, 5L0P; TestDiet) *ad libitum* as previously described (29). WD is high in sucrose and fructose content, together accounting for 19% of WD and less than 3% of CD. Offspring from 47 dams are included in this study. 32 of these animals remained lean (Ln) while consuming CD prior to and throughout pregnancy and lactation. 18 dams developed obesity (Ob) after switching to WD for a minimum of 2 years prior to and throughout pregnancy, giving two maternal phenotypes: LnCD and ObWD.

All births were singleton and delivered vaginally as described (29). Offspring remained in their home colony until weaning at ~7-8 months of age. Of the 36 offspring born to LnCD dams, 20 were weaned to WD while the remaining 16 were maintained on a postweaning (pw)CD. To better address how maternal adiposity and diet further contribute to pwWD phenotypes in offspring, all ObWD offspring (n = 20) were weaning to WD and none to CD. Juvenile offspring were maintained on their assigned pw diet until studied at 14 months-old. 56 juvenile offspring were included in this study. No more than two offspring from the same dam were included in the same offspring group. Groups and sample size include: 16 LnCD/pwCD (8 female [F], 8 male

[M]), 20 LnCD/pwWD (9 F, 11 M), and 20 ObWD/pwWD (8 F, 12 M). All animals were not used for every experiment, however all three offspring groups were equally represented and balanced by sex for each experiment and subsequent analysis. Group size and offspring sex for each experiment can be found in its corresponding figure legend.

Offspring Anthropometrics & Glucose Tolerance Testing

Nonfat mass, fat mass, lean mass, and bone mineral content were measured by DEXA within one month prior to necropsy (258). Intravenous glucose tolerance tests (i.v. GTT) occurred 1-2 months before necropsy (~12 months-old) as previously reported (29; 258). In short, baseline blood samples were collected prior to glucose infusion and at 1, 3, 5, 10, 20, 40, and 60 min after infusion. Data generated after processing of these samples as described in detail here (29) provide measures of offspring fasting blood glucose and insulin concentrations, HOMA-IR, and glucose and insulin AUC.

Offspring Necropsy Collection

Juvenile animals were necropsied at 14 mon-old as previously described (252; 309). Juvenile skeletal muscles, including gastrocnemius (gastroc), were rapidly dissected of fascia and were either flash frozen or placed in biopsy preservation solution (BIOPS) and shipped overnight for mitochondrial analysis by flow cytometry. Frozen muscle was stored at -80°C for future experiments.

Protein Analysis

Frozen gastroc muscle (50-100 mg) were chemically and mechanically homogenized as described previously (29; 194). Protein concentration was determined via BCA kit (Pierce and Thermo Fisher Scientific). To measure protein abundance by Western blot, equal amounts of protein (40 µg unless otherwise indicated) was prepared and loaded onto 10% or 12% TGX Stain-Free FastCast acrylamide gels per manufacturer's instructions (Bio-Rad Laboratories, Hercules, CA). Following electrophoresis (150V for 40-60 min or until dye front runs out), gels were activated for 45 sec before being transferred to PVDF membrane. Images of activated proteins successfully transferred from gel to membrane were then acquired prior to blocking. Primary antibody staining occurred overnight at 4°C with gentle agitation. After washing, membranes were stained with

secondary antibody made in 2% milk dissolved in 1X TBST and rocked for 2 hours at room temp. Membranes were then washed and incubated for 5 min with ECL substrate and data collected via chemiluminescence. Gel activation, total protein imaging, and chemiluminescence detection was accomplished using a ChemiDoc MP Imaging System (Bio-Rad Laboratories, Hercules, CA).

Mitochondrial DNA Copy Number

DNA was extracted from frozen gastroc (<25 mg) with Quick-DNA Miniprep kits (Zymo Research, Irvine, CA). DNA was quantified with a NanoDrop 2000 spectrophotometer (Thermo Fisher Scientific). Genes (*CYTB* and *HBB*) were measured in triplicate with SsoAdvanced Universal SYBR Green Supermix and gene amplification detected using a CFX384 real-time PCR instrument (Bio-Rad Laboratories). Mitochondrial DNA copy number was calculated as the ratio of *CYTB* (mitochondrial genome) to *HBB* (nuclear genome).

Mitochondrial Lipidome

Enrichment of crude mitochondria from frozen gastroc (100-200 mg) was processed for lipidomic analysis using glass/Teflon Potter Elvehjem homogenizers (Kontes Glass Co., Vineland, NJ). Briefly, frozen gastroc was weighed into glass homogenizer with 1 mL of ice-cold Mito Isolation Buffer (MIM, 300 mM sucrose, 10 mM HEPES, 1 mM EGTA and 1 mg/mL fatty-acid free BSA added fresh day of tissue processing). Samples were always kept on ice. Tissue was homogenized at 500 rpm in a final volume of 2 mL MIM for 25 passes on ice. Homogenate was spun at 800*g for 10 min at 4°C and supernatants was collected into fresh tubes before spinning again at 12,000*g for 10 min at 4°C. After careful removal of the supernatant, pellets were resuspended in 200 µL fresh MIM and spun again (12,000*g, 10 min, at 4°C). After removing supernatant again, mito enriched pellets were resuspended one more time in 100 µL fresh MIM. 10 µL were aliquoted for future protein quant before freezing both aliquots at -80°C. After measuring protein conc., equal amount of protein (50 µg) from each sample were shipped overnight for lipidomic analysis via mass spectroscopy as previously described (310).

Isolation & Processing of Mitochondria for Flow Cytometry Analysis

Crude mitochondria from fresh gastroc (60-160 mg) shipped overnight in BIOPS were isolated using a Mitochondria Isolation Kit for Tissue (Thermo Scientific) and further processed and

analyzed as previously described (311). In short, fresh mitochondria were stained with MitoSpy Green FM, per manufacturer's instructions, for 30 min at room temperature before being washed, fixed, and analyzed by flow cytometry. Samples were run on a 3 laser, 10 color Gallios flow cytometer (Beckman Coulter) and analyzed using Kaluza acquisition software v. 1.0. Flow data were processed and analyzed by Kaluza analysis software v. 2.1.

Statistical Analysis

Individual data points with group median, minimum, maximum, and interquartile range are shown in each graph. Sample sizes were calculated *a priori* with variance from previously published data in 3-year-old offspring (29) using G*Power software v.3.1.9.7. To detect a similar (large) effect with $\alpha = 0.05$ and 80% power, the current study required ~14-16 animals (n) per group. This corresponded with number of females/males needed to detect sex specific differences by treatment (e.g., m diet or pw diet) with $\alpha = 0.05$ and 80% power, which is $n = 7$ females/males, 14 offspring total, per group.

Data were analyzed by two-way ANOVA for main effects of offspring group (m diet/pw diet) and sex, and interactive effects (offspring group by biological sex). Significant main or interactive effects ($p < 0.05$) are listed above each figure. If significant main/interactive effects were identified, post hoc analysis using unpaired Student's t-test was used to determine significance between subgroups and is represented by asterisks (*).

RESULTS

Markers of Mitochondrial Network Dynamics in Adolescent Offspring Muscle

We have previously characterized the metabolic profile of adolescent (3Y) offspring exposed to mWD ± further WD stress after weaning (29). In adolescent offspring gastrocnemius, abundance of mitochondrial oxidative phosphorylation (OXPHOS) enzymes and abundance of saturated lipid species were decreased or increased, respectively, in both groups of offspring consuming pwWD (Fig. 3.2 and 3.5). Importantly, pwWD offspring with prior mWD exposure demonstrated a more dramatic phenotype than mCD/pwWD offspring in a manner consistent with elevated risk for eventual development of metabolic disruption. As changes in mitochondrial network structure are shown to correspond with changes in metabolic health and oxidative metabolism (312-316) as

previously demonstrated in this model, we next measured components of mitochondrial network dynamics, i.e., components governing mitochondrial fusion and fission events. Optic atrophy 1 (OPA1) abundance, a dynamin-related protein required for inner mitochondrial membrane fusion and maintaining cristae integrity, was decreased in offspring of mWD with pairwise comparisons showing significant reductions in mWD compared to mCD offspring on the pwWD (Fig. 4.1A). Similarly, for mitofusin-2 (MFN2), required for outer mitochondrial membrane (OMM) fusion, there was a significant interactive effect of maternal and postweaning WD such that MFN2 abundance was decreased with pwWD in mWD but not mCD offspring (Fig. 4.1B). The abundance of dynamin-related protein 1 (DRP1), a GTPase essential in mitochondrial fission, was not different by maternal or postweaning diet (Fig. 4.1C); however, there was a significant main effect of maternal diet on phosphorylation of DRP1 at serine-616 ($pDRP1^{S616}$), which stimulates mitochondrial fission, is significantly reduced with pairwise comparisons to suggest significantly reduced stimulation of fission in mWD/pwWD (Fig. 4.1D).

In addition to fission and fusion dynamics, mitochondrial networks rely on membrane interactions at the endoplasmic reticulum (ER) to facilitate transfer of ions (e.g. Ca^{+2}, Fe^{+2}) (317-319) and phospholipids (320; 321). MitoNEET, an OMM protein, and MFN2 tether mitochondrial membranes to the ER (318; 320; 322), the disruption of which is associated with metabolic dysfunction (306; 323; 324). In addition to the reduced MFN2 (Fig. 4.1B), there was a significant main effect of maternal diet and a maternal and postweaning diet interaction on MitoNEET abundance (Fig 4.1E). Specifically, in response to pwWD, MitoNEET was reduced in muscle from mWD but not mCD offspring (Fig. 4.1B). PTEN-induced putative kinase 1 (PINK1) is a kinase that accumulates in depolarized or damaged mitochondrial membranes to initiate PINK1/PARK2-mediated mitophagy. There was a main effect of postweaning diet on PINK1 with pairwise comparisons showing increased PINK1 abundance in with pwWD in mWD offspring (Fig. 4.1F). While not significant, mitochondrial DNA copy #, indicative of mito-ER associated membranes where mitochondrial DNA biosynthesis occurs (325), appears to be reduced in the majority of a small subset of pwWD offspring from mWD compared to mCD (Fig. 4.1G). Together, these data suggest that mWD moderately impacts mitochondrial fission/fusion dynamics, ER-tethering, and network quality control in offspring skeletal muscle in a way that is significantly amplified with pwWD.

Mitochondrial Fission & Fusion Profile in Younger Juvenile Skeletal Muscle

In contrast to what was observed in adolescent 3Y offspring muscle, fetal gastroc from obese pregnancies collected earlier in this study had increased mitochondrial Electron Transport System (ETS) activity – specifically Complex (C)I, CI+III, and CIV – but no difference in *MFN2* gene expression (194). Therefore, 1 yr-old juvenile offspring (roughly age 4 in humans (326)) present a unique opportunity to investigate subtle changes in muscle mitochondrial structure and function potentially implicated in the pathogenesis of metabolic disease with mWD exposure. Due to the relatively minor change in abundance of mitochondrial networking proteins in pwCD animals from mWD, they were not included in this study.

Mitochondrial dynamics were measured in gastroc of 1Y juveniles consuming CD or WD born to lean dams on a CD (LnCD/CD and LnCD/WD) and postweaning WD animals born to dams with obesity and WD (ObWD/WD) during pregnancy/lactation. In contrast to what was observed in 3Y offspring, both short and long isoforms of the IMM protein OPA1 were increased with postweaning WD independent of maternal diet (Fig. 4.2A and B). Similarly, MFN2 was slightly, but statistically insignificantly, also increased in pwWD animals relative to LnCD/CD controls (Fig. 4.2C). FIS1 content, a mitochondrial fission factor that regulates mitochondrial morphology, was no different across groups (Fig. 4.2D). Lastly, while total DRP1 abundance is increased in LnCD/WD offspring relative to controls, stimulation of DRP1-mediated fission by phosphorylation at S616 is no different (Fig. 4.2 E and F). Taken together, postweaning WD influences markers of mitochondrial fusion/fission independent of early life environment in skeletal muscle at this timepoint in development. Interestingly, these data – particularly in OPA1 abundance – seem to oppose what was observed in these proteins in 3Y gastroc, presenting a possible role for aging in the dysregulation of mitochondrial fission/fusion dynamics.

Abundance of Enzymes Implicated in Cellular Stress

Given the dynamic nature of mitochondria in response to environmental cues and intracellular stress that could explain this unanticipated phenotype in juvenile skeletal muscle, we measured the abundance of OMA1, the protease that cleaves long (L)-OPA1 to short (S)-OPA1 in response to mitochondrial membrane depolarization. To this end, we find no difference in OMA1 abundance in offspring muscle (Fig 4.3A). However, the calcium-dependent protease activated by calcium stress associated with the ER is significantly elevated only with ObWD in pwWD gastroc

compared to LnCD/WD offspring (Fig. 4.3B). Calpain 1 is the only enzyme whose abundance is significantly influenced by sex with female ObWD/WD offspring driving this increase in abundance relative to males (data not shown). A downstream target susceptible to proteolytic cleavage by Calpain 1 following activation by calcium stress is mitochondrial Complex I (315), which is significantly decreased in ObWD animals on WD relative to LnCD/WD animals (Fig. 4.3C). Neither MitoNEET, an iron-sulfur protein with roles in redox sensing and ER-interactions, nor the mitochondria-specific antioxidant Manganese Superoxide Dismutase (MnSOD2) different in offspring muscle (Figure 4.3D and E).

Maintenance of Mitochondrial Network Quality Control & Protein Turnover

Abundance of PINK1 and Parkin were not different in response to WD consumption or maternal ObWD in juvenile gastroc (Fig. 4.4A and B). Ubiquitin content, a downstream substrate in PINK1/PARK2-mediated mitochondrial turnover, was similarly unchanged (Fig. 4.4C). The OMM transporter Voltage Dependent Anion Channel 1 (VDAC1), a protein that shown to regulated flux of metabolites, ions, and Reactive Oxygen Species (ROS) in/out of the mitochondrion is significantly reduced in ObWD/WD juvenile muscle relative to LnCD/WD offspring (Fig 4.4D). Too determine whether this observation was unique to VDAC1, we also measured the abundance of Adenine Nucleotide Translocator (ANT1) and part of the OMM protein translocase complex (TOM40), neither of which different by postweaning diet or maternal phenotype in offspring muscle (Fig. 4.4E and F). These data support the notion that VDAC1 abundance is sensitive to the combination of offspring WD and maternal ObWD exposure in juveniles prior to other markers previously observed to be impacted by pwWD and mWD in the gastroc of adolescent-age offspring (Fig. 4.1).

Mitochondrial Lipidome & Mitochondrial Coupling Efficiency in Gastroc of pwWD Juveniles

To improve the sensitivity of our investigation into the architecture and functional outcomes of the mitochondrial network described in these studies, we enriched for the mitochondrial fraction in the gastroc of these offspring to ascertain the composition of their mitochondrial membrane lipids (327). Initial Principal Component Analysis (PCA) of the entire mitochondrial lipidome in these three groups show that both pwWD groups cluster together in a manner that suggests minimal influence, or the masking of any potential phenotype, created by maternal metabolic phenotype

(Fig. 4.5B). Importantly, this analysis regards each lipid species as a separate and equally important entity associated with the mitochondrial membranes in the muscle of these animals. Upon closer examination into specific species of interest like cardiolipin, a phospholipid that is exclusive to mitochondrial membranes whose abundance most accurately reflects "mitochondrial abundance" in lieu of microscopy or imaging/visual techniques. Similar to L-OPA1 and S-OPA1 content, cardiolipin (CL) abundance presented as a percentage of total mitochondrial lipids was significantly higher in ObWD/WD offspring relative to controls and, uniquely, also significantly higher in ObWD/WD offspring relative to LnCD/WD animals (Fig. 4.5C). Another mitochondria-specific phospholipid, phosphatidylglycerol (PG) content relative to total mito lipids recapitulates this observation with a higher % of PG in ObWD/WD offspring compared to controls (Fig. 4.5D). Of particular interest is abundance of phosphotidylserine (PS), which is synthesized exclusively in the ER junctions and is trafficked to the mitochondria via mito-ER junctions (328). In contrast to CL and PG patterns across offspring groups, the fraction of PS is significantly reduced in both pw WD groups relative to controls (Fig. 4.5E). This could contribute further to the theory that mito-ER junctions and or calcium stress may be present in WD offspring muscle.

Next, we sought to determine whether these findings in protein abundance of enzymes regulating mitochondrial morphology and in the mitochondrial lipidome translated to functional ramifications in the muscle of these animals. Mitochondrial function was assayed via high-resolution respirometry in living PMFBs freshly isolated from the gastroc of these offspring. Of particular interest were functional discrepancies existing between the two pwWD groups that were associated with early life ObWD exposure per our initial hypothesis. Mitochondrial function is presented here as Coupling Efficiency, or proton "leak" relative to maximal oxidative phosphorylation capacity in the presence of saturating ADP concentrations with a value of 1.00 representing 100% efficiency in the coupling of protons that are pumped into the intermembrane space to rate of oxygen flux specific to ATP synthesis. While there is no significant differences in the coupling efficiency between these groups during carbohydrate (CHO) oxidation (Fig. 4.5F), ObWD/WD offspring demonstrate a significant reduction in coupling efficiency in the context of lipid-specific substrate oxidation (Fig. 4.5G). When separated and plotted independently, this difference in coupling efficiency with lipid substrate is driven, significantly, by elevations in LEAK respiration (Fig. 4.5H) in muscle mitochondria from WD offspring exposed to maternal ObWD and not by any significant differences in maximal respiration with lipid substrate at

saturating amounts of ADP between these same two groups (Fig. 4.5I). Altogether, these data provide compelling indicators that markers of mitochondrial network dynamics do not directly reflect mitochondrial or skeletal muscle physiology in offspring exposed to both maternal ObWD as well as postweaning WD consumption.

DISCUSSION

Studies in humans and animals have shown reduced mitochondrial abundance and network integrity develop in tandem with insulin resistance (302; 308) and obesity (224). Mitochondrial network adaptation to acute and chronic stress is mediated by fission and fusion events and activation of quality control pathways that result in mitophagic pruning of dysfunctional network components. The interaction between mitochondrial network's structure and function is evident in distinct subpopulations of mitochondria that redirect lipid and glucose metabolism depending on network structure (329-331). Loss of mitochondrial fusion through depletion of MFN or OPA1 leads to swollen, spherical mitochondria with collapsed cristae and reduced membrane polarization (332). Excessive mitochondrial fission promotes fragmentation of the mitochondrial network (333) and negatively correlates with markers of insulin sensitivity and fatty acid oxidation in muscle (334; 335). In our model, mWD offspring challenged with a pwWD shifts mitochondrial network dynamics toward suppression of mitochondrial fusion and increased fission in offspring skeletal muscle. In rodents, maternal obesity is associated with reduced OXPHOS protein abundance and skewed mitochondrial fission/fusion machinery in offspring skeletal and cardiac muscle and persisted into subsequent generations in both male and female progeny (13). One explanation for elevated fission in mWD offspring in response to pwWD may be due to mitochondrial calcium stress and oxidative stress. Decreased mitoNEET, VDAC1 and MFN2 abundance would correspond with calcium-induced loss of mitochondrial-associated membrane (MAM) interactions and redox imbalance (317; 336; 337). Consistent with reductions in CI abundance, CI respiration, and reduced markers of network quality control in mWD offspring in the present study, calcium stress has been shown to activate mitochondrial and cytosolic calpains that degrade CI and inhibit the clearance of damaged mitochondria by depleting substrates necessary for mitophagy (315).

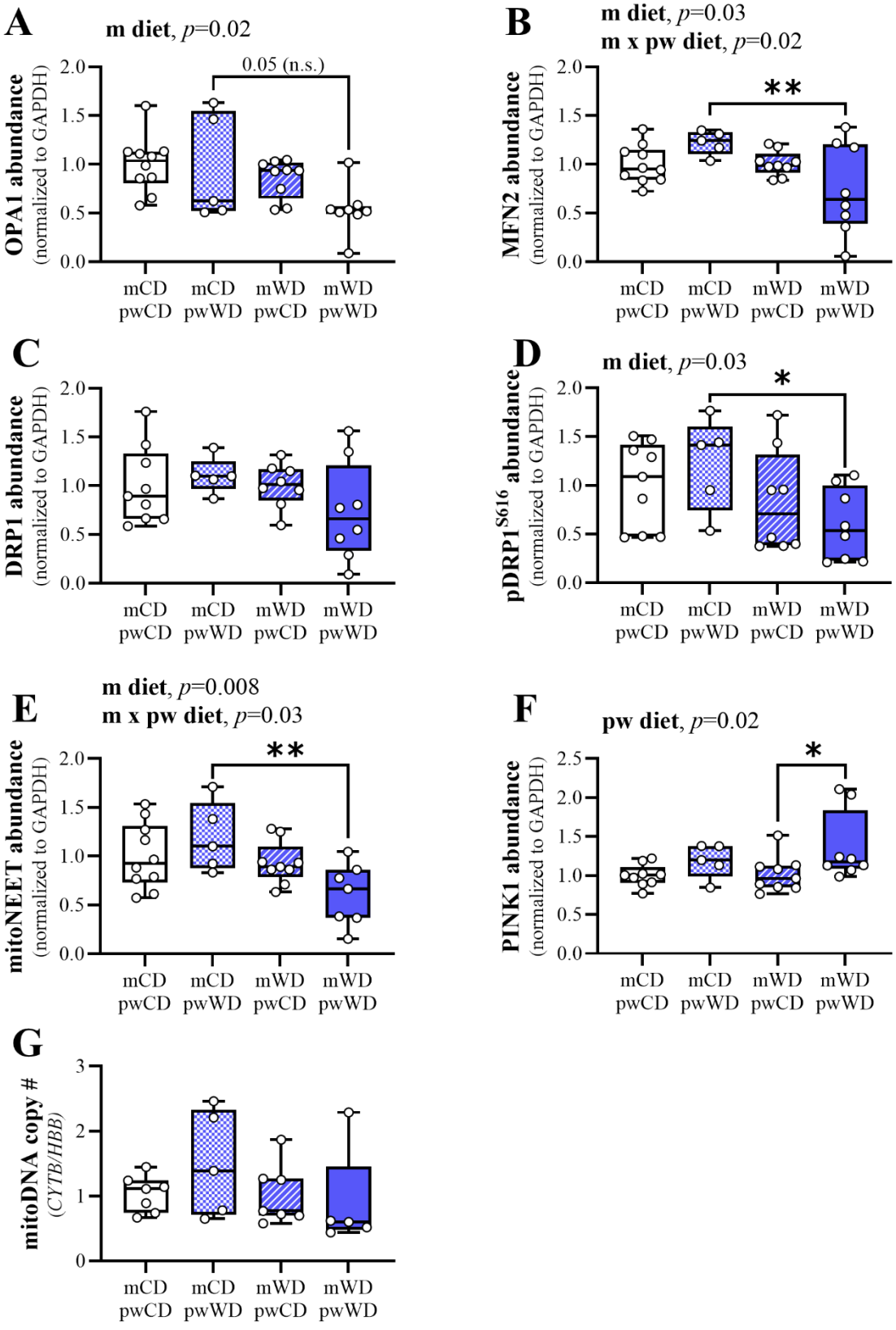
A
m diet, p=0.02
0.05 (n.s.)
OPA1 abundance
(normalized to GAPDH)
B
m diet, p=0.03
m x pw diet, p=0.02
**
MFN2 abundance
(normalized to GAPDH)
C
DRP1 abundance
(normalized to GAPDH)
D
m diet, p=0.03
*
pDRP1S616 abundance
(normalized to GAPDH)
E
m diet, p=0.008
m x pw diet, p=0.03
**
mitoNEET abundance
(normalized to GAPDH)
F
pw diet, p=0.02
*
PINK1 abundance
(normalized to GAPDH)
G
mitoDNA copy #
(CYTB/HBB)
mCD pwCD
mCD pwWD
mWD pwCD
mWD pwWD

Figure 4.1 – Protein abundance of enzymes regulating mitochondrial network dynamics and represent mitochondrial homeostasis were measured by Simple Western for OPA1 (A), MFN2 (B), DRP1 (C), phosphorylated (p)-DRP1 at S616 (D), mitoNEET (E), PINK1 (F), and mitoDNA copy # (G) in 3Y offspring gastroc. Individual protein abundance was normalized to housekeeping protein GAPDH. Data were analyzed by 2-way ANOVA for significant main effects of maternal or postweaning diet or interactions with Sidak's multiple comparisons test. *P*-values for significant main effects are listed above each graph. For post-hoc analysis, carets (^p<.05, ^^p<.01) indicate significant differences by maternal diet within the same postweaning diet group and asterisks (*p<.05) indicate significant differences by postweaning diet within the same maternal diet group. Individual data points for offspring are shown with group minimum, maximum, median, and interquartile range. Male (M) offspring are indicated by circles and female (F) offspring by triangles. Sample size for each group by sex: mCD/pwCD, 5-6F/4M; mCD/pwWD, 2F/3M; mWD/pwCD, 3F/5-6M; mWD/pwWD, 5F/2-3M. For mitoDNA copy #, n = mCD/pwCD, 4F/3M; mCD/pwWD, 2F/3M; mWD/pwCD, 3F/4M; mWD/pwWD, 3F/2M.

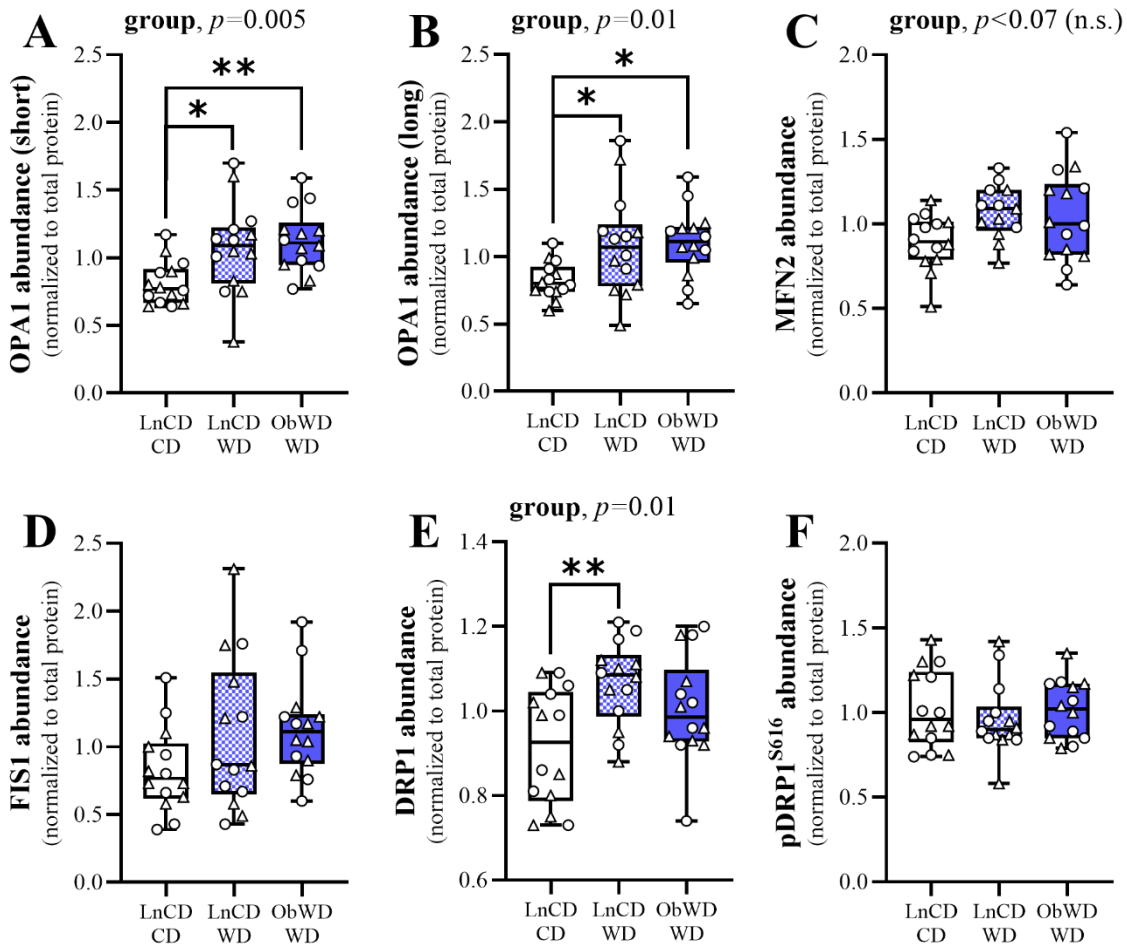

Figure 4.2 – Regulators of mitochondrial fusion and fission were measured by Western blot in gastroc of juvenile (1Y) offspring weaned to a WD ± early life obesogenic exposure (ObWD). Protein abundance of OPA1, including short (A) and long (B) isoforms, MFN2 (C), FIS1 (D), DRP1 (E), and phosphorylated (p)-DRP1 at S616 (F) were measured and normalized to total protein abundance (TGX Stain-free technology, Bio-Rad). Data were analyzed by 2-way ANOVA for significant main effects of offspring group or sex or interactions with Tukey's multiple comparisons test. *P*-values for significant main or interactive effects are listed above each graph. For post-hoc analysis, asterisks (*p<.05, **p<.01) indicate significant differences by offspring group. Individual data points for offspring are shown with group minimum, maximum, median, and interquartile range. Male (M) offspring are indicated by circles and female (F) offspring by triangles. Sample size for each group by sex: LnCD/CD, 7F/7M; LnCD/WD, 6-7F/7M; ObWD/WD, 7F/7M.

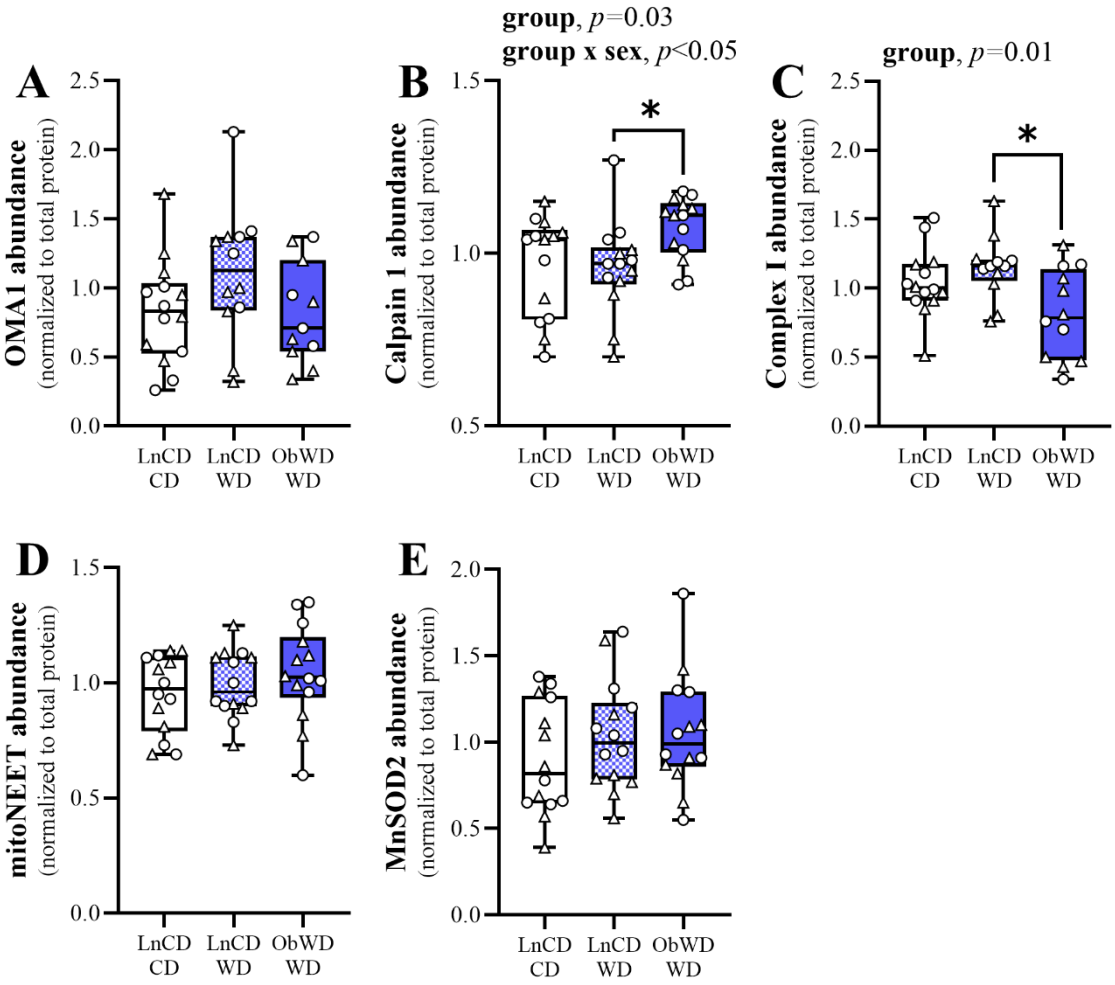

Figure 4.3 – Enzymes involved in cellular stress responses and redox balance – OMA1 (A), Calpain I (B), Complex 1 (C), mitoNEET (D), and MnSOD2 (E) – were measured by Western blot in juvenile gastroc. Individual proteins were normalized to total protein abundance. Data were analyzed by 2-way ANOVA for significant main effects of offspring group or sex or interactions with Tukey's multiple comparisons test. *P*-values for significant main or interactive effects are listed above each graph. For post-hoc analysis, an asterisk (*p<.05) indicate significant differences by offspring group. Individual data points for offspring are shown with group minimum, maximum, median, and interquartile range. Male (M) offspring are indicated by circles and female (F) offspring by triangles. Sample size for each group by sex: LnCD/CD, 7F/7M; LnCD/WD, 6-7F/6-7M; ObWD/WD, 5-7F/6-7M.

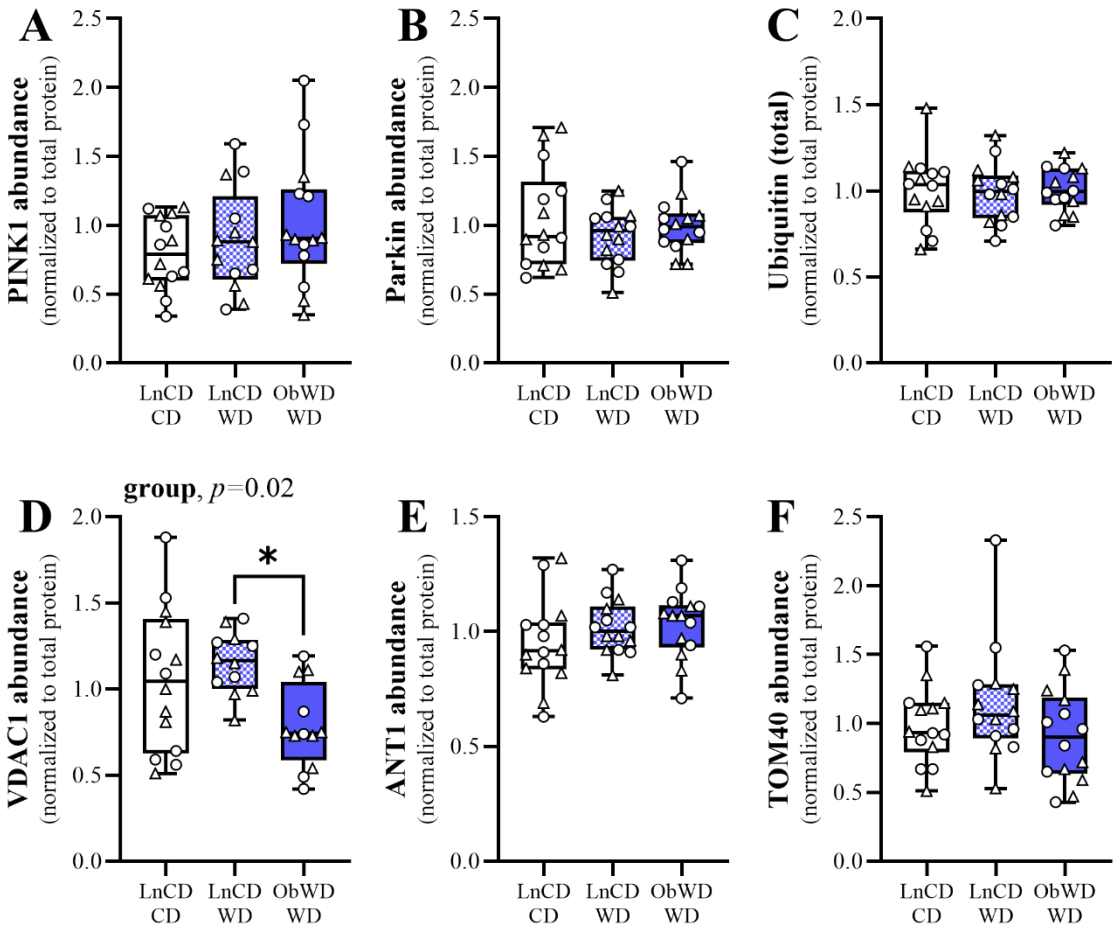

Figure 4.4 – Protein content of proteins involved in mitophagy, like PINK1 (A), Parkin (B), total ubiquitin (C), and VDAC1 (D), in addition to mitochondrial transporters ANT1 (E) and TOM40 (F) were measured by Western blot in juvenile gastroc. Data were analyzed by 2-way ANOVA for significant main effects of offspring group or sex or interactions with Tukey's multiple comparisons test. *P*-values for significant main or interactive effects are listed above each graph. For post-hoc analysis, an asterisk (*p<.05) indicate significant differences by offspring group. Individual data points for offspring are shown with group minimum, maximum, median, and interquartile range. Male (M) offspring are indicated by circles and female (F) offspring by triangles. Sample size for each group by sex: LnCD/CD, 7F/7M; LnCD/WD, 6-7F/6-7M; ObWD/WD, 6-7F/6-7M.

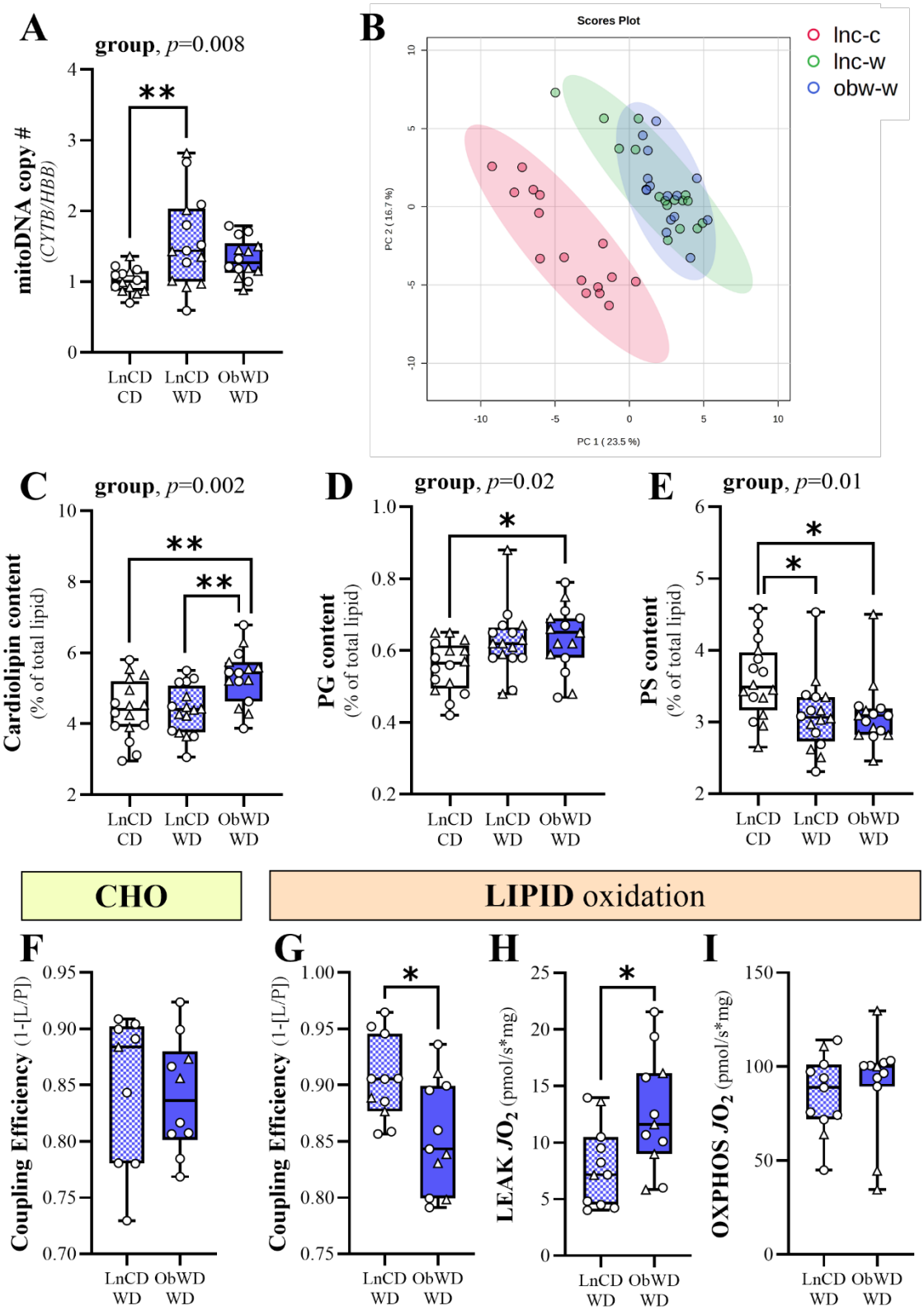
A
group, p=0.008
mitoDNA copy #
(CYTB/HBB)
**
LnCD CD
LnCD WD
ObWD WD
B
Scores Plot
lnc-c
lnc-w
obw-w
PC 2 (16.7 %)
PC 1 (23.5 %)
C
group, p=0.002
Cardiolipin content
(% of total lipid)
**
**
D
group, p=0.02
PG content
(% of total lipid)
*
E
group, p=0.01
PS content
(% of total lipid)
*
*
CHO
LIPID oxidation
F
Coupling Efficiency (1-[L/P])
G
Coupling Efficiency (1-[L/P])
*
H
LEAK JO2 (pmol/s*mg)
*
I
OXPHOS JO2 (pmol/s*mg)

Figure 4.5 – Mitochondrial (mito)DNA relative to nuclear DNA, or mito copy # (A), was assessed in juvenile gastroc. Mitochondrial phospholipid content was measured as % of total mito lipids in crude mitochondria enriched from juvenile gastroc. Principle Component Analysis shows overlap of all mito lipidome subspecies by group (B). Phospholipids specific to mitochondrial membranes, cardiolipin (C) and PG (D), as well as ER-specific phospholipid PS (E), are shown. Mitochondrial coupling efficiency ratios with both carbohydrate (F) and lipid (G) substrates are shown in PMFB from gastroc of pw WD offspring from LnCD or ObWD. Oxygen flux (JO_2) with lipid substrate at LEAK (H) and maximal OXPHOS (I) states are presented normalized to tissue weight. MitoDNA copy # and individual phospholipid data were analyzed by 2-way ANOVA for significant main effects of offspring group or sex or interactions with Tukey's multiple comparisons test. *P*-values for significant main or interactive effects are listed above each graph. For post-hoc analysis, an asterisk (**p*<.05, ***p*<.01) indicate significant differences by offspring group. Respirometry data analyzed by Student's t-test with significant effects by ObWD represented as **p*<0.05. Individual data points for offspring are shown with group minimum, maximum, median, and interquartile range. Male (M) offspring are indicated by circles and female (F) offspring by triangles.

V. EXPERIMENTAL PARADIGM: MATERNAL HYPERANDROGENEMIA

MODELS of MATERNAL ANDROGEN STRESS

Within the context of DOHaD, experiments in animal models have demonstrated that the timing of androgen exposure during fetal development dictates the degree and extent of adverse reproductive and metabolic outcomes in offspring. Prenatal androgen exposure during early- to mid-gestation in sheep results in reduced ovarian reserve (338), FGR, altered insulin sensitivity, and catch-up growth during early life in female offspring with minimal to no alterations to insulin sensitivity by adulthood (14; 339). Prenatal exposure to excess androgens during late gestation in rodents resulted in complicated fetal development – i.e., smaller embryos and fetuses (340) – and reduced cardiomyocyte proliferation in fetal hearts resulting in cardiac hypertrophy in adulthood (341). Female mice exposed to maternal HA in late gestation demonstrated neuroendocrine abnormalities, dysfunctional pancreatic islets, visceral adipocyte hypertrophy, and impaired glucose tolerance as adults (342). Rodent studies of fetal exposure to maternal HA provide evidence of adverse, multigenerational consequences to fetal growth and glucose and lipid metabolism in subsequent generations (155; 343). These models suggest that the added metabolic complications introduced by maternal WD/obesity in combination with prenatal androgen exposure have a more dramatic impact on adverse outcomes in offspring than either treatment alone (340; 344).

The reproducibility, reliability, and translatability of findings in these pre-clinical models is challenged by variations in the source of exogenous testosterone (T) and the timing/duration of HA induction/exposure (141). These challenges are compounded by the metabolic and hormonal milieu of obesity, glucose intolerance, and insulin resistance, metabolic abnormalities that may result from blunted glucose uptake due to loss of insulin sensitivity in skeletal muscle (345; 346). Much work remains in understanding the independent and interactive impact of chronic androgen exposure and diet-induced obesity over time on the metabolic integrity of skeletal muscle in reproductive-aged females and their offspring.

DEPICTION of the RHESUS MACAQUE

Rhesus macaques are one of the most genetically similar models available for human biomedical research (347). *Homo sapiens* share ~93% of their DNA sequence (348), and 97% of their exomes, with Rhesus macaques (347; 349). Similar susceptibility to environmental obesogenic pressures as humans (350), and the natural occurrence of hyperandrogenemia in female Rhesus macaques who present with phenotypes observed with human PCOS (351), make them an attractive model of PCOS and female health, fertility, and offspring outcomes (352).

In addition to naturally occurring HA in female rhesus macaques, experimental induction of HA has been studied chronologically in this animal model to understand the etiology of PCOS (141). Prenatal exposure to excess androgens during early and/or late gestation altered female reproductive anatomy (353), neuroendocrine development and function (353-355), behavior patterns (355), and increases adult abdominal fat deposition (356) in exposed females. A single dose of T administered to neonates within 24-hours of delivery did not impact ovarian function (357). Short-term exposure to HA (3-10 days) in adult females was sufficient to induce polyfollicular ovaries (358). While long-term (13-16 months) administration of low- or high-dose T (80 ng/dL or 115 ng/dL serum, respectively) was not observed to have an effect on ovarian morphology, high T reduced menstrual cycle frequency in these females (359). To build upon this line of investigation requires the design of a primate model able to capture the complexities of chronic androgen excess with and without dietary metabolic adversity observed in human pathogenesis of T2D and CVD.

Previous Findings in Rhesus macaque

Extensive work by R.L. Stouffer and colleagues at the Oregon National Primate Research Center over the last decade has characterized the reproductive and metabolic impacts of elevated androgens (i.e., testosterone, T) with and without additional WD stress in young female macaques. Initial investigations assessed the outcome of chronic T prior to and throughout puberty on neuroendocrine patterns and insulin sensitivity in adulthood. T implants were placed subcutaneously in juvenile female macaques at 1-year of age (360). While LH response to GnRH and pulse frequency was increased in T-treated animals at ages 4 and 5, respectively, insulin

sensitivity remained unchanged (360). To determine the combined effect of T with diet-induced obesity, these animals were maintained on a WD beginning at 5.5 years old. After consuming WD for 16-months, body fat increased >13% in controls and >17% in T-treated females. Importantly, central or visceral fat, a marker associated with reduced insulin sensitivity (361), was increased by 15.7% in WD controls and 21.2% in T+WD animals, suggesting augmented WD-induced weight gain in the presence of androgen (326). Similarly, after 12 months on WD, only the combination of T with WD show signs of insulin resistance, suggesting that the addition of androgen with obesity was more deleterious than obesity alone at this timepoint (326). Visceral white adipose tissue (WAT) collected at this timepoint is prone to lipid storage and resistant to lipolysis in T-treated WD females, indicating an exaggerated phenotype with a propensity for visceral fat accumulation with the combination of T+WD (362). Exacerbated adipose tissue dysfunction after 3 years of T, WD, and T+WD have been confirmed (363) in parallel with accelerated fat mass accumulation and insulin resistance (364). In addition to adverse metabolic signatures, this group has also shown that WD-induced obesity and HA impedes reproductive outcomes through impaired fertility (365-369), decreased oocyte quality (370), and pregnancy complications (371; 372) in these female rhesus monkeys.

PROJECT DESIGN

Study 1: Hyperandrogenemia & Obesity Impact on Young Female Monkey Metabolism

To determine how chronic T impacts female systemic and skeletal muscle insulin sensitivity with and without diet-induced obesity, young (2 to 2.5 years-old) female rhesus macaques were assigned to one of four groups (n=10/group). These groups include 1) control, 2) T-treated, 3) WD, and 4) T+WD-treated. No animals had reached menarche at time of assignment but were expected to in Year (Y)1. Animals were maintained on their assigned hormonal and/or diet treatment for 4 years (from age 2 to 6 years-old).

Chronic Testosterone Treatment

Exogenous Testosterone (T) treatment was initiated at time of assignment in half (n=20) of study animals via subcutaneous implant of T-releasing capsules as previously reported (360). Initially, T was mixed with cholesterol at a 1:10 ratio and concentration adjusted, along with capsule length,

until target T in serum was achieved/maintained in all female monkeys in Groups #2 and #4. T concentration was between 1.0 and 1.5 ng/mL. This target amount is 3-4 times higher than what is normal for young female monkeys and reiterates the modest elevation in androgens observed in pubertal girls with PCOS (373; 374). Remaining control animals (*n*=20) not assigned to T treatment – i.e., Groups #1 and #3 – received an identical subcutaneous Vehicle (V) implant containing only cholesterol following group assignment. T implants were changed if serum T fell below the 1.2 ng/mL threshold in T-treated animals (approx. every 4-8 weeks). Cholesterol control implants (Vehicle, V) were replaced at a matching rate for the duration of the study.

Chronic Western-style Diet Treatment

10 females from the T-treated group and 10 non-T-treated controls will be placed on a fiber-balanced monkey chow/control diet (CD) (Primate Diet no. 5000; Purina LabDiet, St. Louis, MO). These groups – Groups #1 and #2 – will be fed twice a day with meals supplemented with fresh fruits and vegetables. The remaining 20 animals will be placed on a high fat, calorically dense Western-style Diet (WD) (5L0P; Purina LabDiet, St. Louis, MO) and fed *ad libitum.* WD was also supplemented with calorically dense peanut butter treats and high fructose (20%) beverages were also provided.

Study 2: Gestational HA & Obesity on Fetal Muscle Metabolism

The second part of this study was a fertility study. During the first half of Y4, all female animals were paired with fertile males. Pregnancy was confirmed as previously described (375). Animals that did not become pregnant during this first round were re-mated during the second half (6 months) of Y4. A subset of fetal skeletal muscle tissues were collected after caesarian section on gestational day (G) 130.

Aim #3

The first part of Aim #3 will investigate the impact of chronic androgen (T) exposure starting pre-puberty with and without WD-induced obesity on young female skeletal muscle function. Oxidative metabolism and insulin signaling will be assessed in conjunction with the development of systemic glucose dynamics and obesity after two years of treatment. The second

part of Aim #3 will investigate how T +/- WD impact offspring skeletal muscle metabolism in late gestation. Altogether, these experiments will provide evidence of how skeletal muscle function responds to HA and obesity, how these alterations may contribute to development of MetS in exposed females, and how these stressors are translated to fetal muscle function toward the end (third-term) of gestation.

VI. AIM #3

CHRONIC HYPERANDROGENEMIA IMPAIRS SKELETAL MUSCLE INSULIN SENSITIVITY and MITOCHONDRIAL METABOLISM in the ABSENCE of OBESITY in FEMALE RHESUS MACAQUES

Greyslak KT, Campodonico-Burnett W, Hetrick B, Carey K, True C, Takahashi DL, Spangenburg EE, Gertsman I, Stouffer RL, Roberts CT, McCurdy CE. *Manuscript in preparation.*

INTRODUCTION

To date, this group has not investigated the independent and combined impacts of chronic exposure to T and WD on skeletal muscle function. Therefore, the final aim of this dissertation will characterize aspects of skeletal muscle physiology to identify potential mechanisms underlying metabolic dysfunction and how it contributes to the broader picture of this NHP collaboration. Furthermore, the influence of these environmental stressors on the programming of fetal skeletal muscle function in a small cohort of offspring will be assessed and interpreted through the lens of potential contributions to future T2D or CVD development.

METHODS

Animals

All animal procedures were conducted under regulatory compliance at the Oregon National Primate Research Center (ONPRC) and Oregon Health & Science University, which is accredited by the Association for Assessment and Accreditation of Laboratory Animal Care (AAALAC) International. Experiments were designed and reported with reference to the Animals in Research: Reporting In Vivo Experiments (ARRIVE) guidelines (271).

To determine how chronic T impacts female systemic and skeletal muscle insulin sensitivity with and without diet-induced obesity, young (2 to 2.5 years-old) female rhesus

macaques were assigned to one of four groups (*n*=10/group). These groups include 1) control, 2) T-treated, 3) WD, and 4) T+WD-treated. No animals had reached menarche at time of assignment but were expected to in Year (Y)1. Animals were maintained on their assigned hormonal and/or diet treatment for 4 years (from age 2 to 6 years-old).

Chronic Testosterone Treatment

Exogenous Testosterone (T) treatment was initiated at time of assignment in half (*n*=20) of study animals via subcutaneous implant of T-releasing capsules as previously reported (360). Initially, T was mixed with cholesterol at a 1:10 ratio and concentration adjusted, along with capsule length, until target T in serum was achieved/maintained in all female monkeys in Groups #2 and #4. T concentration was between 1.0 and 1.5 ng/mL. This target amount is 3-4 times higher than what is normal for young female monkeys and reiterates the modest elevation in androgens observed in pubertal girls with PCOS (373; 374). Remaining control animals (*n*=20) not assigned to T treatment – i.e., Groups #1 and #3 – received an identical subcutaneous Vehicle (V) implant containing only cholesterol following group assignment. T implants were changed if serum T fell below the 1.2 ng/mL threshold in T-treated animals (approx. every 4-8 weeks). Cholesterol control implants (Vehicle, V) were replaced at a matching rate for the duration of the study.

Chronic Western-style Diet Treatment

10 females from the T-treated group and 10 non-T-treated controls will be placed on a fiber-balanced monkey chow/control diet (CD) (Primate Diet no. 5000; Purina LabDiet, St. Louis, MO). These groups – Groups #1 and #2 – will be fed twice a day with meals supplemented with fresh fruits and vegetables. The remaining 20 animals will be placed on a high fat, calorically dense Western-style Diet (WD) (5L0P; Purina LabDiet, St. Louis, MO) and fed *ad libitum.* WD was also supplemented with calorically dense peanut butter treats and high fructose (20%) beverages were also provided.

Anthropometric Measures

Nonfat mass, fat mass, lean mass, and bone mineral content were measured with DEXA in young female macaques as previously described (258).

Intravenous Glucose Tolerance Testing

Intravenous glucose tolerance tests (i.v. GTT) were conducted as previously described (195; 258). Baseline blood samples were obtained prior to the infusion and at 1, 3, 5, 10, 20, 40, and 60 min after infusion. Glucose was measured immediately with OneTouch Ultra blood glucose monitor (LifeScan), and the remainder of the blood was kept in heparinized tubes on ice for insulin measurement. After centrifugation, samples were stored at -80°C until assayed. Insulin measurements were performed by the Endocrine Technologies Core at ONPRC using a chemiluminescence-based automatic clinical platform (cobase 411; Roche Diagnostics, Indianapolis, IN). HOMA of insulin resistance (HOMA-IR) was calculated from fasting insulin and glucose values with the following formula: (insulin (mU/L) * glucose (mg/dL))/405.

Adult Glucose-Stimulated Muscle Biopsy, Biological Measures & Tissue Collection

All 40 female animals underwent metabolic profiling via intravenous Glucose/Insulin Tolerance Testing (i.v. GTT and i.v. ITT, respectively) and Dual Energy X-Ray Absorptiometry (DEXA) scans twice a year through Y4. Pre- and post-stimulated muscle biopsies were collected from female monkeys in Y2. In short, skeletal muscle biopsies (~30 mg) were collected from gastrocnemius muscle before (basal) and 10 minutes after (post-stim) administering a glucose bolus (0.6 g/kg) in anesthetized animals. ~10 mg of basal biopsy tissue was shipped fresh in ice-cold BIOPS (biopsy preservation solution) to measure substrate metabolism by high-resolution respirometry (HRR). The remaining basal biopsy (20 mg) and post-stim biopsy were flash-frozen and saved for (i) measurement of intramuscular insulin signaling and (ii) metabolomics.

In the fetal programming study, anthropometric fetal data including weight, crown-rump length, head circumference, etc. was recorded at time of necropsy (G130). Gastroc and soleus muscles (10-15 mg) were placed in ice-cold BIOPS and shipped overnight for next-day respirometry analysis using HRR.

Fetal Necropsy Collection

As previously reported (194; 239).

Permeabilized Muscle Fiber Bundle Preparation & Respirometry

Mitochondrial respiratory function was measured in permeabilized muscle fiber bundles (PMFBs) with high-resolution respirometry with an Oxygraph-2k system (Oroboros Instruments, Innsbruck, Austria). Muscles fiber bundles (3–5 mg) were dissected from gastroc and then permeabilized with 30 mg/mL saponin in BIOPS for 30 min, washed, blotted dry, and weighed. All respirometry data were collected at 37°C in a super-oxygenated environment (200–400 mmol/L O2), and two titration protocols were run in parallel to measure respiration with lipid and nonlipid substrates as previously described (194). Mitochondrial integrity was confirmed by measurement of respiratory responses to cytochrome c.

Protein Analysis

Frozen gastroc (50–100 mg) were homogenized mechanically in 0.6 mL buffer (195) with six 2.8-mm ceramic beads (VWR International) in a Bead Ruptor (OMNI International, Kennesaw, GA) at a rate of 6 m/s for 2 × 30 s intervals kept at 4°C with a cryo-cool instrument adaptor. Homogenate was then rotated for 1 h at 4°C on an orbital platform and then centrifuged at 13,000g for 15 min at 4°C. Protein concentration was determined with a BCA kit (Pierce and Thermo Fisher Scientific). Protein abundance was analyzed by capillary immunoassay on a Wes instrument per manufacturer instructions (ProteinSimple, Bio-Techne; San Jose, CA) with 3 mL of 0.25 or 1.25 mg/mL of sample. Antibody concentrations were optimized and multiplexed with target protein abundance quantified with Compass software (ProteinSimple, Bio-Techne) and normalized to a loading control protein.

RESULTS

Baseline Characteristics of Female Juveniles

40 juvenile (prepubertal) female Rhesus Macaques ~2.5 years-old were assigned to one of four groups. 10 young females were assigned a chow diet (CD) with a vehicle control implant containing cholesterol (group “C”); 10 were assigned to chow diet with exogenous testosterone (T) treatment (i.e., group “T”); 10 were assigned to a high fat, high sugar Western Diet (WD, group “W”); and the remaining 10 females were assigned to WD with exogenous testosterone implant (group “T+W”). There was a main effect by T-treatment on age and % body fat such that females assigned to T or T+W conditions were significantly younger and leaner (Table 6.1). Importantly,

there was no difference in glucose tolerance or systemic insulin resistance across groups at the start of this study (Table 6.1).

Adiposity & Development of Insulin Resistance in Young Females

After 2 years on their assigned treatment, body fat distribution and glucose/insulin dynamics were assessed in these adolescent females. As intended, both groups treated with exogenous T had a statistically similar average circulating T conc. between 1.0 and 1.5 ng/mL (Table 6.2). While increased body mass was not statistically significant in T+W females, these animals were >1.0 kg heavier, on average, than the other 3 groups (Table 6.2 and Fig. 6.1A). Indeed, % fat mass in animals consuming WD was significantly higher than females consuming CD and is driven by T+W females (Table 6.2, Fig. 6.1B). Android body fat distribution, typically observed in male obesity development, is associated with poorer insulin sensitivity relative to gynoid body fat distribution, which is typical of female overweight and obesity development. With the addition of another year of treatment (i.e., at Year 3), females chronically consuming WD had significantly more android fat relative to total body fat which was exacerbated with the addition of T supplementation (Fig. 6.1C). Interestingly, both T groups had significantly less gynoid fat relative to total body fat in this third year of treatment (Fig 6.1D). The combined significant increase in android fat and significant decrease in gynoid fat in T+W females in Year 3 would suggest a pronounced loss in insulin sensitivity in these female animals at this timepoint. By Year 2, this phenotype in adipose tissue deposition was far less robust, however there was a significant increase in android fat in both WD groups (Table 6.2).

In contrast to these modest shifts in body fat at Year 2, WD groups were significantly more hyperinsulinemic and insulin resistant per i.v. GTTs (Table 6.2). While glucose tolerance is able to be maintained in Year 2 relative to baseline across groups, it is clear this is the result of insulin hypersecretion in response to a glucose load predominantly seen in T+W females (Fig. 6.1E and F). Per the Homeostatic Model Assessment for Insulin Resistance, or HOMA-IR, this development of systemic insulin resistance with WD was significantly amplified upon addition of exogenous T after only 2 years (Fig. 6.1G). Due to the minute changes in regional adipose tissue accruement and burgeoning loss in insulin sensitivity at this earlier timepoint and given skeletal muscles primary role in glucose uptake in response to insulin, we chose to evaluate skeletal muscle's role

in the pathogenesis of metabolic dysfunction after only 2 years of hyperandrogenemia and obesogenic diet.

Insulin Signaling in Skeletal Muscle of Young Females After Years of HA and/or Obesity

To better understand skeletal muscle's contribution to systemic insulin resistance *in vivo*, skeletal muscle response to insulin stimulation was determined using biopsies taken from the gastroc of these animals in Year 2 of treatment. In scenarios of insulin sensitivity/successful response to insulin signaling, the binding of insulin to its receptor transmits its signal across the cell membrane, triggering the autophosphorylation of insulin receptor substrate 1 (IRS1) at tyrosine residues like Y687. While there was no difference in total IRS1 abundance across groups, there was a significant increase in phosphorylation (p) of IRS1 @Y687 observed in W+T muscle that rivaled what was observed in controls but was absent in WD females with no T (Fig. 6.2A and B). Similarly, while there is no significant difference in total abundance of Akt, its activation via phosphorylation at S473 downstream of pIRS@Y687 are seen in T and T+W gastroc, albeit to a lesser extent than that of C females (Fig. 6.2C and E). While trending in controls, the contribution of Akt activation by the additional phosphorylation of Akt @T308 following glucose bolus was not significant in any group (Fig. 6.2D). While the response to insulin *in vivo* in skeletal muscle from T+W females initially seemed to rival the degree of insulin sensitivity observed in control female gastroc, subsequent analysis of blood insulin concentration in these animals at time of biopsy show that WD groups, namely T+W, animals were hyperinsulinemic prior to glucose bolus (Fig, 6.2F). Therefore, skeletal muscle insulin sensitivity in T+W females was not comparable to healthy control females but rather conflated by preexisting metabolic dysfunction.

Mitochondrial Function in Females at Year 2

In skeletal muscle from adult patients with Type 2 Diabetes or obesity, mitochondrial dysfunction is associated with loss of insulin sensitivity. Therefore, to see how mitochondrial function in skeletal muscle corresponds with the previous findings in skeletal muscle *in vivo* insulin sensitivity, we measured oxidative capacity in PMFB partitioned from the "basal" biopsy of these females. While there are some minor nuances in how T or W independently result in decreased oxidation rates for both lipid (Fig. 6.3A) and carbohydrate (Fig. 6.3B) substrates, both lipid and

carbohydrate oxidation in T+W muscle mirror our findings in skeletal muscle insulin sensitivity within this same group (Fig. 6.3).

Mitochondrial Function in Fetal Skeletal Muscle of T & W Pregnancies

To determine how maternal hyperandrogenemia (HA) and metabolic health translate to fetal skeletal muscle function, we measured lipid oxidation (Fig. 6.4A-C) and nonlipid oxidation (Fig. 6.4D-I) in fetal gastroc at gestational day (G)130. In all offspring, there is a significant interactive effect by sex and diet on proton leak normalized to maximal ADP-stimulated phosphorylation capacity (Leak/OXPHOS) in the presence of lipid substrate (Fig. 6.4A). Smaller Leak/OXPHOS values represent better coupling efficiency between the proton gradient generated by lipid oxidation to phosphorylation capacity at saturating concentrations of ADP. Upon separation of these groups by sex, it appears that this effect is driven by female offspring muscle exposed to maternal hyperandrogenemia (HA) who have reduced Leak/OXPHOS that is not observed in the other female groups nor in male fetuses (Fig. 6.4B and C).

Regarding carbohydrate oxidation in the gastroc of these animals, there appears to be a similar interactive effect between fetal sex and maternal diet observed with fetal lipid oxidation. These ratios include maximal Complex (C)I-linked (CI-flux) OXPHOS (Fig. 6.4D-F) or maximal ADP-stimulated OXPHOS (Fig. 6.4G-I) both normalized by maximally uncoupled Electron Transport System (ETS) capacity in the presence of nonlipid substrate. Smaller values of CI-flux/ETS capacity could result from reduced CI contribution to mitochondrial oxygen consumption and/or an increased reserve in maximal ETS ability to pass electrons. To this end, it appears that offspring exposed to maternal T+W rely more on CI and/or have decreased maximal ETS capacity (Fig. 6.4D). When analyzing these data independently by sex, this phenotype is not driven by females (Fig. 6.4E) but by males exposed to mWD (Fig. 6.4F). This observation is maintained with OXPHOS/ETS such that fetal offspring exposed to mWD appear to have a larger response to saturating concentrations of ADP and/or have less spare ETS capacity (Fig. 6.4G). This phenotype in the gastroc of exposed fetal offspring is not caused by females (Fig. 6.4H) but by males from mWD independent of maternal androgen treatment (Fig. 6.4I).

DISCUSSION

Hyperandrogenemia (HA) is a hallmark of Polycystic Ovary Syndrome (PCOS), the most common endocrinopathy in individuals during their childbearing years (142). HA is often present alongside the development of obesity and is a leading cause of infertility worldwide (376). To better understand how the addition of HA in the presence of obesity impact fetal physiology and skeletal muscle phenotypes, we first sought to better understand how maternal metabolic health is impacted by chronic HA (testosterone, T) with and without chronic Western (WD) diet consumption in young, healthy females prior to pregnancy. We find that the difference made by one year – i.e., from two to three years of treatment – was enough to shift adipose tissue distribution in a pattern associated with amplified resistance to insulin (i.e., abdominal fat) only in W+T treated females (361). Previous work on adipocyte dysfunction in these animals show a more robust phenotype at year 3 of treatment relative to year 2 (363). However, after two years of treatment, WD consuming females were hyperinsulinemic, glucose intolerant, and insulin resistant – the presence of which was driven by W+T group (Table 6.2). As skeletal muscle accounts for up to 80% of glucose uptake in response to insulin, we were curious if subtle shifts in insulin sensitivity and oxidative capacity were present at year 2 in biopsies from these females in response to a glucose bolus. We see that insulin signaling is suppressed in animals consuming WD at the level of IRS1 (upstream) and Akt (downstream) activation that, unexpectedly, appears to be rescued by the addition of T in T+W animals (Fig. 6.2). However, at time of biopsy, this is due to hyperinsulinemia in T+W females, who had ~2-times the concentration of insulin compared to control females (Fig. 6.2F). Chronic hyperinsulinemia is a primary feature of MetS and is implicated in the pathogenesis of insulin resistance and eventual T2D and CVD. Therefore, this seemingly intact insulin signaling in T+WD animals at 2 years of treatment is likely driven by compensatory hyperinsulinemia in response to systemic insulin resistance, an adaptation able to maintain muscle insulin response at this early timepoint but unlikely to be maintained indefinitely, ultimately resulting in more severe metabolic dysfunction upon aging.

We also find that mitochondrial oxidative capacity in skeletal muscle *ex vivo* corresponds with markers of insulin signaling such that the addition of T appears to rescue reduced oxidation by chronic WD consumption to that of controls. Of interest is the reduction in mitochondrial respiration (i.e., oxidative capacity) in T-treated females at this timepoint independent of WD with lipid or non-lipid substrates. WD alone appears to impact lipid oxidation more significantly than non-lipid oxidation, a phenotype that is revealed upon maximal stimulation of coupled and

uncoupled CI+II respiration with non-lipid fuels. Although subtle, mitochondrial dysfunction is present by year 2 of T treatment prior to dysregulated insulin signaling in this group. While not enough to confirm that mitochondrial dysfunction precedes insulin resistance in skeletal muscle of HA females at this timepoint, these data support this possibility. These data confirm prior studies in rodent models of PCOS and insulin resistance that show impaired mitochondrial function, decreased autophagy, and increased activation of mTORC1 in skeletal muscle of PCOS-induced females *in vivo* and *in vitro* (377). Human women with PCOS present with mitochondrial DNA variants that may contribute to or induce mitochondrial dysfunction (378). Oxidative stress may underly these mitochondrial impairments, as gender-affirming testosterone therapy for individuals born with ovaries induces mitochondrial dysfunction and elevated oxidative stress in isolated leukocytes (379). Additional support for the implication of ROS in development of mitochondrial dysfunction can be seen in a rat model of PCOS treated with the antioxidant MitoQ, upon which mitochondrial ATP production, markers of oxidative stress, and antioxidant proteins were rescued relative to those not receiving MitoQ treatment (380). While not a mechanistic explanation of how androgen alters mitochondrial function, there is evidence to suggest the steroid hormone 17β-estradiol improves mitochondrial respiration and ROS generation in skeletal muscle (381) through a mechanism involving mitochondrial membrane viscosity (382). A similar direct or indirect mechanism may describe the phenotype caused by excess androgens in these young females, however more work is still needed.

We have previously demonstrated that early life exposure to obesogenic stress redirects offspring skeletal muscle: oxidative capacity, substrate utilization, insulin sensitivity and glucose uptake, lipid handling, oxidative stress dynamics, mitochondrial lipidome composition and network dynamics. These phenotypes are observed at fetal, juvenile, and/or adolescent timepoints of offspring development. However, how the addition of maternal hyperandrogenemia (HA), a hallmark of PCOS, contributes to these phenotypes in fetal skeletal muscle in this model was lacking. To this end, we find an interactive effect of offspring sex by maternal diet in offspring skeletal muscle. Unexpectedly, our results demonstrate that exposure to maternal HA did not significantly influence offspring respirometry and that the effect of maternal WD was driven by male offspring rather than female offspring. This phenotype appears to be more sensitive in conditions reliant upon non-lipid oxidation and at higher rates of coupled electron flux when normalized to maximal uncoupled electron transport. While a preliminary assessment of fetal

muscle metabolism, these are novel findings, to our knowledge, that demonstrate maternal WD significantly alters maximal coupled-to-uncoupled electron flux with non-lipid metabolism in male offspring. How these shifts in male gastroc oxidation, or lack of metabolic shift in females, evolves during childhood, adolescence, and early-adulthood may reflect an entirely different phenotype requiring further investigation.

This study was originally intended to be a fertility study with these fetal experiments supplemented for the purpose of maximizing potential findings from this longitudinal study. Within this context, the reduced number of fetal offspring from T+W dams reflects subfertility complications previously described in detail in this model (369; 371) and also observed in clinical populations with PCOS (376). However, the small sample size of this group (T+W fetuses) shown to have exacerbated metabolic dysfunction – further truncated after separating by fetal sex for the purpose of testing for sex-specific differences – reduces the statistical power needed for these analyses. However, the presence of sex specific differences in males with only 2-3 additional offspring in W or T+W cohorts speaks to the magnitude that these metabolic and hormonal insults may have on fetal muscle metabolism by the end of gestational development. Further investigation using more sensitive techniques that measure markers of oxidative stress, OXPHOS proteins, insulin signaling regulators, and ER-mito dynamics in these prenatal tissues may provide insight that is replete with data better able to support or refute the phenotypes of fetal muscle function previously observed in other animal models (383).

	C (n = 10)	**T** (n = 10)	**W** (n = 10)	**T+W** (n = 10)	Diet	treatment	d x t
Age (yrs)	2.4 ± 0.1	2.3 ± 0.02	2.6 ± 0.1	2.3 ± 0.05	ns	**0.02**	ns
Body mass (kg)	3.3 ± 0.01	3.2 ± 0.1	3.3 ± 0.1	3.0 ± 0.1	ns	**0.04**	ns
Fat mass (% total mass)	10.5 ± 0.3	11.3 ± 0.5	10.3 ± 0.4	10.3 ± 0.3	ns	ns	ns
Fasting glucose (mg/dL)	61 ± 3	65 ± 3	66 ± 3	61 ± 4	ns	ns	ns
Fasting insulin (µU/mL)	13.2 ± 4.4	9.3 ± 1.2	6.4 ± 0.7	8.5 ± 2.5	ns	ns	ns
Glucose AUC, from zero ($x10^3$)	8.09 ± 0.46	8.21 ± 0.29	8.93 ± 0.36	8.47 ± 0.38	ns	ns	ns
Insulin AUC, from zero ($x10^3$)	2.86 ± 0.52	2.82 ± 0.33	1.93 ± 0.31	2.41 ± 0.24	0.08 (ns)	ns	ns
HOMA-IR	1.9 ± 0.6	1.5 ± 0.2	1.1 ± 0.2	1.5 ± 0.5	ns	ns	ns

Table 6.1 – Baseline phenotypic data in young females.

Young, 2-yr-old females were assigned to one of two treatments, either a cholesterol vehicle implant or testosterone implant, and one of two diets, fiber-balanced chow or a high fat, high sugar Western diet, creating four groups: chow + vehicle control (C), chow + testosterone (T), Western diet + vehicle (W), and Western diet + testosterone (W+T). Age, body composition, fasting glucose and insulin serum values, AUC, and HOMA-IR presented as group mean ± SEM. Glucose and insulin AUC calculated from zero during an i.v. GTT. Data were analyzed by 2-way ANOVA for main effect by diet (d), testosterone treatment (t) or interactions with Sidak's multiple comparisons test. *P*-values are listed and bolded for main or interactive effects.

	C (*n* = 10)	**T** (*n* = 10)	**W** (*n* = 10)	**T+W** (*n* = 10)	diet	treatment	d x t
Testosterone (ng/mL)	--	1.31 ± 0.06	--	1.34 ± 0.05	--	ns	--
Body mass (kg)	6.1 ± 0.4	6.3 ± 0.4	6.2 ± 0.3	7.5 ± 0.6	ns	0.08 (ns)	ns
Fat mass (% total mass)	20.5 ± 3.2	21.9 ± 2.7	24.9 ± 1.9	33.3 ± 3.8	**0.01**	ns	ns
Android fat (% total fat)	9.9 ± 0.6	9.8 ± 0.7	10.6 ± 0.5	11.7 ± 0.6	**0.04**	ns	ns
Gynoid fat (% total fat)	16.9 ± 0.6	17.5 ± 0.9	17.9 ± 1.0	18.6 ± 0.6	ns	ns	ns
Fasting glucose (mg/dL)	50 ± 2	49 ± 2	57 ± 2	52 ± 3	0.05 (ns)	ns	ns
Fasting insulin (μU/mL)	15.1 ± 2.5	20.6 ± 4.4	22.8 ± 3.3	38.0 ± 7.0*	**0.01**	**0.03**	ns
Glucose AUC, Zero (x10^3)	6.99 ± 0.36	6.86 ± 0.26	7.74 ± 0.47	8.24 ± 0.49*	**0.01**	ns	ns
Insulin AUC, Zero (x10^3)	5.11 ± 1.33	5.84 ± 1.22	5.96 ± 0.92	11.37 ± 3.14	ns	ns	ns
HOMA-IR	1.9 ± 0.3	2.5 ± 0.6	3.3 ± 0.5	4.6 ± 0.8*	**0.005**	ns	ns

Table 6.2 – Female phenotypic data at year 2 of treatment.

Young females AFTER 2-years on assigned diet **±** testosterone treatment, i.e., chow + vehicle control (C), chow + testosterone (T), Western diet + vehicle (W), or Western diet + testosterone (W+T). Testosterone concentration, body composition, fasting glucose and insulin serum values, AUC, and HOMA-IR presented as group mean ± SEM. Glucose and insulin AUC calculated from zero during an i.v. GTT. Differences between testosterone concentration in T and T+W females were analyzed using Student's *t*-test. Data were analyzed by 2-way ANOVA for main effect of diet (d), testosterone treatment (t), or interactions (d x t). *P*-values are listed and bolded for main or interactive effects. An asterisk (*p<0.05) represents significant differences by testosterone treatment within the same diet using Sidak's multiple comparisons test.

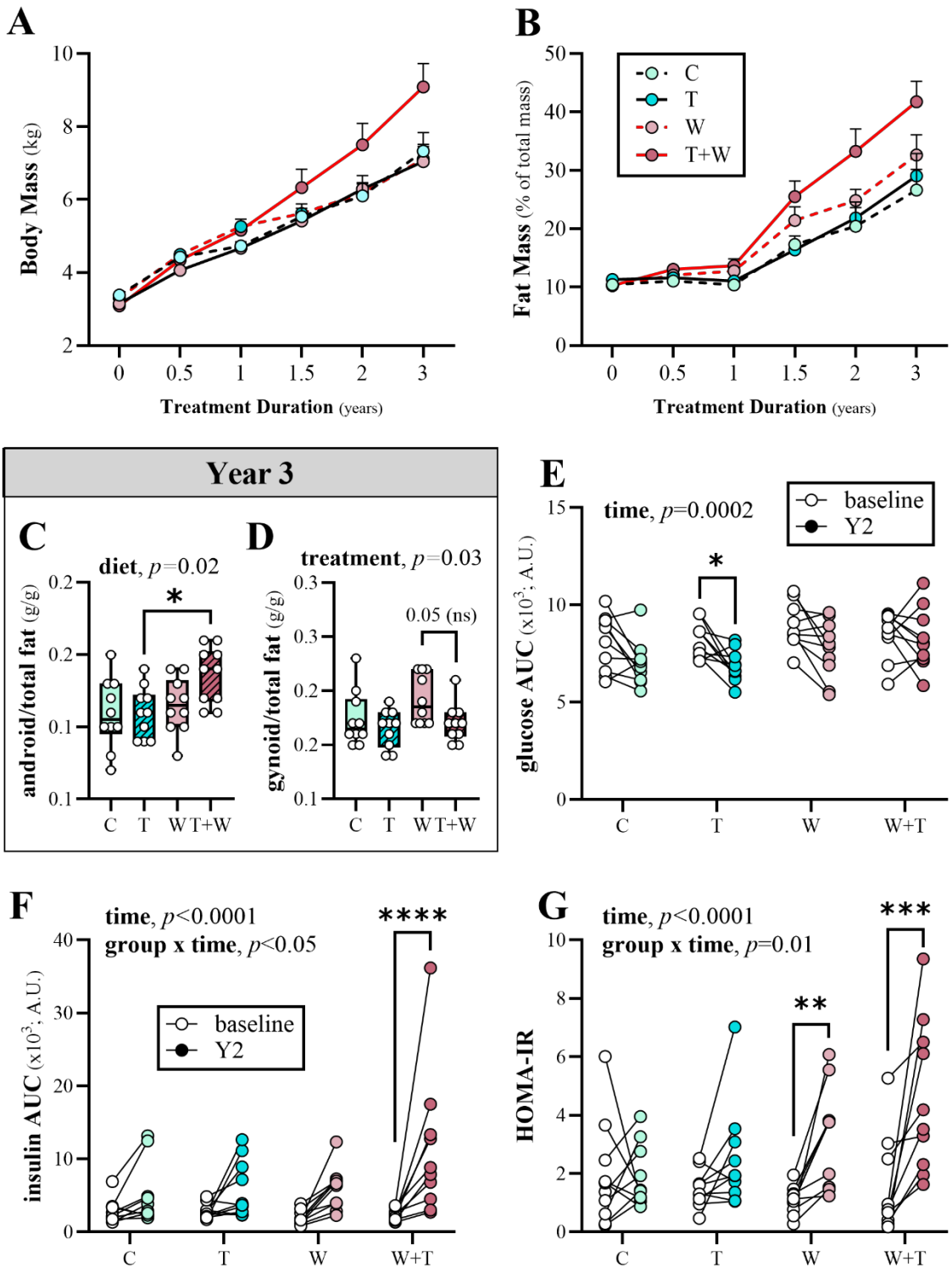
A
Body Mass (kg)
Treatment Duration (years)
B
Fat Mass (% of total mass)
C
T
W
T+W
Treatment Duration (years)
Year 3
C
diet, p=0.02
android/total fat (g/g)
D
treatment, p=0.03
gynoid/total fat (g/g)
0.05 (ns)
E
time, p=0.0002
baseline
Y2
glucose AUC (x10³; A.U.)
F
time, p<0.0001
group x time, p<0.05
insulin AUC (x10³; A.U.)
G
time, p<0.0001
group x time, p=0.01
HOMA-IR

Figure 6.1 – Body composition and i.v. glucose tolerance test metrics in young females from baseline to year 3 of study.

Body mass (A) and fat mass (B) over 3-yr time course shown in control ("C"), testosterone supplemented ("T"), Western Diet ("W"), testosterone with Western Diet ("W+T") animals. Ratio of android (C) and gynoid (D) fat depots to total fat presented after year 3 of treatment. Glucose AUC (E), insulin AUC (F), and HOMA-IR (G) from baseline (open symbols) to year 2 (Y2, closed symbols) shown across groups. Android and gynoid fat ratios were analyzed by 2-way ANOVA for significant main effects of diet or treatment (± testosterone) or interactions with Tukey's multiple comparisons test. *P*-values for significant main or interactive effects are listed above each graph. For post-hoc analysis of fat depots (C and D), an asterisk (**p*<.05) indicate significant differences by diet within testosterone treated animals. i.v. GTT analyses were analyzed by 2-way ANOVA with repeated measures for significant main effects by time (baseline to year 2) or treatment/diet group or interactive effects with Sidak's multiple comparisons test. *P*-values for significant main or interactive effects are listed above each graph. For post-hoc analysis of i.v. GTT data (E-G), asterisks (**p*<.05, ***p*<.01, ****p*<.001, *****p*<.0001) indicate significant differences by study duration (time) within each group. Individual data points are shown.

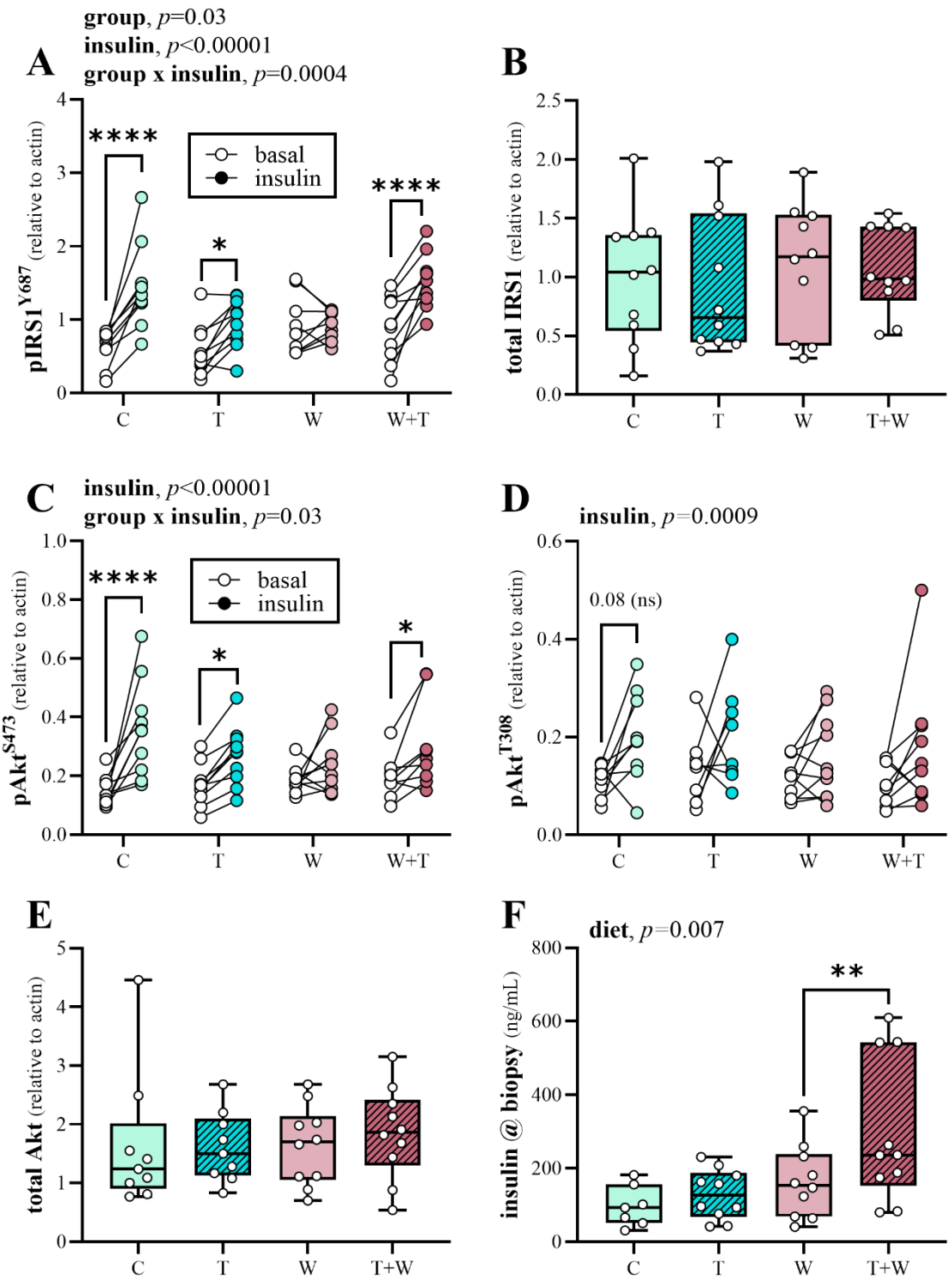
A
group, p=0.03
insulin, p<0.00001
group x insulin, p=0.0004
pIRS1Y687 (relative to actin)
basal
insulin
****
*
****
C
T
W
W+T
B
total IRS1 (relative to actin)
C
T
W
T+W
C
insulin, p<0.00001
group x insulin, p=0.03
pAktS473 (relative to actin)
basal
insulin
****
*
*
D
insulin, p=0.0009
pAktT308 (relative to actin)
0.08 (ns)
E
total Akt (relative to actin)
F
diet, p=0.007
insulin @ biopsy (ng/mL)
**

Figure 6.2 – Skeletal muscle signaling in response to insulin stimulation.

Protein abundance of key markers of insulin signaling were measured in muscle biopsies taken both before (basal) and 10 min after insulin bolus (insulin) in young females after 2-yrs of treatment with testosterone (T) and/or Western Diet (W). Phosphorylated (p)IRS1 at Y687 (A), total IRS1 (B), pAkt at S473 (C) and T308 (D), and total Akt (E) were measured by Wes immunoassay and normalized to housekeeping protein actin. Serum insulin concentration (F) was also taken at time of biopsies. Total IRS1, total Akt, and serum insulin were analyzed by 2-way ANOVA for significant main effects of diet or treatment (± testosterone) or interactions with Tukey's multiple comparisons test. *P*-values for significant main or interactive effects are listed above each graph. For post-hoc analysis, asterisks (**p<.01) indicate significant differences by testosterone within diet. Pre/post bolus biopsy data were analyzed by 2-way ANOVA with repeated measures for significant main effects by time (basal or insulin) or treatment/diet group or interactive effects with Sidak's multiple comparisons test. *P*-values for significant main or interactive effects are listed above each graph. For post-hoc analysis, asterisks (*p<.05, ****p<.0001) indicate significant differences by insulin stimulation (insulin) within each group. Individual data points are shown. Group minimum, maximum, median, and interquartile range are shown in B, E, and F.

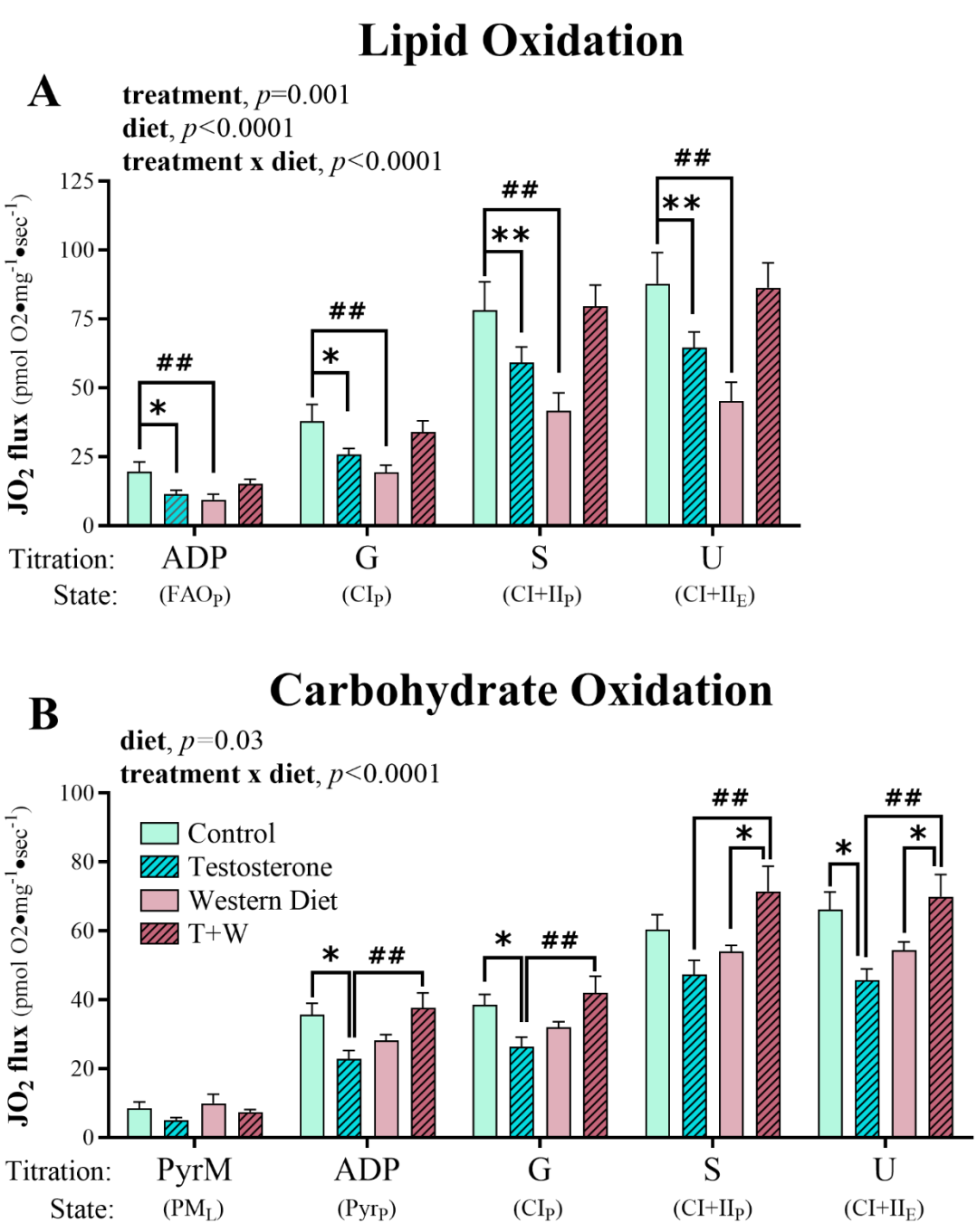
Lipid Oxidation
A
treatment, p=0.001
diet, p<0.0001
treatment x diet, p<0.0001
JO2 flux (pmol O2•mg-1•sec-1)
125
100
75
50
25
0
##
*
##
*
##
**
##
**
Titration: ADP G S U
State: (FAOP) (CIP) (CI+IIP) (CI+IIE)
Carbohydrate Oxidation
B
diet, p=0.03
treatment x diet, p<0.0001
Control
Testosterone
Western Diet
T+W
JO2 flux (pmol O2•mg-1•sec-1)
100
80
60
40
20
0
* ##
* ##
##
*
##
*
*
*
Titration: PyrM ADP G S U
State: (PML) (PyrP) (CIP) (CI+IIP) (CI+IIE)

Figure 6.3 – Lipid and carbohydrate oxidative capacity in young female skeletal muscle at year-2 of treatment.

Average group oxygen flux (JO_2; pmols/s*mg) was measured in permeabilized muscle fiber bundles (PMFB) with lipid (A) or without lipid (B) and normalized to tissue wet weight in gastrocnemius of females at year 2 of treatment. Rate was measured in the presence of saturating ADP with serial additions of lipid and malate (FAO_P), glutamate (G) for CI OXPHOS capacity (CI_P), succinate (S) for maximal CI+CII OXPHOS capacity ($CI+II_P$), and FCCP for uncoupled (U) capacity ($CI+II_E$). Respiration rate without lipid (carbohydrate oxidation) was measured in the presence of saturating pyruvate (Pyr) and malate (M) (PM_L), ADP (Pyr_P), G, S, and FCCP. Respiratory flux data were analyzed by 3-way ANOVA with Sidak's multiple comparisons. *P*-values for significant main effects of treatment or diet or interactive effects are listed above each graph. For post-hoc analysis, asterisks (*p<.05, **p<.01) indicate significant differences by testosterone treatment within the same diet group; octothorps ($^{\#\#}p<.01$) indicate significant differences by diet within the same treatment group. Group average + SEM at each titration stage is shown.

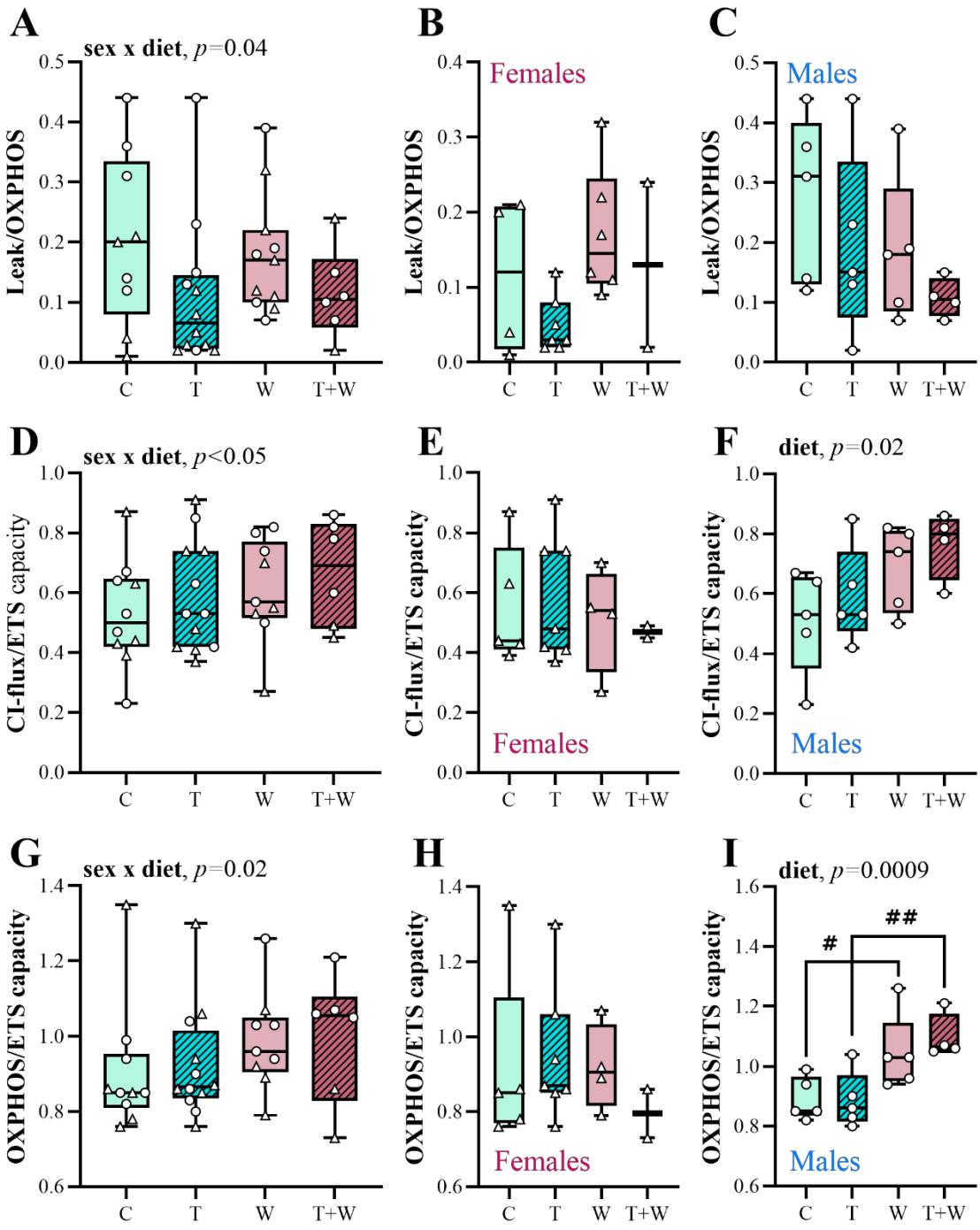
A
sex x diet, p=0.04
Leak/OXPHOS
B
Females
C
Males
D
sex x diet, p<0.05
CI-flux/ETS capacity
E
F
diet, p=0.02
G
sex x diet, p=0.02
OXPHOS/ETS capacity
H
I
diet, p=0.0009
#
##
C
T
W
T+W

Figure 6.4 – Lipid and carbohydrate oxidative capacity in fetal muscle exposed to obesity and hyperandrogenemia during gestation.

Oxygen flux (JO_2; pmols/s*mg) was measured in permeabilized muscle fiber bundles (PMFB) with lipid (A-C) or without lipid (D-E) and normalized to tissue wet weight in gastrocnemius of fetal offspring at gestational day (G) 130. O_2 flux rates were normalized within each run per offspring to generate the following ratios: Non-adenylated lipid oxidation to ADP-stimulated lipid oxidation (Leak/OXPHOS) in all offspring (A) and analyzed by fetal sex, female (B) and male (C). Maximal CI-flux with non-lipid substrate in the presence of ADP normalized to maximal ETS capacity (CI-flux/ETS) was measured in all offspring (D) and analyzed by sex (females, E; males, F). Maximal ADP-stimulated OXPHOS capacity normalized to maximal ETS capacity with nonlipid substrates (OXPHOS/ETS) was measured in all offspring (G) and further analyzed by sex (females, H; males, I). Combined male and female ratios were analyzed by 3-way ANOVA (diet x treatment x sex) with significant *p*-values for interactive effects listed above each graph (A, D, G). Ratios were separated by sex and data analyzed by 2-way ANOVA for main effect of diet or treatment or interactive effect in females and males with Sidak's multiple comparisons. *P*-values for significant main effect of diet is listed above each graph. For post hoc analysis, octothorps ($^{\#}p<0.05$, $^{\#\#}p<.01$) represent significant different by maternal diet within treatments (±testosterone). Individual data points with group minimum, maximum, median, and interquartile range are shown. Male (M) offspring are indicated by circles and female (F) offspring by triangles. Sample size for each fetal group (i.e, maternal exposure) by sex: C, 3-5F/5M; T, 7F/5M; W4-6F/5M; T+W, 2F/4M.

VII. PROJECT SUMMARY & FUTURE DIRECTIONS

This dissertation has addressed the objectives outlined at the onset of this body of work in the following ways…

*...regarding early-life exposure to **obesogenic stress**:*

- In lean, active adolescent offspring (3Y), a postweaning Western-Style diet (pwWD) leads to shifts in body fat distribution that are associated with poorer insulin sensitivity independent of exposure to mWD.
- Adolescent offspring weaned to WD had increased amounts of intramuscular saturated lipid and bioactive lipid molecules, like ceramide and sphingomyelin, which are associated with insulin resistance and are exacerbated upon prior exposure to mWD.
- Fatty acid oxidative metabolism was reduced in skeletal muscles from 3Y offspring exposed to maternal Western-style diet even when weaned to a healthy control diet for years. Furthermore, this reduction in mitochondrial oxidative capacity was present in these offspring even though they were significantly more active than offspring born to mCD dams. Finally, the mCD dams were also significantly younger than mWD dams, further emphasizing the magnitude of this offspring muscle phenotype resulting from mWD.
- Like previous work from our lab measuring insulin-stimulated glucose uptake *ex vivo*, 1Y juvenile skeletal muscle appears to have a milder metabolic phenotype than fetal muscle glucose uptake (195). In these studies, markers of mitochondrial network morphology and protein turnover/network quality control via PINK1/Parkin-mediated mitophagy appear less robust than that seen in adolescent offspring at 3-years-old. This may be caused by differences in duration of time offspring spent consuming WD (i.e., ~7 months in juveniles v. ~30 months in adolescent offspring). Alternatively, this juvenile timepoint may represent a developmental window of metabolic transition. Specifically, ETS complex activities were significantly higher in fetal gastroc from ObWD pregnancies (a phenotype corroborated by this thesis as fetal gastroc of WD pregnancies had elevated OXPHOS/ETS capacity that was driven primarily in males independent of maternal HA (Chapter VI, Aim #3)). However, in mWD exposed animals

aged to adolescence, we observe markers of reduced substrate flexibility and OXPHOS capacity – primarily through CI (Chapter III, Aim #1). In short, this phenotypic flip following early life obesogenic stress occurred between ~GD 135 and 3 years-old and may be represented by this 1Y juvenile timepoint.

- pwWD appeared to mask potentially subtle differences in the protein abundance of mitochondrial morphology markers in 1Y offspring muscle born to ObWD mothers. Importantly, this did not translate to similar mitochondrial coupling efficiency with lipid substrates. Even though both pwWD groups demonstrated an increase in short and long OPA1 content and CL content, which typically correspond with higher oxidative capacity in skeletal muscle, they showed modest but significant differences in mitochondrial function between these pwWD groups in a manner suggesting that the addition of maternal ObWD in early life decreases mitochondrial function in the muscle of these offspring. This marks a significant timepoint during primate development and skeletal muscle function as it relates to mitochondrial physiology and associated insulin sensitivity in the pathogenesis of metabolic diseases like CVD and T2D.
- Reduced content of oxidative phosphorylation complexes I-V and VDAC1 abundance partially explains decreased skeletal muscle respiration in 3Y offspring exposed to early life mWD.
- Relatedly, two of the only proteins whose abundance in 1Y juveniles were consistent with 3Y juveniles following exposure to mWD and pwWD are CI and VDAC1, both of which were reduced following exposure to early life obesogenic stress. This supports the premise that these proteins, or the roles that they fulfill, are differentially programmed by at least 1 year of age.

*...regarding **female/maternal hyperandrogenemia ± diet-induced obesity**:*

- Juvenile females had increased % body fat as early as 1.5 years after switching to WD with or without the addition of HA. However, from 1.5 years of consuming WD and on, % body fat was dramatically exacerbated with the additional presence of HA (testosterone [T] treatment resulting in hyperandrogenemia [HA] induced at the same time as induction of WD).
- After 2 years in their assigned group, both WD groups had increased android adiposity without further accruement with high T. Only a year later, android fat storage was most severely

elevated in T+W group. This suggests a relatively rapid change in body composition at this young age in response to these metabolic and hormonal factors.

- At Year 2 of treatment, young females consuming WD show signs of systemic insulin resistance and glucose intolerance that is amplified with the addition of T.
- Contrary to what was initially hypothesized, the least insulin sensitive group, T+W, appear to respond to insulin stimulation *in vivo* as effectively as control females and significantly better than females exposed to either T or WD alone over the same two years. However, this was the result of sustained hyperinsulinemia in T+W females, suggesting an earlier manifestation of metabolic dysfunction in this group relative to either condition alone. This likely expedites development of MetS and ultimately CVD or T2D in these young female animals.
- Skeletal muscle oxidative capacity mirrors this observation in skeletal muscle insulin signaling. Maximal oxidation is elevated with both lipid and nonlipid substrates in T+W comparable to what is seen in controls while groups with T or W exposure alone have consistently lower rates of oxidative flux. It is unlikely that this increased mitochondrial flux can be sustained indefinitely without functional consequences in the form of oxidative stress, mitochondrial damage, etc.
- Oxidation of nonlipids in fetal gastroc muscle appears to be more sensitive to maternal WD consumption and not HA during the third term of gestation. These respirometry studies also indicate that there is a sex-specific impact by sex such that male fetal muscle drives the observed changes in rates of nonlipid oxidation among offspring groups. Better representation by sex and maternal T+W exposure is needed to draw more definitive conclusions in the muscle of these fetal offspring groups.

FUTURE DIRECTIONS

- In offspring exposed to early life obesogenic stress, there appears to be shifts in systemic and skeletal muscle metabolism that is age- and/or time-dependent. Future studies should investigate how these phenotypes continue to transform throughout puberty and into later life. This would also assist in better understanding the evolution of sex-specific differences caused by this early life stress. Importantly, sex-specific differences have little to no impact on the outcomes of these studies conducted at these young stages of offspring development.

- Given the highly dynamic nature of mitochondrial functional and morphological adaptations in response to metabolic and energetic stress, future assessment of mitochondrial networking and stress response similar to those addressed in Aim #2 would greatly benefit from the introduction of nutrient or hormonal stress into a living system. Specifically, the presence of exogenous stress may better tease out the mitochondrial network discrepancies initially hypothesized but ultimately not present in the muscle of 1Y juveniles consuming WD with or without early life maternal ObWD exposure.
- Additionally, with evidence suggesting a lack of mito-ER interactions and or calcium stress response in these animals, future work should consider how these relationships between intramuscular organelles contribute to the development of metabolic diseases at this timepoint and moving forward. Important to note is how unique skeletal muscle is regarding the populations of mitochondria it contains (intermyofibrillar and subsarcolemmal) as well as its specialized ER (i.e., sarcoplasmic reticulum). More work that takes these unique aspects of skeletal muscle anatomy and physiology in these offspring into account as it relates to the development of insulin resistance and mitochondrial dysfunction is lacking yet warranted.
- Skeletal muscle insulin signaling is likely constitutively activated in skeletal muscle of young females after 2 years of being assigned to T+W. Hyperinsulinemia is a hallmark of MetS and is featured in the pathogenesis of chronic metabolic diseases like T2D. For this reason, future work should focus on how these phenotypes – both in skeletal muscle insulin signaling and in oxidative capacity – continue to change over time with maintained WD-induced obesity and HA in these young females.
- The decrease in VDAC1 and CI abundance in 3Y muscle also seen in juveniles at 1Y warrants future research into earlier (and later) timepoints of development to elucidate the importance or contribution of these proteins in programing offspring metabolic dysfunction and future health outcomes.

APPENDIX A:
SUPPLEMENTAL TABLES

Supplemental Table 1. Pre-pregnancy characteristics of adult female dams

Variable	**mCD/pwCD**	**mCD/pwWD**	**mWD/pwCD**	**mWD/pwWD**	**m diet**	**pw diet**
Dams (*n*)	9	4	9	7	-	-
Offspring (n)	12 (7F, 5M)	5 (2F, 3M)	12 (4F, 8M)	9 (5F, 4M)	-	-
Maternal age (years)	11.3 (8-13)	10.5 (9-12)	**7.1^^^^ (6-8)**	**7.5^ (6-8)**	**<0.0001**	*ns*
Parity	5.6 (4-8)	4.4 (4-6)	**2.5^^^^ (2-3)**	**2.3^ (1-4)**	**<0.0001**	*ns*
Time on WD (years)	-	-	2.3 (1-3)	2.3 (2-3)	-	*ns*
Body weight (kg)	7.1 ± 0.2	7.0 ± 0.6	6.6 ± 0.2	7.4 ± 0.6	*ns*	*ns*
Adiposity (% fat)	20 ± 2	15 ± 2	20 ± 2	14 ± 2	*ns*	**0.02**
Fasting glucose (mg/dL)	50 ± 2	50 ± 2	56 ± 3	49 ± 5	*ns*	*ns*
Fasting insulin (µU/mL)	21.5 ± 5.9	12.3 ± 5.5	33.5 ± 9.4	14.6 ± 2.4	*ns*	*ns*
Glucose AUC	6180 ± 398	5685 ± 694	5290 ± 245	5974 ± 385	*ns*	*ns*
Insulin AUC	2310 ± 382[#]	2138 ± 531	3917 ± 797	3135 ± 429	*ns*	*ns*

Adult females are separated by offspring group indicated in columns (maternal diet/postweaning diet). Data were analyzed by 2-way ANOVA with Sidak's multiple comparisons test or a Student's *t*-test. *P* values are listed for main effects. Carets (^p<0.05, ^^^^p<0.0001) indicate significant differences between maternal diet within same postweaning diet using Sidak's multiple comparisons test. ns, no significant difference. Data for maternal age, parity and time on diet are presented as mean with interquartile range in parentheses. All other data are the mean ± SEM. No more than two offspring per dam were included in each group. Insulin and glucose AUC was calculated from baseline. (#) missing n=1.

Supplemental Table 2. Description of primary and secondary antibodies used to measure relative protein abundance via Wes immunoassay or traditional immunoblotting

Target	Species	Manufacturer	Catalogue ID	Multiplex Group(s)	Antibody Dilutions	Protein Conc. (mg/mL)
OXPHOS (CI-CV)	Ms	MitoProfile (Abcam)	MS601	A*	1:100	1.00
GAPDH	Ms	Santa Cruz Biotech	sc-47724	B*#	1:4000[AB]	1.00
AMPKα2	Rb	Cell Signaling	2757	C	1:100	1.00
GAPDH	Rb	Santa Cruz Biotech	sc-25778	C, D, E, F	1:5000[CD] 1:1000[EF]	0.20[EF], 1.00[CD]
p-AMPKα @thr172	Rb	Cell Signaling	2535	D	1:100	1.00
VLCAD	Rb	abcam	ab155138	E	1:100	0.20
CPT2	Rb	abcam	ab181114	G	1:50	1.00
Vinculin	Rb	Cell Signaling	4650	G, H†, I†, K, M, N	1:50[G] 1:100[HIKMN]	1.00[GHIKMN]
ACCα/β †	Rb	Cell Signaling	3676	H†	1:100	1.00
p-ACCα/β @ser79 †	Rb	Cell Signaling	3661	I†	1:100	1.00
α-tubulin	Rb	Thermo Fisher	PA516891	J	1:1	1.00
PGC1α	Rb	EMD Millipore	AB3242	J	1:50	1.00
ETFα	Rb	Thermo Fisher	PA5-28201	K	1:20	1.00
ETFDH	Rb	Thermo Fisher	PA5-72484	L	1:20	1.00
GAPDH	Rb	Cell Signaling	2118	L	1:4000	1.00
VDAC1/2	Rb	abcam	ab154856	M	1:20	1.00
CPT1β	Rb	Thermo Fisher	PA5-79065	N	1:200	1.00
VDAC2	Rb	abcam	ab126120	N	1:20	1.00
anti-Ms HRP (2°) #	Gt	Bio-Rad	170-5047	T #	1:20,000	n/a
HADHA #	Ms	Santa Cruz Biotech	sc-515278	T #	1:1000	2.50

(*) data in multiplex A normalized to loading control (GAPDH) for each animal in multiplex group B
(†) immunoassay conducted on High Molecular Weight (66-440 kDa) Wes separation module
(#) antibodies used for traditional western blot analysis

Supplemental Table 3. Description of OXPHOS and housekeeping primers

Gene name	Symbol	Genome	A_E	Annealing temp (°C)	Forward primer	Reverse primer
NADH dehydrogenase subunit 2	*nd2*	mito	.90	64.5	ACAACCGCCCTCGCCATAAAAC	AGGGGTGTTCCTTGGGTGACT
Cytochrome B	*cytb*	mito	.94	64.5	ACCTCCACGCCAATGGTGCC	GCCGTAGTAAAGGCCCCGACC
Cytochrome C oxidase subunit 2	*coxii*[#]	mito	.94	61.6	ACTAAGCCTGCAAGACGCCACA	GTGAGCGTTGAGAGCAGGGCATA
ATP synthase subunit 8	*atp8*	mito	.93	61.6	TGCCCCAGTTAGACACATCGACA	GGGGTGGTTGGTAGTGGTTCGT
NADH dehydrogenase 1 beta subcomplex 8	*ndufb8*[#]	nuclear	.96	64.5	TGGGACCAACCGGACCTGAG	GCCAGGAAACCGAAGAGGTGC
Succinate dehydrogenase complex subunit B	*sdhb*[#]	nuclear	.101	64.5	TGTGGCCCCATGGTATTGGAT	TGTTCATTGCACAAGAGCCAC
Ubiquinol-cytochrome C reductase core protein 2	*uqcrc2*[#]	nuclear	.90	64.5	TCAACATGAGGGGTGGGTTTGGT	CCTCTGCACTTCCCGCGACA
Cytochrome C oxidase subunit 5a	*cox5a*	nuclear	.90	64.5	CCAGAGGAACTGGGCCTTGACA	GCAGTGTCAATAAATCCGTGGGGAA
ATP synthase F1 subunit alpha	*atp5f1a*[#]	nuclear	.91	61.6	ATCCACTGTTGCCCAGTTGGTGA	TGAAGTGGGGCAGCATCCGAG
Ribosomal protein S15	*rps15**	nuclear	.73	64.5	TTTCTGAGCATCCGGCAAGA	CATCAGCTGCTCGTAGGACAT
28s ribosomal RNA	*28s**	nuclear	.96	61.6	GAGGGTGTAAATCTCGCGCCGG	TCCGGCTTGCCGACTTCCCTTA
Ribosomal protein L13a	*rpl13a**	nuclear	.92	61.6	CCTGGAGGAGGAGAGGAAAGA	TTGAGGACCTCTGTGTATTTG

Supplemental Table 4. Sex-specific differences by maternal diet in key outcome measures.

Anthropometrics			
	mDiet	Sex	Interaction
n	16 mCD/21 mWD	17 F/20 M	~
Body mass	0.99	**0.001**	0.28
Fat mass	0.38	0.14	0.44
Oxidative capacity			
	mDiet	Sex	Interaction
n	14 mCD/15 mWD	12 F/17 M	~
Lipid+pyr (D-state)	**0.0004**	0.11	0.50
CI	**0.0001**	0.08	0.54
CII	**0.01**	0.99	0.90
Lipids			
	mDiet	Sex	Interaction
n	13 mCD/16 mWD	14 F/15 M	~
TAG saturation	0.87	0.75	0.92
Sphingomyelin (18:0)	0.80	>0.05	0.12
Ceramide (18:0)	0.69	0.43	0.50
Oxidative stress			
	mDiet	Sex	Interaction
n	14-15 mCD/16-17 mWD	14-15 F/16-17M	~
VDAC1/2	**0.00001**	0.46	0.89
Lipid peroxidation	**0.03**	0.32	0.52
Protein carbonylation	0.24	0.54	0.46

Main and interactive effects of sex and maternal diet (mDiet) were tested by 2-way ANOVA for primary outcome variables from the current study. Sample size for mDiet (CD/WD) and sex (F/M) are provided with *p*-values per measure listed beneath. Significant *p*-values are in bolded.

Supplemental Table 5. Sex-specific differences by postweaning diet in key outcome measures.

Anthropometrics			
	pwDiet	Sex	Interaction
n	23 pwCD/14 pwWD	17 F/20 M	~
Body mass	0.82	**0.002**	0.6
Fat mass	**0.03**	0.15	0.95
Oxidative capacity			
	pwDiet	Sex	Interaction
n	17 pwCD/12 pwWD	12F/17 M	~
Lipid+pyr (D-state)	0.64	0.41	0.31
CI	0.49	0.39	0.19
CII	0.46	0.84	0.49
Lipids			
	pwDiet	Sex	Interaction
n	16 pwCD/13 pwWD	14 F/15 M	~
TAG saturation	**0.00005**	0.86	0.27
Sphingomyelin (18:0)	0.24	0.06	0.39
Ceramide (18:0)	0.38	0.40	0.30
Oxidative stress			
	pwDiet	Sex	Interaction
n	18-19 pwCD/12-13 pwWD	14-15 F/16-17M	~
VDAC1/2	**0.002**	0.82	0.73
Lipid peroxidation	0.53	0.55	0.92
Protein carbonylation	**0.03**	0.60	0.76

Main and interactive effects of sex and postweaning diet (pwDiet) were tested by 2-way ANOVA for primary outcome variables from the current study. Sample size for pwDiet (CD/WD) and sex (F/M) are provided with *p*-values per measure listed beneath. Significant *p*-values are bolded.

Compound	mCD/pwCD (n = 8)	mCD/pwWD (n = 5)	mWD/pwCD (n = 8)	mWD/pwWD (n = 8)	mDiet	pwDiet	m x pw
Acyl-C4	12.9 ± 2	8.1 ± 0.8	6.2 ± 0.8^^	6.00 ± 0.7	**0.01**	ns	ns
Acyl-C6	12.5 ± 1.5	13.0 ± 2.3	7.8 ± 1.1	9.61 ± 1.6	**0.02**	ns	ns
Acyl-C8	29.7 ± 5.1	38 ± 8	18.8 ± 4.3	30 ± 6	ns	ns	ns
Acyl-C10	36.2 ± 5.9	54 ± 12	19.6 ± 4.3	55 ± 13*	ns	**0.006**	ns
Acyl-C12	24.7 ± 3.4	38 ± 11	12.1 ± 3.1	41 ± 10**	ns	**0.004**	ns
Acyl-C14	88 ± 15	118 ± 35	34 ± 10	130 ± 32*	ns	**0.01**	ns
Acyl-C16	642 ± 147	709 ± 236	213 ± 56	732 ± 183	ns	ns	ns
Acyl-C16:1	114 ± 21	179 ± 55	39 ± 9	198 ± 51**	ns	**0.004**	ns
Acyl-C18	350 ± 63	422 ±120	150 ± 29	412 ± 77*	ns	**0.03**	ns
Acyl-C18:1	697 ± 163	1044 ± 380	191 ± 40	1113 ± 264**	ns	**0.007**	ns
Acyl-C18:2	558 ± 158	277 ± 103	135 ± 29^^	331 ± 80	ns	ns	**0.03**
Acyl-C18:3	41 ± 13	12 ± 3	13 ± 2^	16 ± 3	ns	ns	**0.04**

Acylcarnitine (AC) concentration in offspring gastrocnemius was normalized to protein amount. Data in pmols are expressed as the mean ± SEM. Data were analyzed by a 2-way ANOVA for main effects of maternal (m) diet and postweaning (pw) diet and interactions (m x pw). *P* values are listed for significant main effects or interactions. (*) indicates significant differences between postweaning diet within same maternal diet group (*p<0.05, **p<0.01) and carets indicate significant differences between maternal diet within same postweaning diet group (^p<0.05, ^^p<0.01) using Sidak's multiple comparisons test. ns, no significant difference.

Supplemental Table 6. Adolescent offspring intramuscular acylcarnitine abundance

Compound	mCD/CD (n = 7-8)	mCD/WD (n = 4-5)	mWD/CD (n = 6-8)	mWD/WD (n = 6-8)	mDiet	pwDiet	m x pw
TG 48:0	472 ± 89	911 ± 147*	252 ± 24	762 ± 135**	ns	**<0.0001**	ns
TG 48:1	500 ± 74	1663 ± 418**	335 ± 58	1355 ± 298**	ns	**<0.0001**	ns
TG 48:2	554 ± 98	1156 ± 336*	448 ± 87	1055 ± 197*	ns	**0.001**	ns
TG 48:3	339 ± 65	709 ± 163	270 ± 49	973 ± 306**	ns	**0.008**	ns
TG 50:0	455 ± 81	861 ± 122*	256 ± 40	923 ± 160***	ns	**<0.0001**	ns
TG 50:1	2525 ± 480	7728 ± 1122***	1617 ± 228	5977 ± 1246**	ns	**<0.0001**	ns
TG 50:2	3606 ± 689	6699 ± 1486	2932 ± 547	5790 ± 1306	ns	**0.006**	ns
TG 50:3	1483 ± 348	2098 ± 661	1208 ± 262	1724 ± 410	ns	ns	ns
TG 50:4	527 ± 114	457 ± 110	524 ± 138	394 ± 145	ns	ns	ns
TG 52:0	131 ± 29	225 ± 18	70 ± 11	307 ± 49****	ns	**<0.0001**	**0.04**
TG 52:1	1543 ± 300	4429 ± 601***	913 ± 135	3447 ± 610***	ns	**<0.0001**	ns
TG 52:2	5563 ± 1037	13145 ± 1604**	4116 ± 812	11353 ± 1976**	ns	**<0.0001**	ns
TG 52:3	8562 ± 1761	12689 ± 2329	7155 ± 1566	8749 ± 1491	ns	ns	ns
TG 52:4	4950 ± 731	4177 ± 657	6201 ± 1494	4061 ± 1213	ns	ns	ns
TG 52:5	1167 ± 165	553 ± 119	1055 ± 326	553 ± 213	ns	**0.02**	ns
TG 54:1	135 ± 25	671 ± 113****	118 ± 26	406 ± 83**^	**0.03**	**<0.0001**	ns
TG 54:2	1050 ± 177	3564 ± 354****	859 ± 183	2576 ± 506***	ns	**<0.0001**	ns
TG 54:3	3383 ± 714	8620 ± 672***	3045 ± 729	5606 ± 980^	**0.048**	**<0.0001**	ns
TG 54:4	6092 ± 1363	8222 ± 209	5741 ± 1348	5689 ± 930	ns	ns	ns
TG 54:5	5104 ± 790	4459 ± 196	6327 ± 1527	2911 ± 530	ns	ns	ns
TG 54:6	2637 ± 426	748 ± 62*	2623 ± 652	1095 ± 417*	ns	**0.001**	ns
TG 56:3	37 ± 11	292 ± 48****	46 ± 16	137 ± 20**	ns	**<0.0001**	ns
TG 56:4	142 ± 49	486 ± 52***	122 ± 37	337 ± 55**	ns	**<0.0001**	ns
TG 56:5	327 ± 55	635 ± 53**	306 ± 79	416 ± 55	ns	**0.005**	ns
TG 56:6	625 ± 152	1228 ± 78*	451 ± 79	1077 ± 206*	ns	**0.0005**	ns
TG 56:7	1008 ± 188	1511 ± 156	706 ± 96	1233 ± 246	ns	**0.01**	ns

Triacylglyceride (TG) concentration was normalized to protein amount. Data in pmols are expressed as the mean ± SEM. Data for TG species were analyzed by 2-way ANOVA for main effects of maternal (m) diet, postweaning (pw) diet and interactions (m x pw). *P* values are listed for significant main effects or interactions. (*) indicates significant differences by postweaning diet within same maternal diet group (*p<0.05, **p<0.01, ***p<0.001 ****p<0.0001) and carets indicate significant differences by maternal diet within same postweaning diet group (^p<0.05) using Sidak's multiple comparisons test. ns, no significant difference.

Supplemental Table 7. Triacylglyceride subspecies abundance in offspring gastrocnemius

Supplemental Table 8. Adolescent offspring complex abundance correlations with lipid peroxidation

OXPHOS Complex(es)	All offspring		LnWD offspring	
	R^2	*p*-value	R^2	*p*-value
Complex I (CI)	**0.3**	**0.006**	**0.5**	**0.005**
Complex II (CII)	0.2	0.02	0.4	0.02
Complex III (CIII)	**0.3**	**0.005**	0.3	<0.05
Complex I+III (CI+III)	**0.3**	**0.003**	0.3	0.03
Complex IV (CIV)	0.1	<0.05	0.3	n.s.
Complex V (CV)	**0.3**	**0.003**	0.4	0.02

A simple linear regression was used to determine the relationship between individual OXPHOS complexes and CI+III abundance and lipid peroxidation (MDA) content in offspring gastroc. Correlation coefficient (R^2) and statistical significance (*p*-values) are shown for all offspring (LnCD/CD, *n*=10; LnCD/WD, *n*=5; LnCD/CD, *n*=8; LnCD/CD, *n*=6) and for LnWD offspring only. OXPHOS complexes with values in bold remained statistically significant after correcting for multiple comparisons using Bonferroni's test (six families, adjusted *p*-value < 0.008).

APPENDIX B:

SUPPLEMENTAL FIGURES

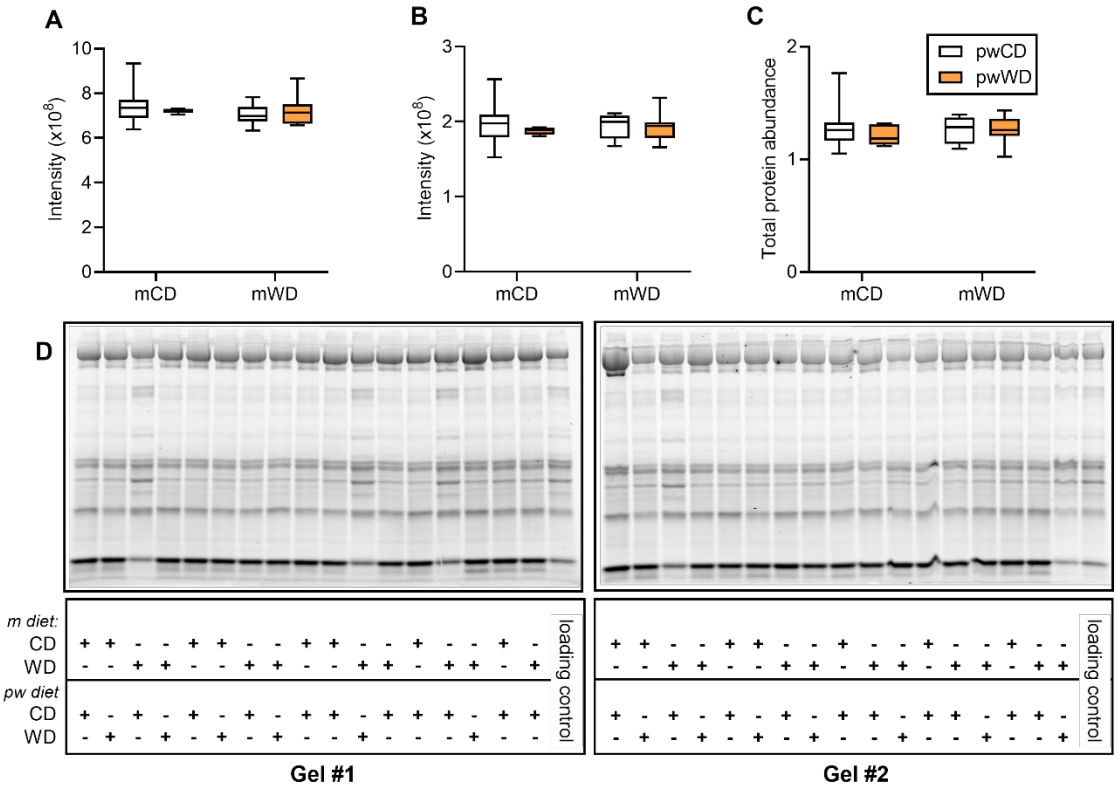

Supplemental Figure 1. Total protein of soleus homogenate from 3Y offspring.

Absolute protein abundance (A) was adjusted for background (B) and calibrated (made relative) to the same "loading control" homogenate (C) run in every gel to ensure consistency across assays (D). Loading control homogenate is combined soleus homogenate from multiple offspring in different treatment groups. Box-and-whisker plots displaying group minimum, maximum, median and interquartile range (A-C) are shown. *Method:* in short, 15 µL of skeletal muscle homogenate was mixed with 15 µL 2X Tris-Glycine SDS Sample Buffer (Novex), heated for 3 minutes at 85°C, and cooled on ice for 5 minutes. 25 µL was loaded per well from animals with OXPHOS abundance data presented in Figure 2. Samples were run in hand-cast Stain-free TGX gels (10%) per manufacturer instructions (Bio-Rad Laboratories; Hercules, CA, USA). Following electrophoresis, gels were activated and imaged using a ChemiDoc MP Imaging System (Bio-Rad Laboratories; Hercules, CA, USA). Total protein was quantified from gel images using Image Lab 5.2 Software (Bio-Rad Laboratories; Hercules, CA, USA) and statistical significance was testing by 2-way ANOVA.

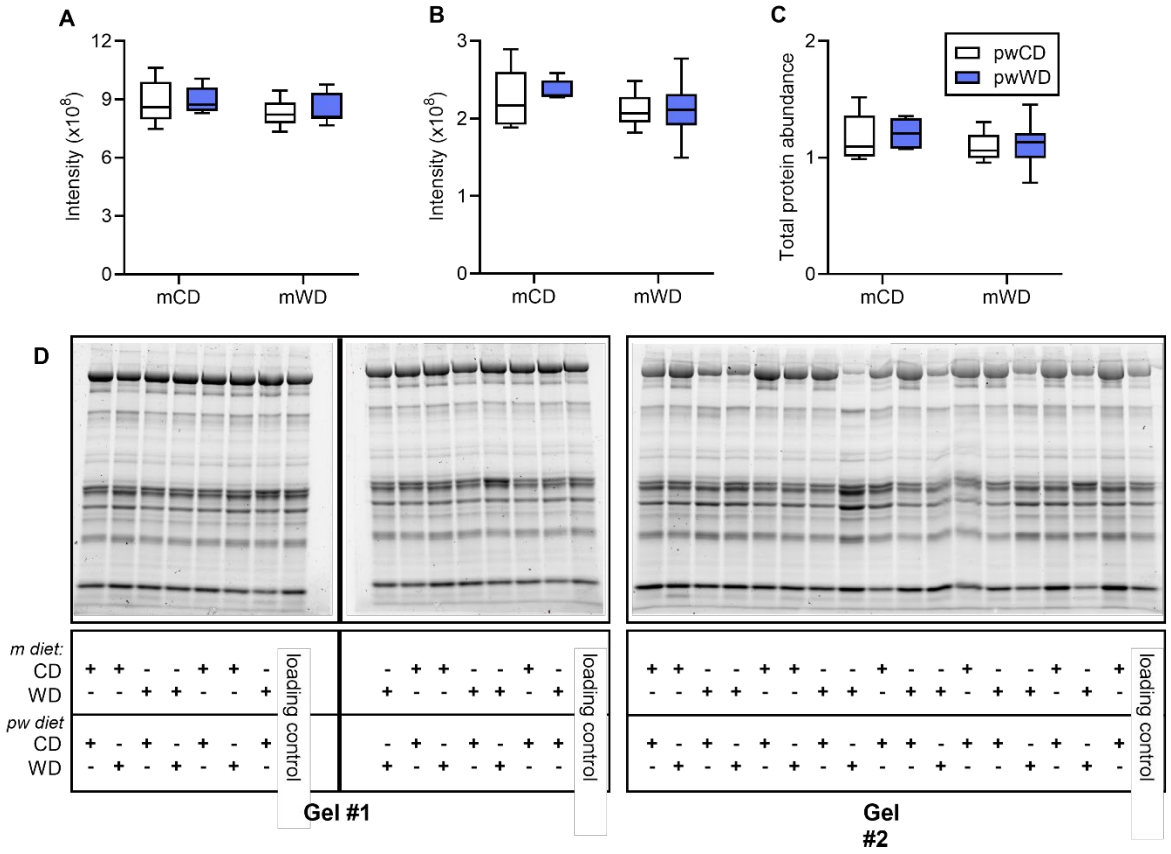

Supplemental Figure 2. Total protein of gastroc homogenate from 3Y offspring.

Absolute protein abundance (A) was adjusted for background (B) and calibrated (made relative) to the same "loading control" homogenate (C) run in every gel to ensure consistency across assays (D). Loading control homogenate is combined soleus homogenate from multiple offspring in different treatment groups. Box-and-whisker plots displaying group minimum, maximum, median and interquartile range (A-C) are shown. *Method:* in short, 15 µL of skeletal muscle homogenate was mixed with 15 µL 2X Tris-Glycine SDS Sample Buffer (Novex), heated for 3 minutes at 85°C, and cooled on ice for 5 minutes. 25 µL was loaded per well from animals with OXPHOS abundance data presented in Figure 2. Samples were run in hand-cast Stain-free TGX gels (10%) per manufacturer instructions (Bio-Rad Laboratories; Hercules, CA, USA). Following electrophoresis, gels were activated and imaged using a ChemiDoc MP Imaging System (Bio-Rad Laboratories; Hercules, CA, USA). Total protein was quantified from gel images using Image Lab 5.2 Software (Bio-Rad Laboratories; Hercules, CA, USA) and statistical significance was testing by 2-way ANOVA.

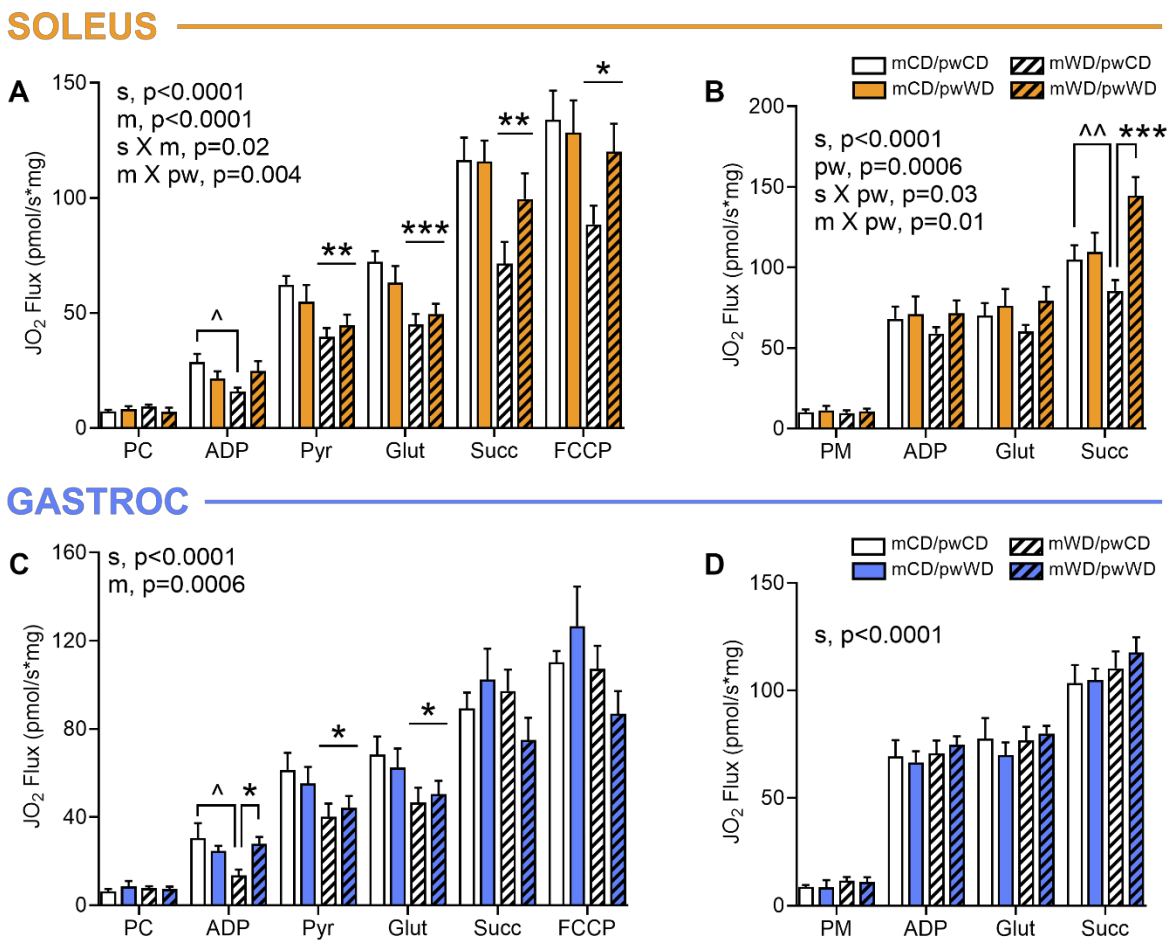

Supplemental Figure 3. Full respirometry SUITs in offspring soleus and gastroc.

Average group oxygen flux (JO_2; pmols/s*mg) was measured in permeabilized muscle fiber bundles (PMFB) and normalized to tissue wet weight in soleus (orange figures, A and B) or gastrocnemius (blue figures, C and D). In soleus, maximal rate of oxygen consumption was measured with (A) or without (B) lipid (palmitoylcarnitine; PC). Oxygen consumption in the gastrocnemius (blue figures, C and D) was also measured with (C) or without (D) PC substrate. Oxygen flux was analyzed by 3-way ANOVA with post hoc 2-way ANOVA analyzed independently per titration state. *P*-values for significant main effects of titration state (s), maternal (m, hatched bars) and postweaning (pw, colored bars) diets and interactive effects (s x m x pw) are listed above each graph. For post-hoc analysis, titration states with a caret (^p<.05) and an asterisk (*p<0.05) indicate a significant interactive effect; asterisks alone (*p<.05, **p<.01, ***p<.001) indicate significant differences by maternal diet. Individual data points with group mean are shown.

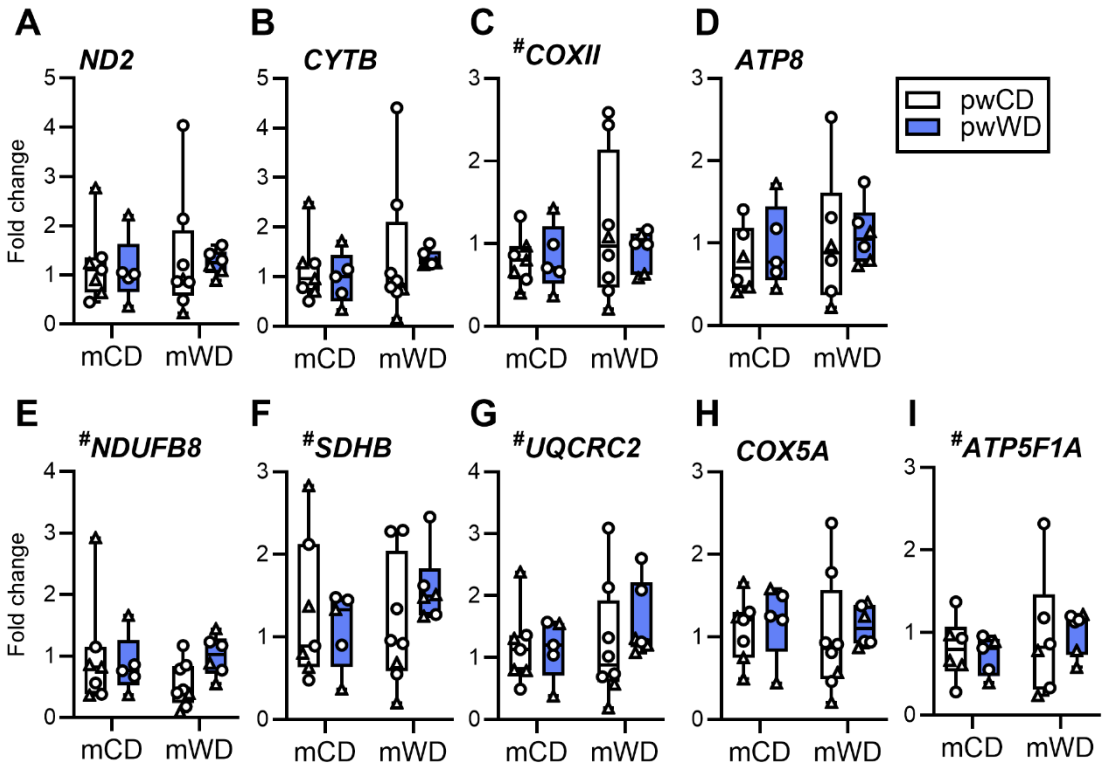

Supplemental Figure 4. OXPHOS gene expression in offspring gastroc.

Gene expression of mitochondrial and nuclear encoded proteins of ETS complexes were measured by qPCR in offspring gastroc. Mitochondrial encoded genes measured were (A) nd2 for CI, (B) cytb for CIII, (C) coxii for CIV and (D) atp8 for CV. Nuclear encoded genes measured were (E) ndufb8 for CI, (F) sdhb for CII, (G) uqcrc for CIII, (H) cox5a for CIV and (I) atp5f1a for CV. Individual gene expression was adjusted to the geometric mean of expression for housekeeper genes *rps15*, *28s* and *rpl13a* expression and presented as fold-change. Data were analyzed by 2-way ANOVA for significant main effects of maternal or postweaning diet or interactions using Sidak's multiple comparisons test. Individual data points for offspring on pwCD (open bars) or pwWD (closed bars) are shown along with group minimum, maximum, median and interquartile range.

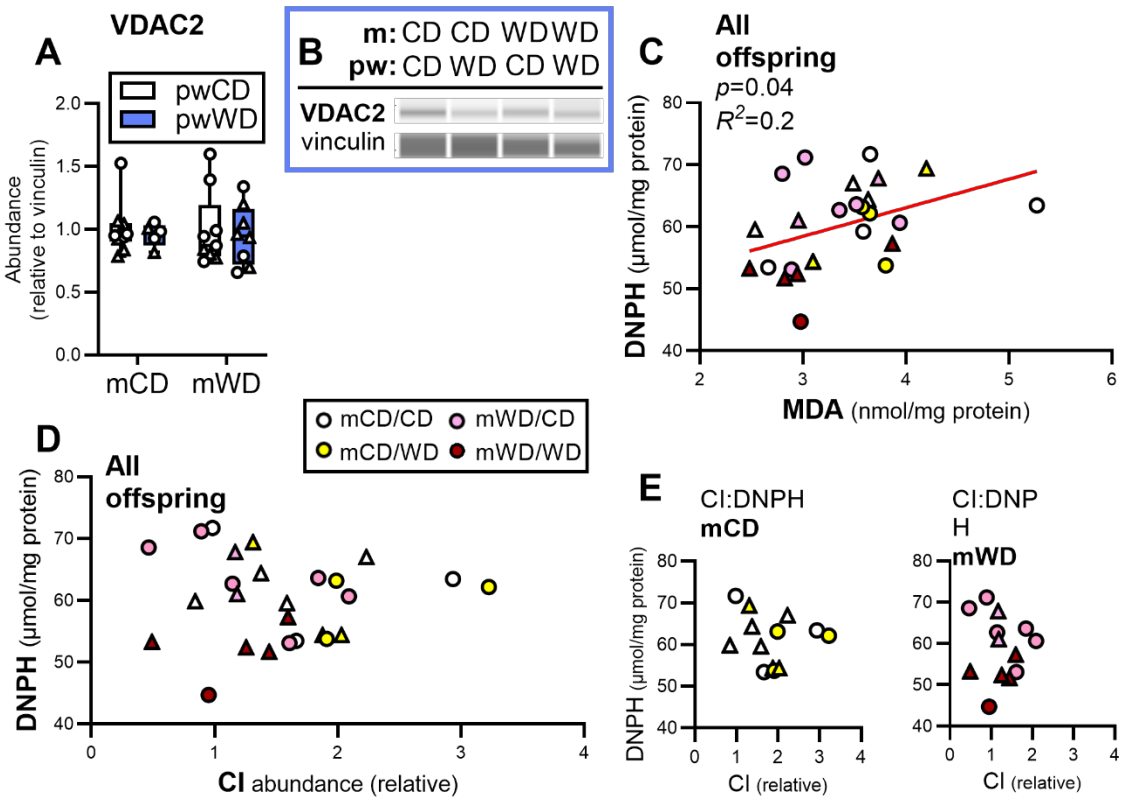

Supplemental Figure 5. Lipid accumulation in offspring gastroc.

Total ceramides (A), saturated ceramides (B) and total SPM (C) were measured in gastroc of 3Y offspring using LC-MS. Data were analyzed by 2-way ANOVA with Sidak's multiple comparisons test. Individual data points for offspring on pwCD (open bars) or pwWD (closed bars) are shown along with group minimum, maximum, median and interquartile range. Male (M) offspring are indicated by circles and female (F) offspring by triangles. Sample size for each group by sex: mCD/pwCD, 5F/3M; mCD/pwWD, 2F/3M; mWD/pwCD, 2F/6M; mWD/pwWD, 5F/3M.

WORKS CITED

1. Kumar S, Kelly AS: Review of Childhood Obesity: From Epidemiology, Etiology, and Comorbidities to Clinical Assessment and Treatment. Mayo Clin Proc 2017;92:251-265

2. Ogden CL, Carroll MD, Kit BK, Flegal KM: Prevalence of childhood and adult obesity in the United States, 2011-2012. JAMA 2014;311:806-814

3. Ward ZJ, Long MW, Resch SC, Giles CM, Cradock AL, Gortmaker SL: Simulation of Growth Trajectories of Childhood Obesity into Adulthood. N Engl J Med 2017;377:2145-2153

4. Isomaa B, Almgren P, Tuomi T, Forsén B, Lahti K, Nissén M, Taskinen MR, Groop L: Cardiovascular morbidity and mortality associated with the metabolic syndrome. Diabetes Care 2001;24:683-689

5. Abbasi F, Brown BW, Jr., Lamendola C, McLaughlin T, Reaven GM: Relationship between obesity, insulin resistance, and coronary heart disease risk. J Am Coll Cardiol 2002;40:937-943

6. Cornier MA, Dabelea D, Hernandez TL, Lindstrom RC, Steig AJ, Stob NR, Van Pelt RE, Wang H, Eckel RH: The metabolic syndrome. Endocrine reviews 2008;29:777-822

7. Spurr S, Bally J, Hill P, Gray K, Newman P, Hutton A: Exploring the Prevalence of Undiagnosed Prediabetes, Type 2 Diabetes Mellitus, and Risk Factors in Adolescents: A Systematic Review. Journal of pediatric nursing 2020;50:94-104

8. Todd JN, Srinivasan S, Pollin TI: Advances in the Genetics of Youth-Onset Type 2 Diabetes. Curr Diab Rep 2018;18:57

9. Mehta NK, Abrams LR, Myrskyla M: US life expectancy stalls due to cardiovascular disease, not drug deaths. Proc Natl Acad Sci U S A 2020;117:6998-7000

10. Basu M, Trask AJ, Garg V: Shaping the future heart: transgenerational outcomes of maternal metabolic syndrome. Am J Physiol Heart Circ Physiol 2019;316:H1141-h1143

11. Dunbar SB, Khavjou OA, Bakas T, Hunt G, Kirch RA, Leib AR, Morrison RS, Poehler DC, Roger VL, Whitsel LP, American Heart A: Projected Costs of Informal Caregiving for Cardiovascular Disease: 2015 to 2035: A Policy Statement From the American Heart Association. Circulation 2018;137:e558-e577

12. Barker DJ: The developmental origins of insulin resistance. Hormone research 2005;64 Suppl 3:2-7

13. Saben JL, Boudoures AL, Asghar Z, Thompson A, Drury A, Zhang W, Chi M, Cusumano A, Scheaffer S, Moley KH: Maternal Metabolic Syndrome Programs Mitochondrial Dysfunction via Germline Changes across Three Generations. Cell Rep 2016;16:1-8

14. Recabarren SE, Padmanabhan V, Codner E, Lobos A, Durán C, Vidal M, Foster DL, Sir-Petermann T: Postnatal developmental consequences of altered insulin sensitivity in female sheep treated prenatally with testosterone. Am J Physiol Endocrinol Metab 2005;289:E801-806

15. Xita N, Tsatsoulis A: Review: fetal programming of polycystic ovary syndrome by androgen excess: evidence from experimental, clinical, and genetic association studies. J Clin Endocrinol Metab 2006;91:1660-1666

16. Friedman JE: Developmental Programming of Obesity and Diabetes in Mouse, Monkey, and Man in 2018: Where Are We Headed? Diabetes 2018;67:2137-2151

17. Oestreich AK, Moley KH: Developmental and Transmittable Origins of Obesity-Associated Health Disorders. Trends in genetics : TIG 2017;33:399-407

18. Barker DJ, Eriksson JG, Forsén T, Osmond C: Fetal origins of adult disease: strength of effects and biological basis. International journal of epidemiology 2002;31:1235-1239

19. Symonds ME, Stephenson T, Gardner DS, Budge H: Long-term effects of nutritional programming of the embryo and fetus: mechanisms and critical windows. Reprod Fertil Dev 2007;19:53-63

20. Critical Periods of Development. In *Mother To Baby | Fact Sheets* Brentwood (TN), Organization of Teratology Information Specialists (OTIS). Copyright by OTIS, March 1, 2021., 1994

21. Malhotra A, Allison BJ, Castillo-Melendez M, Jenkin G, Polglase GR, Miller SL: Neonatal Morbidities of Fetal Growth Restriction: Pathophysiology and Impact. Front Endocrinol (Lausanne) 2019;10:55

22. Gaillard R, Jaddoe VWV: Maternal cardiovascular disorders before and during pregnancy and offspring cardiovascular risk across the life course. Nature reviews Cardiology 2023;20:617-630

23. Barker DJ, Osmond C: Infant mortality, childhood nutrition, and ischaemic heart disease in England and Wales. Lancet 1986;1:1077-1081

24. Barker DJ: The origins of the developmental origins theory. J Intern Med 2007;261:412-417

25. de Boo HA, Harding JE: The developmental origins of adult disease (Barker) hypothesis. Aust N Z J Obstet Gynaecol 2006;46:4-14

26. Barker DJ: Fetal origins of coronary heart disease. BMJ (Clinical research ed) 1995;311:171-174

27. Mortensen OH, Olsen HL, Frandsen L, Nielsen PE, Nielsen FC, Grunnet N, Quistorff B: A maternal low protein diet has pronounced effects on mitochondrial gene expression in offspring liver and skeletal muscle; protective effect of taurine. Journal of biomedical science 2010;17 Suppl 1:S38

28. Roberts VHJ, Gaffney JE, Morgan TK, Frias AE: Placental adaptations in a nonhuman primate model of gestational protein restriction. J Dev Orig Health Dis 2020:1-7

29. Greyslak KT, Hetrick B, Bergman BC, Dean TA, Wesolowski SR, Gannon M, Schenk S, Sullivan EL, Aagaard KM, Kievit P, Chicco AJ, Friedman JE, McCurdy CE: A Maternal Western-Style Diet Impairs Skeletal Muscle Lipid Metabolism in Adolescent Japanese Macaques. Diabetes 2023;72:1766-1780

30. Sureshchandra S, Chan CN, Robino JJ, Parmelee LK, Nash MJ, Wesolowski SR, Pietras EM, Friedman JE, Takahashi D, Shen W, Jiang X, Hennebold JD, Goldman D, Packwood W, Lindner JR, Roberts CT, Jr., Burwitz BJ, Messaoudi I, Varlamov O: Maternal Western-style diet remodels the transcriptional landscape of fetal hematopoietic stem and progenitor cells in rhesus macaques. Stem cell reports 2022;17:2595-2609

31. Dunn GA, Thompson JR, Mitchell AJ, Papadakis S, Selby M, Fair D, Gustafsson HC, Sullivan EL: Perinatal Western-style diet alters serotonergic neurons in the macaque raphe nuclei. Frontiers in neuroscience 2022;16:1067479

32. Hockett CW, Harrall KK, Moore BF, Starling AP, Bellatorre A, Sauder KA, Perng W, Scherzinger A, Garg K, Ringham BM, Glueck DH, Dabelea D: Persistent effects of in utero overnutrition on offspring adiposity: the Exploring Perinatal Outcomes among Children (EPOCH) study. Diabetologia 2019;62:2017-2024

33. Franke K, Clarke GD, Dahnke R, Gaser C, Kuo AH, Li C, Schwab M, Nathanielsz PW: Premature Brain Aging in Baboons Resulting from Moderate Fetal Undernutrition. Front Aging Neurosci 2017;9:92

34. Marshall NE, Abrams B, Barbour LA, Catalano P, Christian P, Friedman JE, Hay WW, Jr., Hernandez TL, Krebs NF, Oken E, Purnell JQ, Roberts JM, Soltani H, Wallace J, Thornburg KL: The importance of nutrition in pregnancy and lactation: lifelong consequences. Am J Obstet Gynecol 2022;226:607-632

35. Burgess DJ, Moritz KM: Prenatal alcohol exposure and developmental programming of mental illness. J Dev Orig Health Dis 2020;11:211-221

36. Wimberly CE, Gulrajani NB, Russ JB, Landi D, Wiemels JL, Towry L, Wiencke JK, Walsh KM: Maternal prenatal use of alcohol, tobacco, and illicit drugs and associations with childhood cancer subtypes. Cancer epidemiology, biomarkers & prevention : a publication of the American Association for Cancer Research, cosponsored by the American Society of Preventive Oncology 2023;

37. Alves-Wagner AB, Kusuyama J, Nigro P, Ramachandran K, Makarewicz N, Hirshman MF, Goodyear LJ: Grandmaternal exercise improves metabolic health of second-generation offspring. Mol Metab 2022:101490

38. Wasinski F, Bacurau RF, Estrela GR, Klempin F, Arakaki AM, Batista RO, Mafra FF, do Nascimento LF, Hiyane MI, Velloso LA, Câmara NO, Araujo RC: Exercise during pregnancy protects adult mouse offspring from diet-induced obesity. Nutrition & metabolism 2015;12:56

39. Raipuria M, Bahari H, Morris MJ: Effects of maternal diet and exercise during pregnancy on glucose metabolism in skeletal muscle and fat of weanling rats. PLoS One 2015;10:e0120980

40. Gustafsson HC, Sullivan EL, Nousen EK, Sullivan CA, Huang E, Rincon M, Nigg JT, Loftis JM: Maternal prenatal depression predicts infant negative affect via maternal inflammatory cytokine levels. Brain Behav Immun 2018;

41. Bolton JL, Bilbo SD: Developmental programming of brain and behavior by perinatal diet: focus on inflammatory mechanisms. Dialogues Clin Neurosci 2014;16:307-320

42. Chan JC, Nugent BM, Bale TL: Parental Advisory: Maternal and Paternal Stress Can Impact Offspring Neurodevelopment. Biol Psychiatry 2018;83:886-894

43. Yehuda R, Bell A, Bierer LM, Schmeidler J: Maternal, not paternal, PTSD is related to increased risk for PTSD in offspring of Holocaust survivors. J Psychiatr Res 2008;42:1104-1111

44. Eisner JR, Barnett MA, Dumesic DA, Abbott DH: Ovarian hyperandrogenism in adult female rhesus monkeys exposed to prenatal androgen excess. Fertil Steril 2002;77:167-172

45. Cardoso RC, Veiga-Lopez A, Moeller J, Beckett E, Pease A, Keller E, Madrigal V, Chazenbalk G, Dumesic D, Padmanabhan V: Developmental Programming: Impact of Gestational Steroid and Metabolic Milieus on Adiposity and Insulin Sensitivity in Prenatal Testosterone-Treated Female Sheep. Endocrinology 2016;157:522-535

46. Kaseva N, Vääräsmäki M, Sundvall J, Matinolli HM, Sipola M, Tikanmäki M, Heinonen K, Lano A, Wehkalampi K, Wolke D, Ruokonen A, Andersson S, Järvelin MR, Räikkönen K, Eriksson JG, Kajantie E: Gestational Diabetes But Not Prepregnancy Overweight Predicts for Cardiometabolic Markers in Offspring Twenty Years Later. J Clin Endocrinol Metab 2019;104:2785-2795

47. Wicklow BA, Sellers EAC, Sharma AK, Kroeker K, Nickel NC, Philips-Beck W, Shen GX: Association of Gestational Diabetes and Type 2 Diabetes Exposure In Utero With the Development of Type 2 Diabetes in First Nations and Non-First Nations Offspring. JAMA Pediatr 2018;172:724-731

48. Leonard SA, Rasmussen KM, King JC, Abrams B: Trajectories of maternal weight from before pregnancy through postpartum and associations with childhood obesity. Am J Clin Nutr 2017;106:1295-1301

49. Wardinger JE, Ambati S: Placental Insufficiency. In *StatPearls* Treasure Island (FL) ineligible companies. Disclosure: Shashikanth Ambati declares no relevant financial relationships with ineligible companies., StatPearls Publishing

50. Gagnon R: Placental insufficiency and its consequences. Eur J Obstet Gynecol Reprod Biol 2003;110 Suppl 1:S99-107

51. Pintican D, Poienar AA, Strilciuc S, Mihu D: Effects of maternal smoking on human placental vascularization: A systematic review. Taiwanese journal of obstetrics & gynecology 2019;58:454-459

52. Black RE, Allen LH, Bhutta ZA, Caulfield LE, de Onis M, Ezzati M, Mathers C, Rivera J: Maternal and child undernutrition: global and regional exposures and health consequences. Lancet 2008;371:243-260

53. Barker DJ, Gluckman PD, Godfrey KM, Harding JE, Owens JA, Robinson JS: Fetal nutrition and cardiovascular disease in adult life. Lancet 1993;341:938-941

54. Jimenez-Chillaron JC, Hernandez-Valencia M, Reamer C, Fisher S, Joszi A, Hirshman M, Oge A, Walrond S, Przybyla R, Boozer C, Goodyear LJ, Patti ME: Beta-cell secretory dysfunction in the pathogenesis of low birth weight-associated diabetes: a murine model. Diabetes 2005;54:702-711

55. Phipps K, Barker DJ, Hales CN, Fall CH, Osmond C, Clark PM: Fetal growth and impaired glucose tolerance in men and women. Diabetologia 1993;36:225-228

56. Hales CN, Barker DJ: The thrifty phenotype hypothesis. Br Med Bull 2001;60:5-20

57. Miller SL, Huppi PS, Mallard C: The consequences of fetal growth restriction on brain structure and neurodevelopmental outcome. J Physiol 2016;594:807-823

58. Thorn SR, Rozance PJ, Brown LD, Hay WW, Jr.: The intrauterine growth restriction phenotype: fetal adaptations and potential implications for later life insulin resistance and diabetes. Semin Reprod Med 2011;29:225-236

59. Phillips DI: Insulin resistance as a programmed response to fetal undernutrition. Diabetologia 1996;39:1119-1122

60. Hattersley AT, Tooke JE: The fetal insulin hypothesis: an alternative explanation of the association of low birthweight with diabetes and vascular disease. Lancet 1999;353:1789-1792

61. Jonker SS, Kamna D, LoTurco D, Kailey J, Brown LD: IUGR impairs cardiomyocyte growth and maturation in fetal sheep. J Endocrinol 2018;239:253-265

62. Dunn PM: Gregor Mendel, OSA (1822-1884), founder of scientific genetics. Archives of disease in childhood Fetal and neonatal edition 2003;88:F537-539

63. Montague CT, Farooqi IS, Whitehead JP, Soos MA, Rau H, Wareham NJ, Sewter CP, Digby JE, Mohammed SN, Hurst JA, Cheetham CH, Earley AR, Barnett AH, Prins JB, O'Rahilly S: Congenital leptin deficiency is associated with severe early-onset obesity in humans. Nature 1997;387:903-908

64. Dabelea D, Mayer-Davis EJ, Saydah S, Imperatore G, Linder B, Divers J, Bell R, Badaru A, Talton JW, Crume T, Liese AD, Merchant AT, Lawrence JM, Reynolds K, Dolan L, Liu LL, Hamman RF: Prevalence of type 1 and type 2 diabetes among children and adolescents from 2001 to 2009. Jama 2014;311:1778-1786

65. Rodgers A, Woodward A, Swinburn B, Dietz WH: Prevalence trends tell us what did not precipitate the US obesity epidemic. The Lancet Public health 2018;3:e162-e163

66. Pinhas-Hamiel O, Zeitler P: The global spread of type 2 diabetes mellitus in children and adolescents. J Pediatr 2005;146:693-700

67. Bendor CD, Bardugo A, Pinhas-Hamiel O, Afek A, Twig G: Cardiovascular morbidity, diabetes and cancer risk among children and adolescents with severe obesity. Cardiovascular diabetology 2020;19:79

68. Galan C, Krykbaeva M, Rando OJ: Early life lessons: the lasting effects of germline epigenetic information on organismal development. Molecular Metabolism 2019;

69. Jaenisch R, Bird A: Epigenetic regulation of gene expression: how the genome integrates intrinsic and environmental signals. Nat Genet 2003;33 Suppl:245-254

70. Suter MA, Aagaard KM: Fetal Epigenetic Origins of Disease. In *Knobil and Neill's Physiology of Reproduction*, 2015, p. 2027-2054

71. Eckersley-Maslin MA, Alda-Catalinas C, Reik W: Dynamics of the epigenetic landscape during the maternal-to-zygotic transition. Nat Rev Mol Cell Biol 2018;19:436-450

72. Al Aboud NM, Tupper C, Jialal I: Genetics, Epigenetic Mechanism. In *StatPearls* Treasure Island (FL) ineligible companies. Disclosure: Connor Tupper declares no relevant financial relationships with ineligible companies. Disclosure: Ishwarlal Jialal declares no relevant financial relationships with ineligible companies., StatPearls Publishing. Copyright © 2023, StatPearls Publishing LLC., 2023

73. He XY, Ou CL, Xiao YH, Han Q, Li H, Zhou SX: LncRNAs: key players and novel insights into diabetes mellitus. Oncotarget 2017;8:71325-71341

74. Kaikkonen MU, Lam MT, Glass CK: Non-coding RNAs as regulators of gene expression and epigenetics. Cardiovascular research 2011;90:430-440

75. Dominguez-Salas P, Moore SE, Baker MS, Bergen AW, Cox SE, Dyer RA, Fulford AJ, Guan Y, Laritsky E, Silver MJ, Swan GE, Zeisel SH, Innis SM, Waterland RA, Prentice AM, Hennig BJ: Maternal nutrition at conception modulates DNA methylation of human metastable epialleles. Nat Commun 2014;5:3746

76. Sato M, Sato K: Maternal inheritance of mitochondrial DNA by diverse mechanisms to eliminate paternal mitochondrial DNA. Biochim Biophys Acta 2013;1833:1979-1984

77. Dumollard R, Duchen M, Carroll J: The role of mitochondrial function in the oocyte and embryo. Current topics in developmental biology 2007;77:21-49

78. Cree LM, Samuels DC, de Sousa Lopes SC, Rajasimha HK, Wonnapinij P, Mann JR, Dahl HH, Chinnery PF: A reduction of mitochondrial DNA molecules during embryogenesis explains the rapid segregation of genotypes. Nat Genet 2008;40:249-254

79. Wai T, Teoli D, Shoubridge EA: The mitochondrial DNA genetic bottleneck results from replication of a subpopulation of genomes. Nat Genet 2008;40:1484-1488

80. Sato K, Sato M: Multiple ways to prevent transmission of paternal mitochondrial DNA for maternal inheritance in animals. J Biochem 2017;162:247-253

81. Boudoures AL, Saben J, Drury A, Scheaffer S, Modi Z, Zhang W, Moley KH: Obesity-exposed oocytes accumulate and transmit damaged mitochondria due to an inability to activate mitophagy. Dev Biol 2017;426:126-138

82. Zhang H, Burr SP, Chinnery PF: The mitochondrial DNA genetic bottleneck: inheritance and beyond. Essays Biochem 2018;62:225-234

83. Wai T, Ao A, Zhang X, Cyr D, Dufort D, Shoubridge EA: The role of mitochondrial DNA copy number in mammalian fertility. Biol Reprod 2010;83:52-62

84. Dimauro S, Davidzon G: Mitochondrial DNA and disease. Ann Med 2005;37:222-232

85. Gemma C, Sookoian S, Alvarinas J, Garcia SI, Quintana L, Kanevsky D, Gonzalez CD, Pirola CJ: Mitochondrial DNA depletion in small- and large-for-gestational-age newborns. Obesity (Silver Spring) 2006;14:2193-2199

86. Mitchell M, Schulz SL, Armstrong DT, Lane M: Metabolic and mitochondrial dysfunction in early mouse embryos following maternal dietary protein intervention. Biol Reprod 2009;80:622-630

87. Luzzo KM, Wang Q, Purcell SH, Chi M, Jimenez PT, Grindler N, Schedl T, Moley KH: High fat diet induced developmental defects in the mouse: oocyte meiotic aneuploidy and fetal growth retardation/brain defects. PLoS One 2012;7:e49217

88. Nehra D, Le HD, Fallon EM, Carlson SJ, Woods D, White YA, Pan AH, Guo L, Rodig SJ, Tilly JL, Rueda BR, Puder M: Prolonging the female reproductive lifespan and improving egg quality with dietary omega-3 fatty acids. Aging Cell 2012;11:1046-1054

89. Kong A, Frigge ML, Masson G, Besenbacher S, Sulem P, Magnusson G, Gudjonsson SA, Sigurdsson A, Jonasdottir A, Jonasdottir A, Wong WS, Sigurdsson G, Walters GB, Steinberg S, Helgason H, Thorleifsson G, Gudbjartsson DF, Helgason A, Magnusson OT, Thorsteinsdottir U, Stefansson K: Rate of de novo mutations and the importance of father's age to disease risk. Nature 2012;488:471-475

90. Morgan CP, Chan JC, Bale TL: Driving the Next Generation: Paternal Lifetime Experiences Transmitted via Extracellular Vesicles and Their Small RNA Cargo. Biol Psychiatry 2019;85:164-171

91. Gapp K, Jawaid A, Sarkies P, Bohacek J, Pelczar P, Prados J, Farinelli L, Miska E, Mansuy IM: Implication of sperm RNAs in transgenerational inheritance of the effects of early trauma in mice. Nature neuroscience 2014;17:667-669

92. Fischer V, Kretschmer M, Germain PL, Kaur J, Mompart-Barrenechea S, Pelczar P, Schürmann D, Schär P, Gapp K: Sperm chromatin accessibility's involvement in the intergenerational effects of stress hormone receptor activation. Transl Psychiatry 2023;13:378

93. Gannon JR, Emery BR, Jenkins TG, Carrell DT: The sperm epigenome: implications for the embryo. Adv Exp Med Biol 2014;791:53-66

94. Hoffmann LB, Li B, Zhao Q, Wei W, Leighton LJ, Bredy TW, Pang TY, Hannan AJ: Chronically high stress hormone levels dysregulate sperm long noncoding RNAs and their embryonic microinjection alters development and affective behaviours. Mol Psychiatry 2023;

95. Rando OJ: Daddy issues: paternal effects on phenotype. Cell 2012;151:702-708

96. Furse S, Morgan HL, Koulman A, Watkins AJ: Characterisation of the Paternal Influence on Intergenerational Offspring Cardiac and Brain Lipid Homeostasis in Mice. Int J Mol Sci 2023;24

97. Shitara H, Kaneda H, Sato A, Inoue K, Ogura A, Yonekawa H, Hayashi JI: Selective and continuous elimination of mitochondria microinjected into mouse eggs from spermatids, but not from liver cells, occurs throughout embryogenesis. Genetics 2000;156:1277-1284

98. Robertson SA: Seminal plasma and male factor signalling in the female reproductive tract. Cell Tissue Res 2005;322:43-52

99. Roach AN, Bhadsavle SS, Higgins SL, Derrico DD, Basel A, Thomas KN, Golding MC: Alterations in sperm RNAs persist after alcohol cessation and correlate with epididymal mitochondrial dysfunction. Andrology 2023;

100. Luo S, Valencia CA, Zhang J, Lee NC, Slone J, Gui B, Wang X, Li Z, Dell S, Brown J, Chen SM, Chien YH, Hwu WL, Fan PC, Wong LJ, Atwal PS, Huang T: Biparental Inheritance of Mitochondrial DNA in Humans. Proc Natl Acad Sci U S A 2018;115:13039-13044

101. Pembrey ME, Bygren LO, Kaati G, Edvinsson S, Northstone K, Sjostrom M, Golding J, Team AS: Sex-specific, male-line transgenerational responses in humans. Eur J Hum Genet 2006;14:159-166

102. Shi X, Li X, Hou Y, Cao X, Zhang Y, Wang H, Wang H, Peng C, Li J, Li Q, Wu C, Xiao X: Paternal hyperglycemia in rats exacerbates the development of obesity in offspring. J Endocrinol 2017;234:175-186

103. Rius R, Cowley MJ, Riley L, Puttick C, Thorburn DR, Christodoulou J: Biparental inheritance of mitochondrial DNA in humans is not a common phenomenon. Genetics in medicine : official journal of the American College of Medical Genetics 2019;21:2823-2826

104. Salas A, Schönherr S, Bandelt HJ, Gómez-Carballa A, Weissensteiner H: Extraordinary claims require extraordinary evidence in asserted mtDNA biparental inheritance. Forensic science international Genetics 2020;47:102274

105. Sutovsky P, Moreno RD, Ramalho-Santos J, Dominko T, Simerly C, Schatten G: Ubiquitinated sperm mitochondria, selective proteolysis, and the regulation of mitochondrial inheritance in mammalian embryos. Biol Reprod 2000;63:582-590

106. Yu Z, O'Farrell PH, Yakubovich N, DeLuca SZ: The Mitochondrial DNA Polymerase Promotes Elimination of Paternal Mitochondrial Genomes. Curr Biol 2017;27:1033-1039

107. Rojansky R, Cha MY, Chan DC: Elimination of paternal mitochondria in mouse embryos occurs through autophagic degradation dependent on PARKIN and MUL1. Elife 2016;5

108. Jimenez-Chillaron JC, Isganaitis E, Charalambous M, Gesta S, Pentinat-Pelegrin T, Faucette RR, Otis JP, Chow A, Diaz R, Ferguson-Smith A, Patti ME: Intergenerational transmission of glucose intolerance and obesity by in utero undernutrition in mice. Diabetes 2009;58:460-468

109. Dunn GA, Bale TL: Maternal high-fat diet effects on third-generation female body size via the paternal lineage. Endocrinology 2011;152:2228-2236

110. Ferey J, Boudoures AL, Reid M, Drury A, Scheaffer S, Modi Z, Kovacs A, Pietka T, DeBosch BJ, Thompson MD, Diwan A, Moley KH: Maternal High-Fat, High-Sucrose Diet Induces Transgenerational Cardiac Mitochondrial Dysfunction Independent of Maternal Mitochondrial Inheritance. Am J Physiol Heart Circ Physiol 2019;

111. Deputy NP, Dub B, Sharma AJ: Prevalence and Trends in Prepregnancy Normal Weight - 48 States, New York City, and District of Columbia, 2011-2015. MMWR Morb Mortal Wkly Rep 2018;66:1402-1407

112. Creanga AA, Catalano PM, Bateman BT: Obesity in Pregnancy. N Engl J Med 2022;387:248-259

113. Chu SY, Callaghan WM, Kim SY, Schmid CH, Lau J, England LJ, Dietz PM: Maternal obesity and risk of gestational diabetes mellitus. Diabetes Care 2007;30:2070-2076

114. Browne K, Park BY, Goetzinger KR, Caughey AB, Yao R: The joint effects of obesity and pregestational diabetes on the risk of stillbirth. The journal of maternal-fetal & neonatal medicine : the official journal of the European Association of Perinatal Medicine, the Federation of Asia and Oceania Perinatal Societies, the International Society of Perinatal Obstet 2021;34:332-338

115. Ehrenberg HM, Mercer BM, Catalano PM: The influence of obesity and diabetes on the prevalence of macrosomia. Am J Obstet Gynecol 2004;191:964-968

116. Kulkarni SR, Kumaran K, Rao SR, Chougule SD, Deokar TM, Bhalerao AJ, Solat VA, Bhat DS, Fall CH, Yajnik CS: Maternal lipids are as important as glucose for fetal growth: findings from the Pune Maternal Nutrition Study. Diabetes Care 2013;36:2706-2713

117. Barbour LA, Farabi SS, Friedman JE, Hirsch NM, Reece MS, Van Pelt RE, Hernandez TL: Postprandial Triglycerides Predict Newborn Fat More Strongly than Glucose in Women with Obesity in Early Pregnancy. Obesity (Silver Spring) 2018;26:1347-1356

118. Josefson JL, Scholtens DM, Kuang A, Catalano PM, Lowe LP, Dyer AR, Petito LC, Lowe WL, Jr., Metzger BE: Newborn Adiposity and Cord Blood C-Peptide as Mediators of the Maternal Metabolic Environment and Childhood Adiposity. Diabetes Care 2021;44:1194-1202

119. Caprio S, Santoro N, Weiss R: Childhood obesity and the associated rise in cardiometabolic complications. Nat Metab 2020;2:223-232

120. Barbour LA, Hernandez TL: Maternal Lipids and Fetal Overgrowth: Making Fat from Fat. Clinical therapeutics 2018;40:1638-1647

121. Adank MC, Benschop L, van Streun SP, Smak Gregoor AM, Mulder MT, Steegers EAP, Schalekamp-Timmermans S, Roeters van Lennep JE: Gestational lipid profile as an early marker of metabolic syndrome in later life: a population-based prospective cohort study. BMC medicine 2020;18:394

122. Herrera E, Desoye G: Maternal and fetal lipid metabolism under normal and gestational diabetic conditions. Hormone molecular biology and clinical investigation 2016;26:109-127

123. Metzger BE, Buchanan TA, Coustan DR, de Leiva A, Dunger DB, Hadden DR, Hod M, Kitzmiller JL, Kjos SL, Oats JN, Pettitt DJ, Sacks DA, Zoupas C: Summary and recommendations of the Fifth International Workshop-Conference on Gestational Diabetes Mellitus. Diabetes Care 2007;30 Suppl 2:S251-260

124. Brumbaugh DE, Tearse P, Cree-Green M, Fenton LZ, Brown M, Scherzinger A, Reynolds R, Alston M, Hoffman C, Pan Z, Friedman JE, Barbour LA: Intrahepatic fat is increased in the neonatal offspring of obese women with gestational diabetes. J Pediatr 2013;162:930-936.e931

125. HERNANDEZ TL, FARABI SS, HIRSCH N, DUNN EZ, HAUGEN EA, BRUMBAUGH D, BROWN MS, FRIEDMAN JE, BARBOUR LA: 352-OR: Maternal Triglycerides in Gestational Diabetes Are Strongly Associated with Increased Newborn Hepatic Fat Independent of Subcutaneous Fat. Diabetes 2019;68

126. Li CC, Young PE, Maloney CA, Eaton SA, Cowley MJ, Buckland ME, Preiss T, Henstridge DC, Cooney GJ, Febbraio MA, Martin DI, Cropley JE, Suter CM: Maternal obesity and diabetes induces latent metabolic defects and widespread epigenetic changes in isogenic mice. Epigenetics 2013;8:602-611

127. Alba-Linares JJ, Pérez RF, Tejedor JR, Bastante-Rodríguez D, Ponce F, Carbonell NG, Zafra RG, Fernández AF, Fraga MF, Lurbe E: Maternal obesity and gestational diabetes reprogram the methylome of offspring beyond birth by inducing epigenetic signatures in metabolic and developmental pathways. Cardiovascular diabetology 2023;22:44

128. Boyle KE, Patinkin ZW, Shapiro ALB, Bader C, Vanderlinden L, Kechris K, Janssen RC, Ford RJ, Smith BK, Steinberg GR, Davidson EJ, Yang IV, Dabelea D, Friedman JE: Maternal obesity alters fatty acid oxidation, AMPK activity, and associated DNA methylation in mesenchymal stem cells from human infants. Mol Metab 2017;6:1503-1516

129. Waldrop SW, Niemiec S, Wood C, Gyllenhammer LE, Jansson T, Friedman JE, Tryggestad JB, Borengasser SJ, Davidson EJ, Yang IV, Kechris K, Dabelea D, Boyle KE: Cord blood DNA methylation of immune and lipid metabolism genes is associated with maternal triglycerides and child adiposity. Obesity (Silver Spring) 2023;

130. Lecoutre S, Oger F, Pourpe C, Butruille L, Marousez L, Dickes-Coopman A, Laborie C, Guinez C, Lesage J, Vieau D, Junien C, Eberlé D, Gabory A, Eeckhoute J, Breton C: Maternal obesity programs increased leptin gene expression in rat male offspring via epigenetic modifications in a depot-specific manner. Mol Metab 2017;6:922-930

131. Zheng S, Rollet M, Pan YX: Protein restriction during gestation alters histone modifications at the glucose transporter 4 (GLUT4) promoter region and induces GLUT4 expression in skeletal muscle of female rat offspring. J Nutr Biochem 2012;23:1064-1071

132. Sugino KY, Mandala A, Janssen RC, Gurung S, Trammell M, Day MW, Brush RS, Papin JF, Dyer DW, Agbaga MP, Friedman JE, Castillo-Castrejon M, Jonscher KR, Myers DA: Western diet-induced shifts in the maternal microbiome are associated with altered microRNA expression in baboon placenta and fetal liver. Frontiers in clinical diabetes and healthcare 2022;3

133. Du M, Yan X, Tong JF, Zhao J, Zhu MJ: Maternal obesity, inflammation, and fetal skeletal muscle development. Biol Reprod 2010;82:4-12

134. Brack AS, Conboy MJ, Roy S, Lee M, Kuo CJ, Keller C, Rando TA: Increased Wnt signaling during aging alters muscle stem cell fate and increases fibrosis. Science 2007;317:807-810

135. Crane JD, Devries MC, Safdar A, Hamadeh MJ, Tarnopolsky MA: The effect of aging on human skeletal muscle mitochondrial and intramyocellular lipid ultrastructure. J Gerontol A Biol Sci Med Sci 2010;65:119-128

136. Savage DB, Watson L, Carr K, Adams C, Brage S, Chatterjee KK, Hodson L, Boesch C, Kemp GJ, Sleigh A: Accumulation of saturated intramyocellular lipid is associated with insulin resistance. J Lipid Res 2019;60:1323-1332

137. Kahn D, Perreault L, Macias E, Zarini S, Newsom SA, Strauss A, Kerege A, Harrison K, Snell-Bergeon J, Bergman BC: Subcellular localisation and composition of intramuscular triacylglycerol influence insulin sensitivity in humans. Diabetologia 2021;64:168-180

138. Boyle KE, Patinkin Z, Shapiro AL, Baker PR, 2nd, Dabelea D, Friedman JE: Mesenchymal stem cells from infants born to obese mothers exhibit greater potential for adipogenesis: the healthy start BabyBUMP Project. Diabetes 2016;65:647-659

139. Witchel SF, Oberfield SE, Peña AS: Polycystic Ovary Syndrome: Pathophysiology, Presentation, and Treatment With Emphasis on Adolescent Girls. J Endocr Soc 2019;3:1545-1573

140. Dumesic DA, Oberfield SE, Stener-Victorin E, Marshall JC, Laven JS, Legro RS: Scientific Statement on the Diagnostic Criteria, Epidemiology, Pathophysiology, and Molecular Genetics of Polycystic Ovary Syndrome. Endocrine reviews 2015;36:487-525

141. Abbott DH, Rogers J, Dumesic DA, Levine JE: Naturally Occurring and Experimentally Induced Rhesus Macaque Models for Polycystic Ovary Syndrome: Translational Gateways to Clinical Application. Medical sciences (Basel, Switzerland) 2019;7

142. Goodarzi MO, Dumesic DA, Chazenbalk G, Azziz R: Polycystic ovary syndrome: etiology, pathogenesis and diagnosis. Nat Rev Endocrinol 2011;7:219-231

143. McCartney CR, Prendergast KA, Chhabra S, Eagleson CA, Yoo R, Chang RJ, Foster CM, Marshall JC: The association of obesity and hyperandrogenemia during the pubertal transition in girls: obesity as a potential factor in the genesis of postpubertal hyperandrogenism. J Clin Endocrinol Metab 2006;91:1714-1722

144. McCartney CR, Blank SK, Prendergast KA, Chhabra S, Eagleson CA, Helm KD, Yoo R, Chang RJ, Foster CM, Caprio S, Marshall JC: Obesity and sex steroid changes across puberty: evidence for marked hyperandrogenemia in pre- and early pubertal obese girls. J Clin Endocrinol Metab 2007;92:430-436

145. Dumesic DA, Akopians AL, Madrigal VK, Ramirez E, Margolis DJ, Sarma MK, Thomas AM, Grogan TR, Haykal R, Schooler TA, Okeya BL, Abbott DH, Chazenbalk GD: Hyperandrogenism Accompanies Increased Intra-Abdominal Fat Storage in Normal Weight Polycystic Ovary Syndrome Women. J Clin Endocrinol Metab 2016;101:4178-4188

146. Evans DJ, Barth JH, Burke CW: Body fat topography in women with androgen excess. International journal of obesity 1988;12:157-162

147. Polderman KH, Gooren LJ, Asscheman H, Bakker A, Heine RJ: Induction of insulin resistance by androgens and estrogens. J Clin Endocrinol Metab 1994;79:265-271

148. Dunaif A, Segal KR, Futterweit W, Dobrjansky A: Profound peripheral insulin resistance, independent of obesity, in polycystic ovary syndrome. Diabetes 1989;38:1165-1174

149. Ding EL, Song Y, Malik VS, Liu S: Sex differences of endogenous sex hormones and risk of type 2 diabetes: a systematic review and meta-analysis. Jama 2006;295:1288-1299

150. Goodarzi MO, Erickson S, Port SC, Jennrich RI, Korenman SG: Relative impact of insulin resistance and obesity on cardiovascular risk factors in polycystic ovary syndrome. Metabolism 2003;52:713-719

151. Alexander CJ, Tangchitnob EP, Lepor NE: Polycystic ovary syndrome: a major unrecognized cardiovascular risk factor in women. Reviews in obstetrics & gynecology 2009;2:232-239

152. Torchen LC, Idkowiak J, Fogel NR, O'Neil DM, Shackleton CH, Arlt W, Dunaif A: Evidence for Increased 5α-Reductase Activity During Early Childhood in Daughters of Women With Polycystic Ovary Syndrome. J Clin Endocrinol Metab 2016;101:2069-2075

153. Sir-Petermann T, Codner E, Maliqueo M, Echiburú B, Hitschfeld C, Crisosto N, Pérez-Bravo F, Recabarren SE, Cassorla F: Increased anti-Müllerian hormone serum concentrations in prepubertal daughters of women with polycystic ovary syndrome. J Clin Endocrinol Metab 2006;91:3105-3109

154. Sir-Petermann T, Ladrón de Guevara A, Codner E, Preisler J, Crisosto N, Echiburú B, Maliqueo M, Sánchez F, Perez-Bravo F, Cassorla F: Relationship between anti-Müllerian hormone (AMH) and insulin levels during different tanner stages in daughters of women with polycystic ovary syndrome. Reprod Sci 2012;19:383-390

155. Risal S, Li C, Luo Q, Fornes R, Lu H, Eriksson G, Manti M, Ohlsson C, Lindgren E, Crisosto N, Maliqueo M, Echiburú B, Recabarren S, Petermann TS, Benrick A, Brusselaers N, Qiao J, Deng Q, Stener-Victorin E: Transgenerational transmission of reproductive and metabolic dysfunction in the male progeny of polycystic ovary syndrome. Cell reports Medicine 2023;4:101035

156. Kent SC, Gnatuk CL, Kunselman AR, Demers LM, Lee PA, Legro RS: Hyperandrogenism and hyperinsulinism in children of women with polycystic ovary syndrome: a controlled study. J Clin Endocrinol Metab 2008;93:1662-1669

157. Farhadi-Azar M, Noroozzadeh M, Ghahremani M, Rahmati M, Saei Ghare Naz M, Azizi F, Ramezani Tehrani F: Maternal androgen excess increases the risk of pre-diabetes mellitus in male offspring in later life: a long-term population-based follow-up study. Journal of endocrinological investigation 2023;46:1775-1785

158. Legro RS, Driscoll D, Strauss JF, 3rd, Fox J, Dunaif A: Evidence for a genetic basis for hyperandrogenemia in polycystic ovary syndrome. Proc Natl Acad Sci U S A 1998;95:14956-14960

159. Torchen LC, Kumar A, Kalra B, Savjani G, Sisk R, Legro RS, Dunaif A: Increased antimüllerian hormone levels and other reproductive endocrine changes in adult male relatives of women with polycystic ovary syndrome. Fertil Steril 2016;106:50-55

160. Vink JM, Sadrzadeh S, Lambalk CB, Boomsma DI: Heritability of polycystic ovary syndrome in a Dutch twin-family study. J Clin Endocrinol Metab 2006;91:2100-2104

161. Urbanek M, Sam S, Legro RS, Dunaif A: Identification of a polycystic ovary syndrome susceptibility variant in fibrillin-3 and association with a metabolic phenotype. J Clin Endocrinol Metab 2007;92:4191-4198

162. Ewens KG, Stewart DR, Ankener W, Urbanek M, McAllister JM, Chen C, Baig KM, Parker SC, Margulies EH, Legro RS, Dunaif A, Strauss JF, 3rd, Spielman RS: Family-based analysis of candidate genes for polycystic ovary syndrome. J Clin Endocrinol Metab 2010;95:2306-2315

163. Dunaif A: Perspectives in Polycystic Ovary Syndrome: From Hair to Eternity. J Clin Endocrinol Metab 2016;101:759-768

164. Dapas M, Sisk R, Legro RS, Urbanek M, Dunaif A, Hayes MG: Family-Based Quantitative Trait Meta-Analysis Implicates Rare Noncoding Variants in DENND1A in Polycystic Ovary Syndrome. J Clin Endocrinol Metab 2019;104:3835-3850

165. Hiam D, Simar D, Laker R, Altıntaş A, Gibson-Helm M, Fletcher E, Moreno-Asso A, Trewin AJ, Barres R, Stepto NK: Epigenetic Reprogramming of Immune Cells in Women With PCOS Impact Genes Controlling Reproductive Function. J Clin Endocrinol Metab 2019;104:6155-6170

166. Xu N, Kwon S, Abbott DH, Geller DH, Dumesic DA, Azziz R, Guo X, Goodarzi MO: Epigenetic mechanism underlying the development of polycystic ovary syndrome (PCOS)-like phenotypes in prenatally androgenized rhesus monkeys. PLoS One 2011;6:e27286

167. Roy S, Abudu A, Salinas I, Sinha N, Cline-Fedewa H, Yaw AM, Qi W, Lydic TA, Takahashi DL, Hennebold JD, Hoffmann HM, Wang J, Sen A: Androgen-mediated Perturbation of the Hepatic Circadian System Through Epigenetic Modulation Promotes NAFLD in PCOS Mice. Endocrinology 2022;163

168. Taniguchi CM, Emanuelli B, Kahn CR: Critical nodes in signalling pathways: insights into insulin action. Nat Rev Mol Cell Biol 2006;7:85-96

169. Facchini FS, Hua N, Abbasi F, Reaven GM: Insulin resistance as a predictor of age-related diseases. J Clin Endocrinol Metab 2001;86:3574-3578

170. Yip J, Facchini FS, Reaven GM: Resistance to insulin-mediated glucose disposal as a predictor of cardiovascular disease. J Clin Endocrinol Metab 1998;83:2773-2776

171. Jellinger PS: Metabolic consequences of hyperglycemia and insulin resistance. Clinical cornerstone 2007;8 Suppl 7:S30-42

172. Reaven GM: Hemostatic abnormalities associated with obesity and the metabolic syndrome. Journal of Thrombosis and Haemostasis 2005:1074-1085

173. Lebovitz HE: Insulin resistance: definition and consequences. Experimental and clinical endocrinology & diabetes : official journal, German Society of Endocrinology [and] German Diabetes Association 2001;109 Suppl 2:S135-148

174. Nilsson P, Nilsson J-Å, Hedblad B, Eriksson K-F, Berglund G: Hyperinsulinaemia as long-term predictor of death and ischaemic heart disease in nondiabetic men: The Malmö Preventive Project. Journal of Internal Medicine 2003;253:136-145

175. Mohan M, Deshmukh H, Maria Choy A, Lang C: 60 Insulin Resistance is Associated with All-cause Mortality and Accelerates the Risk of Progression to Diabetes in Non-diabetic Heart Failure Patients. Heart 2014;100:A34-A34

176. Hu G, Qiao Q, Tuomilehto J, Balkau B, Borch-Johnsen K, Pyorala K, Group ftDS: Prevalence of the Metabolic Syndrome and Its Relation to All-Cause and Cardiovascular Mortality in Nondiabetic European Men and Women. Archives of Internal Medicine 2004;164:1066-1076

177. Ausk KJ, Boyko EJ, Ioannou GN: Insulin Resistance Predicts Mortality in Nondiabetic Individuals in the U.S. Diabetes Care 2010;33:1179-1185

178. Brown MS, Goldstein JL: Selective versus total insulin resistance: a pathogenic paradox. Cell Metab 2008;7:95-96

179. Højlund K: Metabolism and insulin signaling in common metabolic disorders and inherited insulin resistance. Danish medical journal 2014;61:B4890

180. Biddinger SB, Hernandez-Ono A, Rask-Madsen C, Haas JT, Alemán JO, Suzuki R, Scapa EF, Agarwal C, Carey MC, Stephanopoulos G, Cohen DE, King GL, Ginsberg HN, Kahn CR: Hepatic insulin resistance is sufficient to produce dyslipidemia and susceptibility to atherosclerosis. Cell Metab 2008;7:125-134

181. Semple RK, Sleigh A, Murgatroyd PR, Adams CA, Bluck L, Jackson S, Vottero A, Kanabar D, Charlton-Menys V, Durrington P, Soos MA, Carpenter TA, Lomas DJ, Cochran EK, Gorden P, O'Rahilly S, Savage DB: Postreceptor insulin resistance contributes to human dyslipidemia and hepatic steatosis. J Clin Invest 2009;119:315-322

182. Jiang ZY, Lin YW, Clemont A, Feener EP, Hein KD, Igarashi M, Yamauchi T, White MF, King GL: Characterization of selective resistance to insulin signaling in the vasculature of obese Zucker (fa/fa) rats. J Clin Invest 1999;104:447-457

183. Cusi K, Maezono K, Osman A, Pendergrass M, Patti ME, Pratipanawatr T, DeFronzo RA, Kahn CR, Mandarino LJ: Insulin resistance differentially affects the PI 3-kinase- and MAP kinase-mediated signaling in human muscle. J Clin Invest 2000;105:311-320

184. DeFronzo RA, Tripathy D: Skeletal muscle insulin resistance is the primary defect in type 2 diabetes. Diabetes Care 2009;32 Suppl 2:S157-163

185. Kitessa SM, Abeywardena MY: Lipid-Induced Insulin Resistance in Skeletal Muscle: The Chase for the Culprit Goes from Total Intramuscular Fat to Lipid Intermediates, and Finally to Species of Lipid Intermediates. Nutrients 2016;8

186. Koves TR, Ussher JR, Noland RC, Slentz D, Mosedale M, Ilkayeva O, Bain J, Stevens R, Dyck JR, Newgard CB, Lopaschuk GD, Muoio DM: Mitochondrial overload and incomplete fatty acid oxidation contribute to skeletal muscle insulin resistance. Cell Metab 2008;7:45-56

187. Bergman BC, Goodpaster BH: Exercise and Muscle Lipid Content, Composition, and Localization: Influence on Muscle Insulin Sensitivity. Diabetes 2020;69:848-858

188. Perreault L, Newsom SA, Strauss A, Kerege A, Kahn DE, Harrison KA, Snell-Bergeon JK, Nemkov T, D'Alessandro A, Jackman MR, MacLean PS, Bergman BC: Intracellular localization of diacylglycerols and sphingolipids influences insulin sensitivity and mitochondrial function in human skeletal muscle. JCI insight 2018;3

189. Amati F, Dube JJ, Alvarez-Carnero E, Edreira MM, Chomentowski P, Coen PM, Switzer GE, Bickel PE, Stefanovic-Racic M, Toledo FG, Goodpaster BH: Skeletal muscle triglycerides, diacylglycerols, and ceramides in insulin resistance: another paradox in endurance-trained athletes? Diabetes 2011;60:2588-2597

190. Sarabhai T, Koliaki C, Mastrototaro L, Kahl S, Pesta D, Apostolopoulou M, Wolkersdorfer M, Bönner AC, Bobrov P, Markgraf DF, Herder C, Roden M: Dietary palmitate and oleate differently modulate insulin sensitivity in human skeletal muscle. Diabetologia 2022;65:301-314

191. Butterfield WJ, Hanley T, Whichelow MJ: PERIPHERAL METABOLISM OF GLUCOSE AND FREE FATTY ACIDS DURING ORAL GLUCOSE TOLERANCE TESTS. Metabolism 1965;14:851-866

192. Groop LC, Bonadonna RC, DelPrato S, Ratheiser K, Zyck K, Ferrannini E, DeFronzo RA: Glucose and free fatty acid metabolism in non-insulin-dependent diabetes mellitus. Evidence for multiple sites of insulin resistance. J Clin Invest 1989;84:205-213

193. Szendroedi J, Yoshimura T, Phielix E, Koliaki C, Marcucci M, Zhang D, Jelenik T, Müller J, Herder C, Nowotny P, Shulman GI, Roden M: Role of diacylglycerol activation of PKCθ in lipid-induced muscle insulin resistance in humans. Proc Natl Acad Sci U S A 2014;111:9597-9602

194. McCurdy CE, Schenk S, Hetrick B, Houck J, Drew BG, Kaye S, Lashbrook M, Bergman BC, Takahashi DL, Dean TA, Nemkov T, Gertsman I, Hansen KC, Philp A, Hevener AL, Chicco AJ, Aagaard KM, Grove KL, Friedman JE: Maternal obesity reduces oxidative capacity in fetal skeletal muscle of Japanese macaques. JCI insight 2016;1:e86612

195. Campodonico-Burnett W, Hetrick B, Wesolowski SR, Schenk S, Takahashi DL, Dean TA, Sullivan EL, Kievit P, Gannon M, Aagaard K, Friedman JE, McCurdy CE: Maternal Obesity and Western-Style Diet Impair Fetal and Juvenile Offspring Skeletal Muscle Insulin-Stimulated Glucose Transport in Nonhuman Primates. Diabetes 2020;

196. van der Giezen M, Tovar J: Degenerate mitochondria. EMBO Rep 2005;6:525-530

197. Labbé K, Murley A, Nunnari J: Determinants and functions of mitochondrial behavior. Annu Rev Cell Dev Biol 2014;30:357-391

198. Martini H, Passos JF: Cellular senescence: all roads lead to mitochondria. Febs j 2023;290:1186-1202

199. Ni HM, Williams JA, Ding WX: Mitochondrial dynamics and mitochondrial quality control. Redox Biol 2015;4:6-13

200. Friedman JR, Nunnari J: Mitochondrial form and function. Nature 2014;505:335-343

201. Chavez AO, Kamath S, Jani R, Sharma LK, Monroy A, Abdul-Ghani MA, Centonze VE, Sathyanarayana P, Coletta DK, Jenkinson CP, Bai Y, Folli F, Defronzo RA, Tripathy D: Effect of short-term free Fatty acids elevation on mitochondrial function in skeletal muscle of healthy individuals. J Clin Endocrinol Metab 2010;95:422-429

202. Goodpaster BH: Mitochondrial deficiency is associated with insulin resistance. Diabetes 2013;62:1032-1035

203. Tubbs E, Chanon S, Robert M, Bendridi N, Bidaux G, Chauvin MA, Ji-Cao J, Durand C, Gauvrit-Ramette D, Vidal H, Lefai E, Rieusset J: Disruption of Mitochondria-Associated Endoplasmic Reticulum Membrane (MAM) Integrity Contributes to Muscle Insulin Resistance in Mice and Humans. Diabetes 2018;67:636-650

204. Houzelle A, Jörgensen JA, Schaart G, Daemen S, van Polanen N, Fealy CE, Hesselink MKC, Schrauwen P, Hoeks J: Human skeletal muscle mitochondrial dynamics in relation to oxidative capacity and insulin sensitivity. Diabetologia 2021;64:424-436

205. Liesa M, Shirihai OS: Mitochondrial dynamics in the regulation of nutrient utilization and energy expenditure. Cell Metab 2013;17:491-506

206. Ngo J, Choi DW, Stanley IA, Stiles L, Molina AJA, Chen PH, Lako A, Sung ICH, Goswami R, Kim MY, Miller N, Baghdasarian S, Kim-Vasquez D, Jones AE, Roach B, Gutierrez V, Erion K,

Divakaruni AS, Liesa M, Danial NN, Shirihai OS: Mitochondrial morphology controls fatty acid utilization by changing CPT1 sensitivity to malonyl-CoA. Embo j 2023;42:e111901

207. Cogliati S, Enriquez JA, Scorrano L: Mitochondrial Cristae: Where Beauty Meets Functionality. Trends Biochem Sci 2016;41:261-273

208. Cogliati S, Frezza C, Soriano ME, Varanita T, Quintana-Cabrera R, Corrado M, Cipolat S, Costa V, Casarin A, Gomes LC, Perales-Clemente E, Salviati L, Fernandez-Silva P, Enriquez JA, Scorrano L: Mitochondrial cristae shape determines respiratory chain supercomplexes assembly and respiratory efficiency. Cell 2013;155:160-171

209. Drew BG, Ribas V, Le JA, Henstridge DC, Phun J, Zhou Z, Soleymani T, Daraei P, Sitz D, Vergnes L, Wanagat J, Reue K, Febbraio MA, Hevener AL: HSP72 is a mitochondrial stress sensor critical for Parkin action, oxidative metabolism, and insulin sensitivity in skeletal muscle. Diabetes 2014;63:1488-1505

210. Li W, Li H, Zheng L, Xia J, Yang X, Men S, Yuan Y, Fan Y: Ginsenoside CK improves skeletal muscle insulin resistance by activating DRP1/PINK1-mediated mitophagy. Food & function 2023;14:1024-1036

211. Nie Q, Wang C, Song G, Ma H, Kong D, Zhang X, Gan K, Tang Y: Mitofusin 2 deficiency leads to oxidative stress that contributes to insulin resistance in rat skeletal muscle cells. Molecular Biology Reports 2014;41:6975-6983

212. Anderson EJ, Lustig ME, Boyle KE, Woodlief TL, Kane DA, Lin CT, Price JW, 3rd, Kang L, Rabinovitch PS, Szeto HH, Houmard JA, Cortright RN, Wasserman DH, Neufer PD: Mitochondrial H2O2 emission and cellular redox state link excess fat intake to insulin resistance in both rodents and humans. J Clin Invest 2009;119:573-581

213. Cox CS, McKay SE, Holmbeck MA, Christian BE, Scortea AC, Tsay AJ, Newman LE, Shadel GS: Mitohormesis in Mice via Sustained Basal Activation of Mitochondrial and Antioxidant Signaling. Cell Metab 2018;28:776-786 e775

214. Xirouchaki CE, Jia Y, McGrath MJ, Greatorex S, Tran M, Merry TL, Hong D, Eramo MJ, Broome SC, Woodhead JST, D'Souza R F, Gallagher J, Salimova E, Huang C, Schittenhelm RB, Sadoshima J, Watt MJ, Mitchell CA, Tiganis T: Skeletal muscle NOX4 is required for adaptive responses that prevent insulin resistance. Sci Adv 2021;7:eabl4988

215. Willems PH, Rossignol R, Dieteren CE, Murphy MP, Koopman WJ: Redox Homeostasis and Mitochondrial Dynamics. Cell Metab 2015;22:207-218

216. Collins Y, Chouchani ET, James AM, Menger KE, Cochemé HM, Murphy MP: Mitochondrial redox signalling at a glance. J Cell Sci 2012;125:801-806

217. Szendroedi J, Schmid AI, Chmelik M, Toth C, Brehm A, Krssak M, Nowotny P, Wolzt M, Waldhausl W, Roden M: Muscle mitochondrial ATP synthesis and glucose transport/phosphorylation in type 2 diabetes. PLoS Med 2007;4:e154

218. Holloszy JO: Skeletal muscle "mitochondrial deficiency" does not mediate insulin resistance. Am J Clin Nutr 2009;89:463S-466S

219. Holloszy JO: "Deficiency" of mitochondria in muscle does not cause insulin resistance. Diabetes 2013;62:1036-1040

220. Martin SD, Morrison S, Konstantopoulos N, McGee SL: Mitochondrial dysfunction has divergent, cell type-dependent effects on insulin action. Mol Metab 2014;3:408-418

221. Szendroedi J, Schmid AI, Meyerspeer M, Cervin C, Kacerovsky M, Smekal G, Gräser-Lang S, Groop L, Roden M: Impaired mitochondrial function and insulin resistance of skeletal muscle in mitochondrial diabetes. Diabetes Care 2009;32:677-679

222. Hulver MW, Berggren JR, Cortright RN, Dudek RW, Thompson RP, Pories WJ, MacDonald KG, Cline GW, Shulman GI, Dohm GL, Houmard JA: Skeletal muscle lipid metabolism with obesity. Am J Physiol Endocrinol Metab 2003;284:E741-747

223. Gavin TP, Ernst JM, Kwak HB, Caudill SE, Reed MA, Garner RT, Nie Y, Weiss JA, Pories WJ, Dar M, Lin CT, Hubal MJ, Neufer PD, Kuang S, Dohm GL: High Incomplete Skeletal Muscle Fatty Acid Oxidation Explains Low Muscle Insulin Sensitivity in Poorly Controlled T2D. J Clin Endocrinol Metab 2018;103:882-889

224. Kelley DE, He J, Menshikova EV, Ritov VB: Dysfunction of mitochondria in human skeletal muscle in type 2 diabetes. Diabetes 2002;51:2944-2950

225. Morino K, Petersen KF, Dufour S, Befroy D, Frattini J, Shatzkes N, Neschen S, White MF, Bilz S, Sono S, Pypaert M, Shulman GI: Reduced mitochondrial density and increased IRS-1 serine phosphorylation in muscle of insulin-resistant offspring of type 2 diabetic parents. J Clin Invest 2005;115:3587-3593

226. Morino K, Petersen KF, Shulman GI: Molecular mechanisms of insulin resistance in humans and their potential links with mitochondrial dysfunction. Diabetes 2006;55 Suppl 2:S9-S15

227. Petersen KF, Dufour S, Morino K, Yoo PS, Cline GW, Shulman GI: Reversal of muscle insulin resistance by weight reduction in young, lean, insulin-resistant offspring of parents with type 2 diabetes. Proc Natl Acad Sci U S A 2012;109:8236-8240

228. Ukropcova B, Sereda O, de Jonge L, Bogacka I, Nguyen T, Xie H, Bray GA, Smith SR: Family history of diabetes links impaired substrate switching and reduced mitochondrial content in skeletal muscle. Diabetes 2007;56:720-727

229. Befroy DE, Petersen KF, Dufour S, Mason GF, de Graaf RA, Rothman DL, Shulman GI: Impaired mitochondrial substrate oxidation in muscle of insulin-resistant offspring of type 2 diabetic patients. Diabetes 2007;56:1376-1381

230. Chavatte-Palmer P, Tarrade A, Rousseau-Ralliard D: Diet before and during Pregnancy and Offspring Health: The Importance of Animal Models and What Can Be Learned from Them. International journal of environmental research and public health 2016;13

231. Williams L, Seki Y, Vuguin PM, Charron MJ: Animal models of in utero exposure to a high fat diet: a review. Biochim Biophys Acta 2014;1842:507-519

232. Zhang XJ, Chinkes DL, Aarsland A, Herndon DN, Wolfe RR: Lipid metabolism in diet-induced obese rabbits is similar to that of obese humans. J Nutr 2008;138:515-518

233. Paigen B: Genetics of responsiveness to high-fat and high-cholesterol diets in the mouse. Am J Clin Nutr 1995;62:458s-462s

234. Furukawa S, Kuroda Y, Sugiyama A: A comparison of the histological structure of the placenta in experimental animals. Journal of toxicologic pathology 2014;27:11-18

235. Barry JS, Anthony RV: The pregnant sheep as a model for human pregnancy. Theriogenology 2008;69:55-67

236. Guilloteau P, Zabielski R, Hammon HM, Metges CC: Nutritional programming of gastrointestinal tract development. Is the pig a good model for man? Nutrition research reviews 2010;23:4-22

237. Arentson-Lantz EJ, Buhman KK, Ajuwon K, Donkin SS: Excess pregnancy weight gain leads to early indications of metabolic syndrome in a swine model of fetal programming. Nutrition research (New York, NY) 2014;34:241-249

238. Ramírez V, Bautista RJ, Frausto-González O, Rodríguez-Peña N, Betancourt ET, Bautista CJ: Developmental Programming in Animal Models: Critical Evidence of Current Environmental Negative Changes. Reprod Sci 2023;30:442-463

239. McCurdy CE, Bishop JM, Williams SM, Grayson BE, Smith MS, Friedman JE, Grove KL: Maternal high-fat diet triggers lipotoxicity in the fetal livers of nonhuman primates. J Clin Invest 2009;119:323-335

240. Frias AE, Morgan TK, Evans AE, Rasanen J, Oh KY, Thornburg KL, Grove KL: Maternal high-fat diet disturbs uteroplacental hemodynamics and increases the frequency of stillbirth in a nonhuman primate model of excess nutrition. Endocrinology 2011;152:2456-2464

241. Comstock SM, Pound LD, Bishop JM, Takahashi DL, Kostrba AM, Smith MS, Grove KL: High-fat diet consumption during pregnancy and the early post-natal period leads to decreased alpha cell plasticity in the nonhuman primate. Mol Metab 2012;2:10-22

242. Sullivan EL, Grayson B, Takahashi D, Robertson N, Maier A, Bethea CL, Smith MS, Coleman K, Grove KL: Chronic consumption of a high-fat diet during pregnancy causes perturbations in the serotonergic system and increased anxiety-like behavior in nonhuman primate offspring. J Neurosci 2010;30:3826-3830

243. Sullivan EL, Riper KM, Lockard R, Valleau JC: Maternal high-fat diet programming of the neuroendocrine system and behavior. Horm Behav 2015;76:153-161

244. Takahashi T, Higashino A, Takagi K, Kamanaka Y, Abe M, Morimoto M, Kang KH, Goto S, Suzuki J, Hamada Y, Kageyama T: Characterization of obesity in Japanese monkeys (Macaca fuscata) in a pedigreed colony. Journal of medical primatology 2006;35:30-37

245. Thorn SR, Baquero KC, Newsom SA, El Kasmi KC, Bergman BC, Shulman GI, Grove KL, Friedman JE: Early Life Exposure to Maternal Insulin Resistance Has Persistent Effects on Hepatic NAFLD in Juvenile Nonhuman Primates. Diabetes 2014;63:2702-2713

246. Cox J, Williams S, Grove K, Lane RH, Aagaard-Tillery KM: A maternal high-fat diet is accompanied by alterations in the fetal primate metabolome. Am J Obstet Gynecol 2009;201:281.e281-289

247. Schmidt SL, Kealey EH, Horton TJ, VonKaenel S, Bessesen DH: The effects of short-term overfeeding on energy expenditure and nutrient oxidation in obesity-prone and obesity-resistant individuals. Int J Obes (Lond) 2013;37:1192-1197

248. Cornier MA, McFadden KL, Thomas EA, Bechtell JL, Bessesen DH, Tregellas JR: Propensity to obesity impacts the neuronal response to energy imbalance. Frontiers in behavioral neuroscience 2015;9:52

249. True C, Dean T, Takahashi D, Sullivan E, Kievit P: Maternal High-Fat Diet Effects on Adaptations to Metabolic Challenges in Male and Female Juvenile Nonhuman Primates. Obesity (Silver Spring) 2018;26:1430-1438

250. Thompson JR, Gustafsson HC, DeCapo M, Takahashi DL, Bagley JL, Dean TA, Kievit P, Fair DA, Sullivan EL: Maternal Diet, Metabolic State, and Inflammatory Response Exert Unique and Long-Lasting Influences on Offspring Behavior in Non-Human Primates. Front Endocrinol (Lausanne) 2018;9:161

251. Suter MA, Sangi-Haghpeykar H, Showalter L, Shope C, Hu M, Brown K, Williams S, Harris RA, Grove KL, Lane RH, Aagaard KM: Maternal high-fat diet modulates the fetal thyroid axis and thyroid gene expression in a nonhuman primate model. Mol Endocrinol 2012;26:2071-2080

252. Sullivan EL, Rivera HM, True CA, Franco JG, Baquero K, Dean TA, Valleau JC, Takahashi DL, Frazee T, Hanna G, Kirigiti MA, Bauman LA, Grove KL, Kievit P: Maternal and postnatal high-fat diet consumption programs energy balance and hypothalamic melanocortin signaling in nonhuman primate offspring. Am J Physiol Regul Integr Comp Physiol 2017;313:R169-R179

253. Sullivan EL, Nousen EK, Chamlou KA: Maternal high fat diet consumption during the perinatal period programs offspring behavior. Physiol Behav 2014;123:236-242

254. Rivera HM, Kievit P, Kirigiti MA, Bauman LA, Baquero K, Blundell P, Dean TA, Valleau JC, Takahashi DL, Frazee T, Douville L, Majer J, Smith MS, Grove KL, Sullivan EL: Maternal high-fat diet and obesity impact palatable food intake and dopamine signaling in nonhuman primate offspring. Obesity (Silver Spring) 2015;23:2157-2164

255. Wesolowski SR, Mulligan CM, Janssen RC, Baker PR, 2nd, Bergman BC, D'Alessandro A, Nemkov T, Maclean KN, Jiang H, Dean TA, Takahashi DL, Kievit P, McCurdy CE, Aagaard KM, Friedman JE: Switching obese mothers to a healthy diet improves fetal hypoxemia, hepatic metabolites, and lipotoxicity in non-human primates. Mol Metab 2018;

256. Grant WF, Nicol LE, Thorn SR, Grove KL, Friedman JE, Marks DL: Perinatal exposure to a high-fat diet is associated with reduced hepatic sympathetic innervation in one-year old male Japanese macaques. PLoS One 2012;7:e48119

257. Nicol LE, Grant WF, Comstock SM, Nguyen ML, Smith MS, Grove KL, Marks DL: Pancreatic inflammation and increased islet macrophages in insulin-resistant juvenile primates. J Endocrinol 2013;217:207-213

258. Elsakr JM, Dunn JC, Tennant K, Zhao SK, Kroeten K, Pasek RC, Takahashi DL, Dean TA, Velez Edwards DR, McCurdy CE, Aagaard KM, Powers AC, Friedman JE, Kievit P, Gannon M: Maternal Western-style diet affects offspring islet composition and function in a non-human primate model of maternal over-nutrition. Mol Metab 2019;25:73-82

259. Carroll DT, Elsakr JM, Miller A, Fuhr J, Lindsley SR, Kirigiti M, Takahashi DL, Dean TA, Wesolowski SR, McCurdy CE, Friedman JE, Aagaard KM, Kievit P, Gannon M: Maternal Western-style diet in nonhuman primates leads to offspring islet adaptations including altered gene expression and insulin hypersecretion. Am J Physiol Endocrinol Metab 2023;324:E577-e588

260. Fan L, Lindsley SR, Comstock SM, Takahashi DL, Evans AE, He GW, Thornburg KL, Grove KL: Maternal high-fat diet impacts endothelial function in nonhuman primate offspring. Int J Obes (Lond) 2013;37:254-262

261. Ma J, Prince AL, Bader D, Hu M, Ganu R, Baquero K, Blundell P, Alan Harris R, Frias AE, Grove KL, Aagaard KM: High-fat maternal diet during pregnancy persistently alters the offspring microbiome in a primate model. Nat Commun 2014;5:3889

262. Wankhade UD, Thakali KM, Shankar K: Persistent influence of maternal obesity on offspring health: Mechanisms from animal models and clinical studies. Mol Cell Endocrinol 2016;435:7-19

263. Kelley DE, Goodpaster B, Wing RR, Simoneau JA: Skeletal muscle fatty acid metabolism in association with insulin resistance, obesity, and weight loss. Am J Physiol 1999;277:E1130-1141

264. Muoio DM: Metabolic inflexibility: when mitochondrial indecision leads to metabolic gridlock. Cell 2014;159:1253-1262

265. Fleischman A, Kron M, Systrom DM, Hrovat M, Grinspoon SK: Mitochondrial function and insulin resistance in overweight and normal-weight children. J Clin Endocrinol Metab 2009;94:4923-4930

266. Paulsen ME, Rosario FJ, Wesolowski SR, Powell TL, Jansson T: Normalizing adiponectin levels in obese pregnant mice prevents adverse metabolic outcomes in offspring. Faseb j 2019;33:2899-2909

267. Kelly AC, F JR, Chan J, Cox LA, Powell TL, Jansson T: Transcriptomic responses are sex-dependent in the skeletal muscle and liver in offspring of obese mice. Am J Physiol Endocrinol Metab 2022;323:E336-e353

268. Latouche C, Heywood SE, Henry SL, Ziemann M, Lazarus R, El-Osta A, Armitage JA, Kingwell BA: Maternal overnutrition programs changes in the expression of skeletal muscle genes that are associated with insulin resistance and defects of oxidative phosphorylation in adult male rat offspring. J Nutr 2014;144:237-244

269. Roberts AL, Koenen KC, Lyall K, Ascherio A, Weisskopf MG: Women's posttraumatic stress symptoms and autism spectrum disorder in their children. Res Autism Spectr Disord 2014;8:608-616

270. Harris RA, Alcott CE, Sullivan EL, Takahashi D, McCurdy CE, Comstock S, Baquero K, Blundell P, Frias AE, Kahr M, Suter M, Wesolowski S, Friedman JE, Grove KL, Aagaard KM: Genomic Variants Associated with Resistance to High Fat Diet Induced Obesity in a Primate Model. Sci Rep 2016;6:36123

271. Kilkenny C, Browne W, Cuthill IC, Emerson M, Altman DG: Animal research: reporting in vivo experiments: the ARRIVE guidelines. British journal of pharmacology 2010;160:1577-1579

272. Elsakr JM, Zhao SK, Ricciardi V, Dean TA, Takahashi DL, Sullivan E, Wesolowski SR, McCurdy CE, Kievit P, Friedman JE, Aagaard KM, Edwards DRV, Gannon M: Western-style diet consumption impairs maternal insulin sensitivity and glucose metabolism during pregnancy in a Japanese macaque model. Scientific reports 2021;11:12977-12977

273. Bergman BC, Brozinick JT, Strauss A, Bacon S, Kerege A, Bui HH, Sanders P, Siddall P, Wei T, Thomas MK, Kuo MS, Perreault L: Muscle sphingolipids during rest and exercise: a C18:0 signature for insulin resistance in humans. Diabetologia 2016;59:785-798

274. Bergman BC, Perreault L, Strauss A, Bacon S, Kerege A, Harrison K, Brozinick JT, Hunerdosse DM, Playdon MC, Holmes W, Bui HH, Sanders P, Siddall P, Wei T, Thomas MK, Kuo MS, Eckel RH: Intramuscular triglyceride synthesis: importance in muscle lipid partitioning in humans. Am J Physiol Endocrinol Metab 2018;314:E152-E164

275. Dymond JS: Explanatory chapter: quantitative PCR. Methods Enzymol 2013;529:279-289

276. Garcia-Sifuentes Y, Maney DL: Reporting and misreporting of sex differences in the biological sciences. Elife 2021;10

277. Ruiz-Alejos A, Carrillo-Larco RM, Miranda JJ, Gilman RH, Smeeth L, Bernabé-Ortiz A: Skinfold thickness and the incidence of type 2 diabetes mellitus and hypertension: an analysis of the PERU MIGRANT study. Public health nutrition 2020;23:63-71

278. Bergman BC, Hunerdosse DM, Kerege A, Playdon MC, Perreault L: Localisation and composition of skeletal muscle diacylglycerol predicts insulin resistance in humans. Diabetologia 2012;55:1140-1150

279. Di Meo S, Iossa S, Venditti P: Skeletal muscle insulin resistance: role of mitochondria and other ROS sources. J Endocrinol 2017;233:R15-r42

280. Han D, Antunes F, Canali R, Rettori D, Cadenas E: Voltage-dependent anion channels control the release of the superoxide anion from mitochondria to cytosol. J Biol Chem 2003;278:5557-5563

281. Reynolds RM, Allan KM, Raja EA, Bhattacharya S, McNeill G, Hannaford PC, Sarwar N, Lee AJ, Bhattacharya S, Norman JE: Maternal obesity during pregnancy and premature mortality from cardiovascular event in adult offspring: follow-up of 1 323 275 person years. BMJ (Clinical research ed) 2013;347:f4539

282. Dabelea D, Mayer-Davis EJ, Lamichhane AP, D'Agostino RB, Jr., Liese AD, Vehik KS, Narayan KM, Zeitler P, Hamman RF: Association of intrauterine exposure to maternal diabetes and obesity with type 2 diabetes in youth: the SEARCH Case-Control Study. Diabetes Care 2008;31:1422-1426

283. Antoun G, McMurray F, Thrush AB, Patten DA, Peixoto AC, Slack RS, McPherson R, Dent R, Harper ME: Impaired mitochondrial oxidative phosphorylation and supercomplex assembly in rectus abdominis muscle of diabetic obese individuals. Diabetologia 2015;58:2861-2866

284. Galgani JE, Moro C, Ravussin E: Metabolic flexibility and insulin resistance. Am J Physiol Endocrinol Metab 2008;295:E1009-1017

285. Venizelos N, von Dobeln U, Hagenfeldt L: Fatty acid oxidation in fibroblasts from patients with defects in beta-oxidation and in the respiratory chain. J Inherit Metab Dis 1998;21:409-415

286. Weiss R, Dufour S, Taksali SE, Tamborlane WV, Petersen KF, Bonadonna RC, Boselli L, Barbetta G, Allen K, Rife F, Savoye M, Dziura J, Sherwin R, Shulman GI, Caprio S: Prediabetes in obese youth: a syndrome of impaired glucose tolerance, severe insulin resistance, and altered myocellular and abdominal fat partitioning. Lancet 2003;362:951-957

287. Kim JY, Hickner RC, Cortright RL, Dohm GL, Houmard JA: Lipid oxidation is reduced in obese human skeletal muscle. Am J Physiol-Endoc M 2000;279:E1039-E1044

288. Petersen MC, Shulman GI: Mechanisms of Insulin Action and Insulin Resistance. Physiol Rev 2018;98:2133-2223

289. Powell DJ, Hajduch E, Kular G, Hundal HS: Ceramide disables 3-phosphoinositide binding to the pleckstrin homology domain of protein kinase B (PKB)/Akt by a PKCzeta-dependent mechanism. Mol Cell Biol 2003;23:7794-7808

290. Bandet CL, Tan-Chen S, Ali-Berrada S, Campana M, Poirier M, Blachnio-Zabielska A, Pais-de-Barros JP, Rouch C, Ferré P, Foufelle F, Le Stunff H, Hajduch E: Ceramide analog C2-cer induces a

loss in insulin sensitivity in muscle cells through the salvage/recycling pathway. J Biol Chem 2023;299:104815

291. Diaz-Vegas A, Madsen S, Cooke KC, Carroll L, Khor JXY, Turner N, Lim XY, Astore MA, Morris JC, Don AS, Garfield A, Zarini S, Zemski Berry KA, Ryan AP, Bergman BC, Brozinick JT, James DE, Burchfield JG: Mitochondrial electron transport chain, ceramide, and coenzyme Q are linked in a pathway that drives insulin resistance in skeletal muscle. Elife 2023;12

292. Straczkowski M, Kowalska I, Nikolajuk A, Dzienis-Straczkowska S, Kinalska I, Baranowski M, Zendzian-Piotrowska M, Brzezinska Z, Gorski J: Relationship between insulin sensitivity and sphingomyelin signaling pathway in human skeletal muscle. Diabetes 2004;53:1215-1221

293. Tonks KT, Coster AC, Christopher MJ, Chaudhuri R, Xu A, Gagnon-Bartsch J, Chisholm DJ, James DE, Meikle PJ, Greenfield JR, Samocha-Bonet D: Skeletal muscle and plasma lipidomic signatures of insulin resistance and overweight/obesity in humans. Obesity (Silver Spring) 2016;24:908-916

294. Fisher-Wellman KH, Neufer PD: Linking mitochondrial bioenergetics to insulin resistance via redox biology. Trends Endocrinol Metab 2012;23:142-153

295. Kokoszka JE, Coskun P, Esposito LA, Wallace DC: Increased mitochondrial oxidative stress in the Sod2 (+/-) mouse results in the age-related decline of mitochondrial function culminating in increased apoptosis. Proc Natl Acad Sci U S A 2001;98:2278-2283

296. Chaudhuri AD, Choi DC, Kabaria S, Tran A, Junn E: MicroRNA-7 Regulates the Function of Mitochondrial Permeability Transition Pore by Targeting VDAC1 Expression. J Biol Chem 2016;291:6483-6493

297. Pryde KR, Taanman JW, Schapira AH: A LON-ClpP Proteolytic Axis Degrades Complex I to Extinguish ROS Production in Depolarized Mitochondria. Cell Rep 2016;17:2522-2531

298. Mercken EM, Capri M, Carboneau BA, Conte M, Heidler J, Santoro A, Martin-Montalvo A, Gonzalez-Freire M, Khraiwesh H, Gonzalez-Reyes JA, Moaddel R, Zhang Y, Becker KG, Villalba JM, Mattison JA, Wittig I, Franceschi C, de Cabo R: Conserved and species-specific molecular denominators in mammalian skeletal muscle aging. NPJ Aging Mech Dis 2017;3:8

299. Sandovici I, Fernandez-Twinn DS, Hufnagel A, Constância M, Ozanne SE: Sex differences in the intergenerational inheritance of metabolic traits. Nat Metab 2022;4:507-523

300. Rosenberg TJ, Garbers S, Lipkind H, Chiasson MA: Maternal obesity and diabetes as risk factors for adverse pregnancy outcomes: differences among 4 racial/ethnic groups. American journal of public health 2005;95:1545-1551

301. Petersen KF, Dufour S, Savage DB, Bilz S, Solomon G, Yonemitsu S, Cline GW, Befroy D, Zemany L, Kahn BB, Papademetris X, Rothman DL, Shulman GI: The role of skeletal muscle insulin resistance in the pathogenesis of the metabolic syndrome. Proc Natl Acad Sci U S A 2007;104:12587-12594

302. Petersen KF, Dufour S, Befroy D, Garcia R, Shulman GI: Impaired mitochondrial activity in the insulin-resistant offspring of patients with type 2 diabetes. N Engl J Med 2004;350:664-671

303. Chan DC: Mitochondrial Dynamics and Its Involvement in Disease. Annual review of pathology 2020;15:235-259

304. Nowinski SM, Van Vranken JG, Dove KK, Rutter J: Impact of Mitochondrial Fatty Acid Synthesis on Mitochondrial Biogenesis. Curr Biol 2018;28:R1212-R1219

305. Tubbs E, Rieusset J: Metabolic signaling functions of ER-mitochondria contact sites: role in metabolic diseases. J Mol Endocrinol 2017;58:R87-R106

306. Theurey P, Tubbs E, Vial G, Jacquemetton J, Bendridi N, Chauvin MA, Alam MR, Le Romancer M, Vidal H, Rieusset J: Mitochondria-associated endoplasmic reticulum membranes allow adaptation of mitochondrial metabolism to glucose availability in the liver. J Mol Cell Biol 2016;8:129-143

307. Song J, Herrmann JM, Becker T: Quality control of the mitochondrial proteome. Nat Rev Mol Cell Biol 2021;22:54-70

308. Rector RS, Thyfault JP, Uptergrove GM, Morris EM, Naples SP, Borengasser SJ, Mikus CR, Laye MJ, Laughlin MH, Booth FW, Ibdah JA: Mitochondrial dysfunction precedes insulin resistance and hepatic steatosis and contributes to the natural history of non-alcoholic fatty liver disease in an obese rodent model. J Hepatol 2010;52:727-736

309. Pound LD, Comstock SM, Grove KL: Consumption of a Western-style diet during pregnancy impairs offspring islet vascularization in a Japanese macaque model. Am J Physiol Endocrinol Metab 2014;307:E115-123

310. Ferrara PJ, Lang MJ, Johnson JM, Watanabe S, McLaughlin KL, Maschek JA, Verkerke ARP, Siripoksup P, Chaix A, Cox JE, Fisher-Wellman KH, Funai K: Weight loss increases skeletal muscle mitochondrial energy efficiency in obese mice. Life metabolism 2023;2

311. Dent JR, Hetrick B, Tahvilian S, Sathe A, Greyslak K, LaBarge SA, Svensson K, McCurdy CE, Schenk S: Skeletal muscle mitochondrial function and exercise capacity are not impaired in mice with knockout of STAT3. J Appl Physiol (1985) 2019;127:1117-1127

312. Gong G, Song M, Csordas G, Kelly DP, Matkovich SJ, Dorn GW, 2nd: Parkin-mediated mitophagy directs perinatal cardiac metabolic maturation in mice. Science 2015;350:aad2459

313. Del Dotto V, Mishra P, Vidoni S, Fogazza M, Maresca A, Caporali L, McCaffery JM, Cappelletti M, Baruffini E, Lenaers G, Chan D, Rugolo M, Carelli V, Zanna C: OPA1 Isoforms in the Hierarchical Organization of Mitochondrial Functions. Cell Rep 2017;19:2557-2571

314. Mishra P, Carelli V, Manfredi G, Chan DC: Proteolytic cleavage of Opa1 stimulates mitochondrial inner membrane fusion and couples fusion to oxidative phosphorylation. Cell Metab 2014;19:630-641

315. Chen Q, Thompson J, Hu Y, Dean J, Lesnefsky EJ: Inhibition of the ubiquitous calpains protects complex I activity and enables improved mitophagy in the heart following ischemia-reperfusion. Am J Physiol Cell Physiol 2019;317:C910-C921

316. Fernandez-Mosquera L, Yambire KF, Couto R, Pereyra L, Pabis K, Ponsford AH, Diogo CV, Stagi M, Milosevic I, Raimundo N: Mitochondrial respiratory chain deficiency inhibits lysosomal hydrolysis. Autophagy 2019:1-20

317. Ainbinder A, Boncompagni S, Protasi F, Dirksen RT: Role of Mitofusin-2 in mitochondrial localization and calcium uptake in skeletal muscle. Cell Calcium 2015;57:14-24

318. de Brito OM, Scorrano L: Mitofusin 2 tethers endoplasmic reticulum to mitochondria. Nature 2008;456:605-610

319. Ferecatu I, Goncalves S, Golinelli-Cohen MP, Clemancey M, Martelli A, Riquier S, Guittet E, Latour JM, Puccio H, Drapier JC, Lescop E, Bouton C: The diabetes drug target MitoNEET governs a novel trafficking pathway to rebuild an Fe-S cluster into cytosolic aconitase/iron regulatory protein 1. J Biol Chem 2014;289:28070-28086

320. Vernay A, Marchetti A, Sabra A, Jauslin TN, Rosselin M, Scherer PE, Demaurex N, Orci L, Cosson P: MitoNEET-dependent formation of intermitochondrial junctions. Proc Natl Acad Sci U S A 2017;114:8277-8282

321. Schlattner U, Tokarska-Schlattner M, Rousseau D, Boissan M, Mannella C, Epand R, Lacombe ML: Mitochondrial cardiolipin/phospholipid trafficking: the role of membrane contact site complexes and lipid transfer proteins. Chem Phys Lipids 2014;179:32-41

322. Vernay A, Marchetti A, Sabra A, Jauslin TN, Rosselin M, Scherer PE, Demaurex N, Orci L, Cosson P: MitoNEET-dependent formation of intermitochondrial junctions. 2017;114:8277-8282

323. Sebastian D, Hernandez-Alvarez MI, Segales J, Sorianello E, Munoz JP, Sala D, Waget A, Liesa M, Paz JC, Gopalacharyulu P, Oresic M, Pich S, Burcelin R, Palacin M, Zorzano A: Mitofusin 2 (Mfn2) links mitochondrial and endoplasmic reticulum function with insulin signaling and is essential for normal glucose homeostasis. Proc Natl Acad Sci U S A 2012;109:5523-5528

324. Llinàs-Arias P, Rosselló-Tortella M, López-Serra P, Pérez-Salvia M, Setién F, Marin S, Muñoz JP, Junza A, Capellades J, Calleja-Cervantes ME, Ferreira HJ, de Moura MC, Srbic M, Martínez-Cardús A, de la Torre C, Villanueva A, Cascante M, Yanes O, Zorzano A, Moutinho C, Esteller M: Epigenetic loss of the endoplasmic reticulum-associated degradation inhibitor SVIP induces cancer cell metabolic reprogramming. JCI insight 2019;5

325. Lewis SC, Uchiyama LF, Nunnari J: ER-mitochondria contacts couple mtDNA synthesis with mitochondrial division in human cells. Science 2016;353:aaf5549

326. McGee WK, Bishop CV, Pohl CR, Chang RJ, Marshall JC, Pau FK, Stouffer RL, Cameron JL: Effects of hyperandrogenemia and increased adiposity on reproductive and metabolic parameters in young adult female monkeys. Am J Physiol Endocrinol Metab 2014;306:E1292-1304

327. Funai K, Summers SA, Rutter J: Reign in the membrane: How common lipids govern mitochondrial function. Curr Opin Cell Biol 2020;63:162-173

328. Flis VV, Daum G: Lipid transport between the endoplasmic reticulum and mitochondria. Cold Spring Harb Perspect Biol 2013;5

329. Li J, Huang Q, Long X, Guo X, Sun X, Jin X, Li Z, Ren T, Yuan P, Huang X, Zhang H, Xing J: Mitochondrial elongation-mediated glucose metabolism reprogramming is essential for tumour cell survival during energy stress. Oncogene 2017;36:4901-4912

330. Benador IY, Veliova M, Mahdaviani K, Petcherski A, Wikstrom JD, Assali EA, Acin-Perez R, Shum M, Oliveira MF, Cinti S, Sztalryd C, Barshop WD, Wohlschlegel JA, Corkey BE, Liesa M, Shirihai OS: Mitochondria Bound to Lipid Droplets Have Unique Bioenergetics, Composition, and Dynamics that Support Lipid Droplet Expansion. Cell Metab 2018;27:869-885 e866

331. Benador IY, Veliova M, Liesa M, Shirihai OS: Mitochondria Bound to Lipid Droplets: Where Mitochondrial Dynamics Regulate Lipid Storage and Utilization. Cell Metab 2019;

332. Senos Demarco R, Uyemura BS, D'Alterio C, Jones DL: Mitochondrial fusion regulates lipid homeostasis and stem cell maintenance in the Drosophila testis. Nat Cell Biol 2019;21:710-720

333. Moore TM, Zhou Z, Cohn W, Norheim F, Lin AJ, Kalajian N, Strumwasser AR, Cory K, Whitney K, Ho T, Ho T, Lee JL, Rucker DH, Shirihai O, van der Bliek AM, Whitelegge JP, Seldin MM, Lusis AJ, Lee S, Drevon CA, Mahata SK, Turcotte LP, Hevener AL: The impact of exercise on mitochondrial dynamics and the role of Drp1 in exercise performance and training adaptations in skeletal muscle. Mol Metab 2019;21:51-67

334. Kugler BA, Deng W, Francois B, Nasta M, Hinkley JM, Houmard JA, Gona PN, Zou K: Distinct Adaptations of Mitochondrial Dynamics to Electrical Pulse Stimulation in Lean and Severely Obese Primary Myotubes. Medicine and science in sports and exercise 2020;

335. Chang W, Xiao D, Ao X, Li M, Xu T, Wang J: Increased Dynamin-Related Protein 1-Dependent Mitochondrial Fission Contributes to High-Fat-Diet-Induced Cardiac Dysfunction and Insulin Resistance by Elevating Tafazzin in Mouse Hearts. Mol Nutr Food Res 2019;63:e1801322

336. Hu Y, Chen H, Zhang L, Lin X, Li X, Zhuang H, Fan H, Meng T, He Z, Huang H, Gong Q, Zhu D, Xu Y, He P, Li L, Feng D: The AMPK-MFN2 axis regulates MAM dynamics and autophagy induced by energy stresses. Autophagy 2020:1-15

337. McLelland GL, Goiran T, Yi W, Dorval G, Chen CX, Lauinger ND, Krahn AI, Valimehr S, Rakovic A, Rouiller I, Durcan TM, Trempe JF, Fon EA: Mfn2 ubiquitination by PINK1/parkin gates the p97-dependent release of ER from mitochondria to drive mitophagy. Elife 2018;7

338. Steckler T, Wang J, Bartol FF, Roy SK, Padmanabhan V: Fetal programming: prenatal testosterone treatment causes intrauterine growth retardation, reduces ovarian reserve and increases ovarian follicular recruitment. Endocrinology 2005;146:3185-3193

339. Manikkam M, Crespi EJ, Doop DD, Herkimer C, Lee JS, Yu S, Brown MB, Foster DL, Padmanabhan V: Fetal programming: prenatal testosterone excess leads to fetal growth retardation and postnatal catch-up growth in sheep. Endocrinology 2004;145:790-798

340. Risal S, Pei Y, Lu H, Manti M, Fornes R, Pui HP, Zhao Z, Massart J, Ohlsson C, Lindgren E, Crisosto N, Maliqueo M, Echiburú B, Ladrón de Guevara A, Sir-Petermann T, Larsson H, Rosenqvist MA, Cesta CE, Benrick A, Deng Q, Stener-Victorin E: Prenatal androgen exposure and transgenerational susceptibility to polycystic ovary syndrome. Nat Med 2019;25:1894-1904

341. Huo Y, Wang W, Zhang J, Xu D, Bai F, Gui Y: Maternal androgen excess inhibits fetal cardiomyocytes proliferation through RB-mediated cell cycle arrest and induces cardiac hypertrophy in adulthood. Journal of endocrinological investigation 2024;47:603-617

342. Roland AV, Nunemaker CS, Keller SR, Moenter SM: Prenatal androgen exposure programs metabolic dysfunction in female mice. J Endocrinol 2010;207:213-223

343. Abruzzese GA, Ferreira SR, Ferrer MJ, Silva AF, Motta AB: Prenatal Androgen Excess Induces Multigenerational Effects on Female and Male Descendants. Clinical medicine insights Endocrinology and diabetes 2023;16:11795514231196461

344. Bishop CV, Takahashi D, Mishler E, Slayden OD, Roberts CT, Hennebold J, True C: Individual and combined effects of 5-year exposure to hyperandrogenemia and Western-style diet on metabolism and reproduction in female rhesus macaques. Hum Reprod 2021;36:444-454

345. Diamond MP, Grainger D, Diamond MC, Sherwin RS, Defronzo RA: Effects of methyltestosterone on insulin secretion and sensitivity in women. J Clin Endocrinol Metab 1998;83:4420-4425

346. Arslanian SA, Lewy VD, Danadian K: Glucose intolerance in obese adolescents with polycystic ovary syndrome: roles of insulin resistance and beta-cell dysfunction and risk of cardiovascular disease. J Clin Endocrinol Metab 2001;86:66-71

347. Perelman P, Johnson WE, Roos C, Seuánez HN, Horvath JE, Moreira MA, Kessing B, Pontius J, Roelke M, Rumpler Y, Schneider MP, Silva A, O'Brien SJ, Pecon-Slattery J: A molecular phylogeny of living primates. PLoS Genet 2011;7:e1001342

348. Cauvin AJ, Peters C, Brennan F: *Advantages and Limitations of Commonly Used Nonhuman Primate Species in Research and Development of Biopharmaceuticals*. The Nonhuman Primate in Nonclinical Drug Development and Safety Assessment. 2015:379-95. doi: 10.1016/B978-0-12-417144-2.00019-6. Epub 2015 Mar 20.

349. Dumesic DA, Abbott DH, Chazenbalk GD: An Evolutionary Model for the Ancient Origins of Polycystic Ovary Syndrome. Journal of clinical medicine 2023;12

350. Dumesic DA, Padmanabhan V, Chazenbalk GD, Abbott DH: Polycystic ovary syndrome as a plausible evolutionary outcome of metabolic adaptation. Reproductive biology and endocrinology : RB&E 2022;20:12

351. Abbott DH, Rayome BH, Dumesic DA, Lewis KC, Edwards AK, Wallen K, Wilson ME, Appt SE, Levine JE: Clustering of PCOS-like traits in naturally hyperandrogenic female rhesus monkeys. Hum Reprod 2017;32:923-936

352. National Academies of Sciences E, Medicine, Division on E, Life S, Health, Medicine D, Institute for Laboratory Animal R, Board on Health Sciences P, Committee on the State of the S, Future Needs for Nonhuman Primate Model S: The National Academies Collection: Reports funded by National Institutes of Health. In *Nonhuman Primate Models in Biomedical Research: State of the Science and Future Needs* Yost OC, Downey A, Ramos KS, Eds. Washington (DC), National Academies Press (US)

353. Herman RA, Jones B, Mann DR, Wallen K: Timing of prenatal androgen exposure: anatomical and endocrine effects on juvenile male and female rhesus monkeys. Horm Behav 2000;38:52-66

354. Abbott DH, Barnett DK, Levine JE, Padmanabhan V, Dumesic DA, Jacoris S, Tarantal AF: Endocrine antecedents of polycystic ovary syndrome in fetal and infant prenatally androgenized female rhesus monkeys. Biol Reprod 2008;79:154-163

355. Dumesic DA, Abbott DH, Eisner JR, Goy RW: Prenatal exposure of female rhesus monkeys to testosterone propionate increases serum luteinizing hormone levels in adulthood. Fertil Steril 1997;67:155-163

356. Eisner JR, Dumesic DA, Kemnitz JW, Colman RJ, Abbott DH: Increased adiposity in female rhesus monkeys exposed to androgen excess during early gestation. Obes Res 2003;11:279-286

357. Treloar OL, Wolf RC, Meyer RK: Failure of a single neonatal dose of testosterone to alter ovarian function in the Rhesus monkey. Endocrinology 1972;90:281-284

358. Vendola KA, Zhou J, Adesanya OO, Weil SJ, Bondy CA: Androgens stimulate early stages of follicular growth in the primate ovary. J Clin Invest 1998;101:2622-2629

359. Faiman C, Reyes FI, Dent DW, Fuller GB, Hobson WC, Thliveris JA: Effects of long-term testosterone exposure on ovarian function and morphology in the rhesus monkey. The Anatomical record 1988;222:245-251

360. McGee WK, Bishop CV, Bahar A, Pohl CR, Chang RJ, Marshall JC, Pau FK, Stouffer RL, Cameron JL: Elevated androgens during puberty in female rhesus monkeys lead to increased neuronal drive to the reproductive axis: a possible component of polycystic ovary syndrome. Hum Reprod 2012;27:531-540

361. Carey DG, Jenkins AB, Campbell LV, Freund J, Chisholm DJ: Abdominal fat and insulin resistance in normal and overweight women: Direct measurements reveal a strong relationship in subjects at both low and high risk of NIDDM. Diabetes 1996;45:633-638

362. Varlamov O, Chu MP, McGee WK, Cameron JL, O'Rourke RW, Meyer KA, Bishop CV, Stouffer RL, Roberts CT, Jr.: Ovarian cycle-specific regulation of adipose tissue lipid storage by testosterone in female nonhuman primates. Endocrinology 2013;154:4126-4135

363. Varlamov O, Bishop CV, Handu M, Takahashi D, Srinivasan S, White A, Roberts CT, Jr.: Combined androgen excess and Western-style diet accelerates adipose tissue dysfunction in young adult, female nonhuman primates. Hum Reprod 2017;32:1892-1902

364. True CA, Takahashi DL, Burns SE, Mishler EC, Bond KR, Wilcox MC, Calhoun AR, Bader LA, Dean TA, Ryan ND, Slayden OD, Cameron JL, Stouffer RL: Chronic combined hyperandrogenemia and western-style diet in young female rhesus macaques causes greater metabolic impairments compared to either treatment alone. Hum Reprod 2017;32:1880-1891

365. Rodrigues JK, Navarro PA, Zelinski MB, Stouffer RL, Xu J: Direct actions of androgens on the survival, growth and secretion of steroids and anti-Müllerian hormone by individual macaque follicles during three-dimensional culture. Hum Reprod 2015;30:664-674

366. Xu J, McGee WK, Bishop CV, Park BS, Cameron JL, Zelinski MB, Stouffer RL: Exposure of female macaques to Western-style diet with or without chronic T in vivo alters secondary follicle function during encapsulated 3-dimensional culture. Endocrinology 2015;156:1133-1142

367. Bishop CV, Xu F, Xu J, Ting AY, Galbreath E, McGee WK, Zelinski MB, Hennebold JD, Cameron JL, Stouffer RL: Western-style diet, with and without chronic androgen treatment, alters the number, structure, and function of small antral follicles in ovaries of young adult monkeys. Fertil Steril 2016;105:1023-1034

368. Baba T, Ting AY, Tkachenko O, Xu J, Stouffer RL: Direct actions of androgen, estrogen and anti-Müllerian hormone on primate secondary follicle development in the absence of FSH in vitro. Hum Reprod 2017;32:2456-2464

369. Bishop CV, Mishler EC, Takahashi DL, Reiter TE, Bond KR, True CA, Slayden OD, Stouffer RL: Chronic hyperandrogenemia in the presence and absence of a western-style diet impairs ovarian and uterine structure/function in young adult rhesus monkeys. Hum Reprod 2018;33:128-139

370. Bishop CV, Reiter TE, Erikson DW, Hanna CB, Daughtry BL, Chavez SL, Hennebold JD, Stouffer RL: Chronically elevated androgen and/or consumption of a Western-style diet impairs oocyte quality and granulosa cell function in the nonhuman primate periovulatory follicle. Journal of assisted reproduction and genetics 2019;36:1497-1511

371. Bishop CV, Stouffer RL, Takahashi DL, Mishler EC, Wilcox MC, Slayden OD, True CA: Chronic hyperandrogenemia and western-style diet beginning at puberty reduces fertility and increases metabolic dysfunction during pregnancy in young adult, female macaques. Hum Reprod 2018;33:694-705

372. Kuo K, Roberts VHJ, Gaffney J, Takahashi DL, Morgan T, Lo JO, Stouffer RL, Frias AE: Maternal High-Fat Diet Consumption and Chronic Hyperandrogenemia Are Associated With Placental Dysfunction in Female Rhesus Macaques. Endocrinology 2019;160:1937-1949

373. Moran C, Reyna R, Boots LS, Azziz R: Adrenocortical hyperresponsiveness to corticotropin in polycystic ovary syndrome patients with adrenal androgen excess. Fertil Steril 2004;81:126-131

374. Silfen ME, Denburg MR, Manibo AM, Lobo RA, Jaffe R, Ferin M, Levine LS, Oberfield SE: Early endocrine, metabolic, and sonographic characteristics of polycystic ovary syndrome (PCOS): comparison between nonobese and obese adolescents. J Clin Endocrinol Metab 2003;88:4682-4688

375. Keator CS, Lindner JR, Belcik JT, Bishop CV, Slayden OD: Contrast-enhanced ultrasound reveals real-time spatial changes in vascular perfusion during early implantation in the macaque uterus. Fertil Steril 2011;95:1316-1321.e1311-1313

376. Teede HJ, Tay CT, Laven JJE, Dokras A, Moran LJ, Piltonen TT, Costello MF, Boivin J, Redman LM, Boyle JA, Norman RJ, Mousa A, Joham AE: Recommendations From the 2023 International Evidence-based Guideline for the Assessment and Management of Polycystic Ovary Syndrome. J Clin Endocrinol Metab 2023;108:2447-2469

377. Song X, Shen Q, Fan L, Yu Q, Jia X, Sun Y, Bai W, Kang J: Dehydroepiandrosterone-induced activation of mTORC1 and inhibition of autophagy contribute to skeletal muscle insulin resistance in a mouse model of polycystic ovary syndrome. Oncotarget 2018;9:11905-11921

378. Shukla P, Mukherjee S, Patil A: Identification of Variants in Mitochondrial D-Loop and OriL Region and Analysis of Mitochondrial DNA Copy Number in Women with Polycystic Ovary Syndrome. DNA and cell biology 2020;39:1458-1466

379. Victor VM, Rocha M, Bañuls C, Rovira-Llopis S, Gómez M, Hernández-Mijares A: Mitochondrial impairment and oxidative stress in leukocytes after testosterone administration to female-to-male transsexuals. The journal of sexual medicine 2014;11:454-461

380. Ding Y, Jiang Z, Xia B, Zhang L, Zhang C, Leng J: Mitochondria-targeted antioxidant therapy for an animal model of PCOS-IR. Int J Mol Med 2019;43:316-324

381. Torres MJ, Ryan TE, Lin CT, Zeczycki TN, Neufer PD: Impact of 17β-estradiol on complex I kinetics and H(2)O(2) production in liver and skeletal muscle mitochondria. J Biol Chem 2018;293:16889-16898

382. Torres MJ, Kew KA, Ryan TE, Pennington ER, Lin CT, Buddo KA, Fix AM, Smith CA, Gilliam LA, Karvinen S, Lowe DA, Spangenburg EE, Zeczycki TN, Shaikh SR, Neufer PD: 17beta-Estradiol Directly Lowers Mitochondrial Membrane Microviscosity and Improves Bioenergetic Function in Skeletal Muscle. Cell Metab 2018;27:167-179 e167

383. Puttabyatappa M, Ciarelli JN, Chatoff AG, Padmanabhan V: Developmental programming: Metabolic tissue-specific changes in endoplasmic reticulum stress, mitochondrial oxidative and telomere length status induced by prenatal testosterone excess in the female sheep. Mol Cell Endocrinol 2021;526:111207